January 1967

Application of an Electronic Analog Computer to the Problems of River Basin Hydrology

J. Paul Riley

Duane G. Chadwick

APPLICATION OF AN ELECTRONIC ANALOG COMPUTER TO THE PROBLEMS OF RIVER BASIN HYDROLOGY

by

John Paul Riley

Duane G. Chadwick

This report represents a section of the project completion report for a study which was supported in part with funds provided by the Department of the Interior, Office of Water Resources Research under P.L. 88-379, Project Number - B - 011 - Utah, Agreement Number 14 - 0001 - 1 - 53, Investigation period, October 1, 1966, to December 31, 1967. The senior author of the report, Dr. John Paul Riley, was a graduate research assistant supported partly by the above project. The results of his work were utilized as partial fulfillment of the requirements for the Ph.D. degree.

Utah Water Research Laboratory
College of Engineering
Utah State University
Logan, Utah

December 1967

ABSTRACT

APPLICATION OF AN ELECTRONIC ANALOG COMPUTER

TO THE PROBLEMS OF RIVER BASIN HYDROLOGY

As demands upon available water supplies increase, there is an accompanying increase in the need to assess the downstream consequences resulting from changes at specific locations within a hydrologic system. This problem was approached by electronic analog simulation of the hydrologic system.

The complexity of a hydrologic model depends to a large extent upon the magnitude of the time and spatial increments utilized in the model. The increment size selected depends upon the types of problems to be solved. Three models are described, and in each succeeding model the definition in terms of time and/or space is improved. While the improved model is capable of solving the same heirarchy of hydrologic problems as its predecessor, it is also capable of solving many additional problems which require a higher degree of definition.

Preliminary verification studies for both the second and third models have shown close agreement between observed and computed discharge hydrographs from prototype basins.

Riley, John Paul, and Chadwick, Duane G.
APPLICATION OF AN ELECTRONIC ANALOG COMPUTER TO THE PROBLEMS OF RIVER BASIN HYDROLOGY
Research Project Technical Report to Office of Water Resources Research, Department of Interior, December 1967, Washington D. C., 199 p.

KEYWORDS--*hydrologic models/ *hydrologic simulation/ *simulation/ *electronic analog computer/ infiltration/ runoff/ rainfall/ precipitation/ *watershed studies/ *snowmelt/ evapotranspiration/ *hydrology/ *hydrologic research/ *water yields/ *water resource planning and development/ experimental watersheds/ soil moisture/ semiarid watershed studies/ convective storms.

ACKNOWLEDGMENTS

This publication represents a section of the project completion report for a project which was supported in part with funds provided by the Office of Water Resources of the United States Department of the Interior as authorized under the Water Resources Research Act of 1964, Public Law 88-379. The work was accomplished by personnel of the Utah Water Research Laboratory in accordance with a research proposal which was submitted to the Office of Water Resources Research through the Utah center for Water Resources Research at Utah State University. This university is the institution designated to administer the programs of the Office of Water Resources Research in Utah.

The writers are grateful for the facilities of the Utah Water Research Laboratory which contributed to the successful completion of this study, and also acknowledge the technical advice and suggestions provided by Dr. Jay M. Bagley and Professors Jerald E. Christiansen, Joel E. Fletcher, and Eugene K. Israelsen. Others of various agencies have also provided useful suggestions for which appreciation is expressed.

John Paul Riley
Duane G. Chadwick

TABLE OF CONTENTS

TABLE OF CONTENTS (Continued)

LIST OF FIGURES

LIST OF FIGURES (Continued)

LIST OF FIGURES (Continued)

LIST OF FIGURES (Continued)

LIST OF FIGURES (Continued)

LIST OF TABLES

PARTIAL LIST OF SYMBOLS[1]

Symbol	Definition
C_s	volume of water stored within a particular length of surface channel
D_s	quantity of precipitation in surface storage
D_{cs}	surface depression storage capacity as determined by a physiographic study
D_r	rate of inflow to surface depression storage
D_{cr}	maximum rate at which surface water is able to enter depression storage
E_r	evaporation rate
E_{cr}	potential evaporation rate or evaporation capacity
ET_r	evapotranspiration rate
ET_{cr}	potential evapotranspiration rate or evapotranspiration capacity
F_r	infiltration rate
F_{cr}	infiltration capacity or maximum infiltration rate

[1] Notes:
1. All parameters are functions of time.
2. The subscript "r" denotes a rate of change with respect to time.
3. The subscript "s" denotes a stored quantity.
4. Values of all parameters are greater than or equal to zero.
5. Symbols not included in this list are defined within the text of the report.

PARTIAL LIST OF SYMBOLS (Continued)

Symbol	Definition
G_r	deep percolation rate to the groundwater basin (inflow to storage)
G_s	quantity of water stored within the groundwater basin
I_r	rate at which precipitation is entering interception storage
I_{cr}	interception capacity or maximum rate at which precipitation is able to enter interception storage
I_s	the quantity of precipitation in interception storage
I_{cs}	interception storage capacity of the vegetation within a particular area
i_r	net inflow rate to surface channels within a watershed zone
M_s	quantity of water stored within the root zone and available for plant use
M_{cs}	root zone storage capacity of water available to plants
M_{es}	limiting root zone available moisture content below which the actual evapotranspiration rate becomes less than the potential rate
N_r	interflow rate (inflow to storage)
N_s	quantity of water stored as interflow
P	precipitation rate
P_{gr}	precipitation throughfall rate, including stemflow
Q_{rb}	rate of total base flow within the surface channels of a watershed

PARTIAL LIST OF SYMBOLS (Continued)

Symbol	Definition
q_{rb}	rate of flow from the groundwater basin into an effluent channel within a watershed zone
q_{rc}	rate of channel runoff from a particular watershed zone
Q_{rg}	rate of total discharge from the groundwater basin
q_{rg}	rate of seepage loss from a surface channel within a watershed zone
q_{rn}	rate of discharge from interflow storage within a watershed zone
Q_{rs}	rate of total surface discharge from a watershed, including channel base flow
q_{rs}	rate of discharge from surface detention storage within a watershed zone
Q_{rt}	rate of total discharge from a watershed
Q_{ru}	rate of total subsurface discharge from a watershed
S_r	rate at which water is available for surface runoff within a zone (inflow to surface detention storage)
S_s	quantity of water stored as surface detention
T_a	surface air temperature in degrees F
T_o	the surface air temperature in degrees F applied as an index for establishing the form in which precipitation is considered to occur in the model (rain or snow)

PARTIAL LIST OF SYMBOLS (Continued)

Symbol	Definition
W_{gr}	rate at which water is available at the soil surface
W_{rs}	rate at which snowmelt water is available at the soil surface
W_{s}	snow storage in terms of water equivalent

ABSTRACT

Application of an Electronic Analog Computer

to the Problems of River Basin Hydrology

by

John Paul Riley, Doctor of Philosophy

Utah State University, 1967

Major Professor: Dr. Jay M. Bagley
Department: Civil Engineering

As demands upon available water supplies increase, there is an accompanying increase in the need to assess the downstream consequences resulting from changes at specific locations within a hydrologic system. This problem was approached by electronic analog simulation of the hydrologic system.

The complexity of a hydrologic model depends to a large extent upon the magnitude of the time and spatial increments utilized in the model. The increment size selected depends upon the types of problems to be solved. Three models are described, and in each succeeding model the definition in terms of time and/or space is improved. While the improved model is capable of solving the same heirarchy of hydrologic problems as its predecessor, it is also capable of solving many additional problems which require a higher degree of definition.

Preliminary verification studies for both the second and third models have shown close agreement between observed and computed discharge hydrographs from prototype basins. (215 pages)

CHAPTER I

INTRODUCTION

The rapid growth in recent years of a variety of demands upon available water resources has led to an increasing interest in the science of hydrology. In every hydrologic system each upstream use has some effect on the quantity of flow occurring at downstream points. Because many of the factors which affect hydrologic flow systems are subject to management or regulation, the optimum use of an existing water supply depends upon an accurate quantitative assessment of the possible management alternatives.

A hydrologic system is relatively easy to describe from a qualitative standpoint. However, the extension of this qualitative knowledge to obtain specific quantitative results is a difficult problem. The complex interrelation and variable nature of the many different processes occurring simultaneously within a hydrologic system make this so. In addition, compared to many other fields of science, few basic quantitative concepts exist as yet in the area of hydrology. Thus, there is need both to describe the various hydrologic processes in mathematical terms, and to develop a practical method of combining these expressions into models which will facilitate a quick and easy examination of hydrologic parameters as they are affected by management and other changes within a prototype basin.

In an attempt to find a solution to the problem posed by the preceding paragraph, research workers in recent years have turned to modern high-speed electronic computers. Comprehensive simulation models of the entire hydrologic system are now being formulated. Simulation is a technique for investigating the behavior or response of a dynamic system subject to particular constraints and input functions. This technique is usually performed by means of both physical and electronic models. Physical models and also those consisting of electrical resistor-capacitor networks have been used to investigate hydraulic and hydrologic phenomena for many years. However, simulation by means of high-speed electronic computers is a relatively new technique.

Considerable progress in digital computer simulation has been made at Stanford University (1, 7, 8). A simplified digital model of the hydrologic and water quality system of the Lost River in northern California has been developed (62), and work is now in progress on digital models at several universities (46).

Simulation of hydrologic systems by means of electronic analog computers is also under development. Shen (41) discusses the applicability of analog models for analyzing flood flows. The Hydraulic Laboratory of the University of California has built an analog model for the purpose of routing floods in a particular river system (15). In addition, an analog computer program has been developed for simulating flood conditions on the Kitakami River of Japan (31).

Research in electronic analog models of hydrologic systems began at Utah State University in 1962 (3). Professors Bagley and Chadwick envisioned model simulation of an entire watershed and proposed the design and formulation of a pilot model for use in water resource planning. These recommendations were accepted, and the Agricultural Research Service, the Soil Conservation Service, and the Utah Water and Power Board provided funding to proceed with the construction of a test model. An electronic analog computing device was subsequently designed and built at Utah State University. The computer, completed in November 1964 (2), is shown by figure 1. 1.

For the simulation of hydrologic phenomena the electronic analog computer has several important advantages. This type of computer solves problems by behaving electronically in a manner analogous with the problem solution, and it is therefore a parallel device in that all computations proceed simultaneously. Thus, if the size of a problem is doubled, the amount of analog equipment required is also approximately doubled, but the time for solution remains the same.

Many of the processes which occur in nature are time dependent and as such are differential in form. It is in the solution of differential equations that the great speed of the analog computer is particularly apparent because it can integrate the problem variables continuously instead of using numerical approximations. Frequently, design optimization problems or those involving stochastic variables require differential equations to be solved repeatedly, each with slightly different

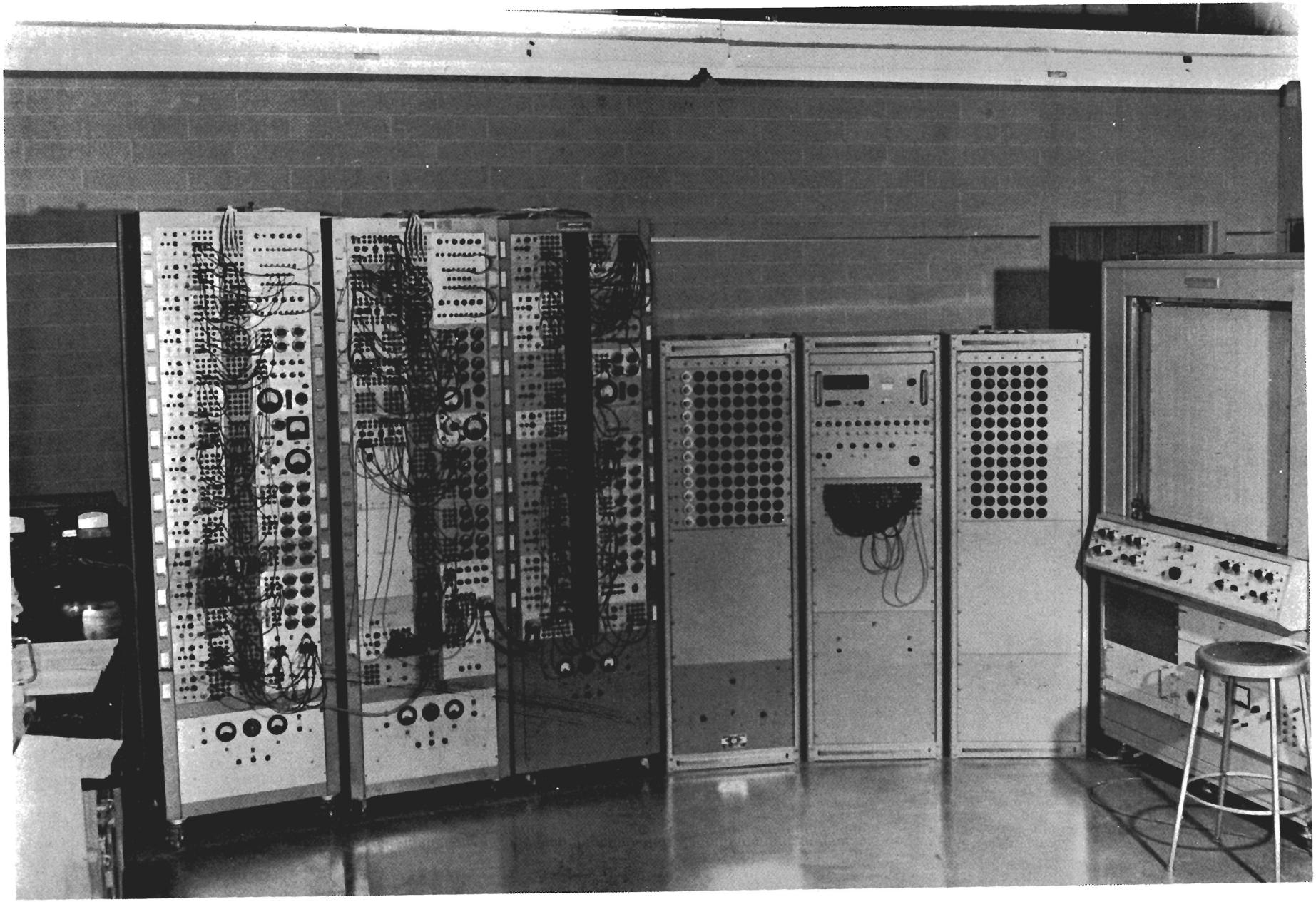

Figure 1.1. The first model of the analog computing facilities developed for simulation studies at Utah State University.

parameters or functions. Because of its capability for continuous output feedback during problem solution, program optimization can be undertaken on the analog computer during the computation process.

Output on an analog computer is presented in graphical form as a continuous plot of the variable quantities involved. The operator can visualize results as being the actual dynamic responses of the physical system under investigation. Also, the results of possible alternative ways of combining the various components of the entire system can be quickly defined as an aid to determining the changes in specific processes that might be necessary to meet prototype conditions. Thus, the analog is very helpful during the exploratory phases of developing both component relationships and a composite model of a hydrologic system.

The fundamental requirement of a computer model of a physical flow system is that the model simulates on a continuous basis all important processes and relationships within the system that it represents. This requirement is met by developing a preliminary model from an analysis of published information and established concepts. Through operation of the model, quantitative relationships and hydrologic concepts are further defined and improved. This evolutionary process of trial, feed-back of information, and improvement in the development of a simulation model of a dynamic system is illustrated by the flow diagram of figure 1.2. When the model is properly verified so that it accurately simulates a particular system, input and individual model

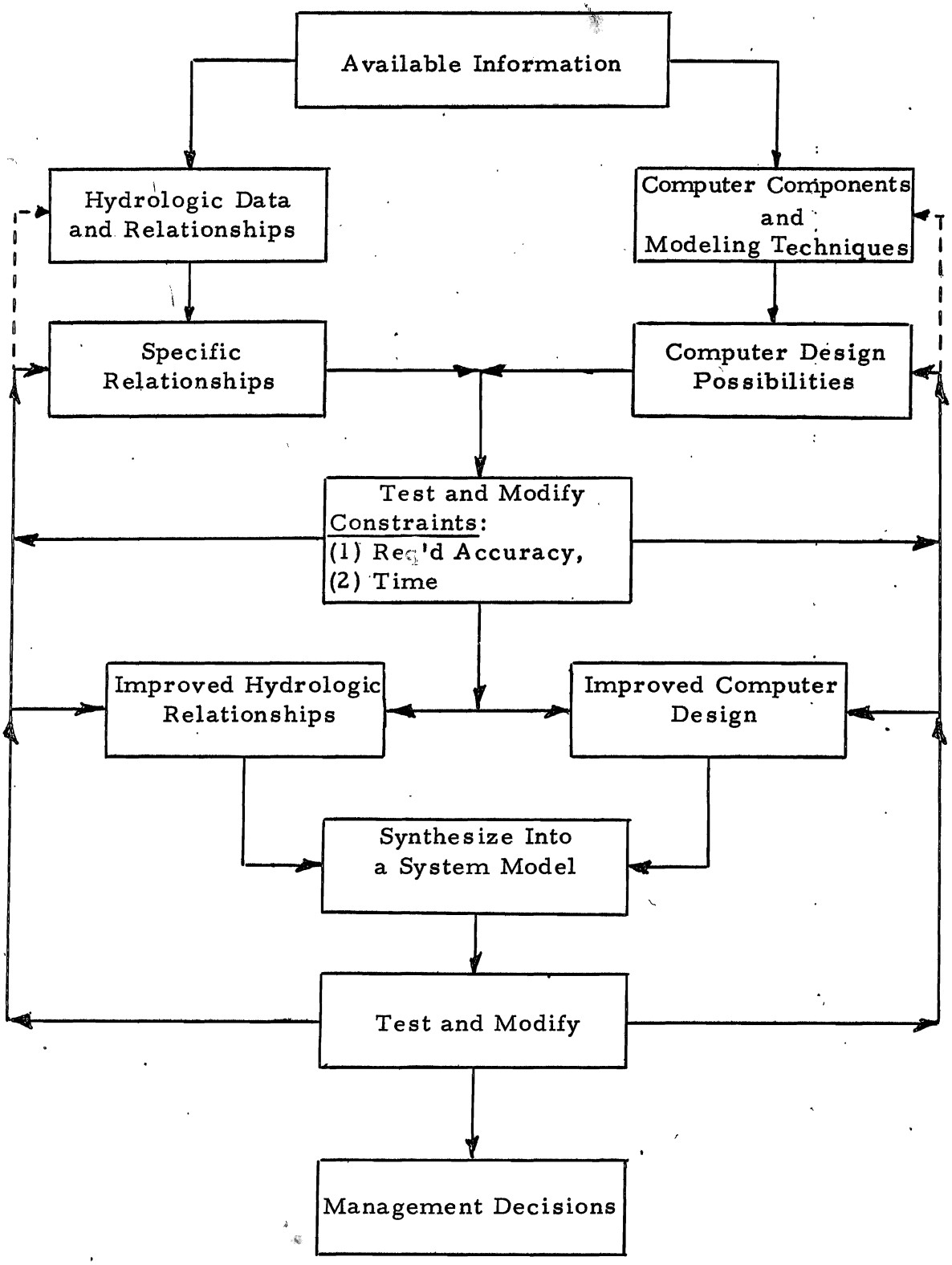

Figure 1.2. Development process of a hydrologic model.

parameters can be varied, and the effects of these changes can be observed at any point in the system.

A dynamic system consists of three basic components, namely the medium or media acted upon, a set of constraints, and an energy supply or driving forces. In a hydrologic system water in any one of its three physical states is the medium of interest. The constraints are applied by the physical nature of the hydrologic basin, and the driving forces are supplied by both direct solar energy and gravity and capillary potential fields. The various functions and operations of the different parts of the system are interrelated by the concepts of continuity of mass and momentum. Unless relatively high velocities are encountered, such as in channel flow, the effects of momentum are negligible, so that for many hydrologic models continuity of mass is the only link among the various processes within the system.

Continuity of mass for a specific control volume or continuum is expressed by the general equation:

$$\text{Input} = \text{Output} \pm \text{Change in Storage} \quad . \quad . \quad . \quad . \quad . \quad . \quad . \quad 1.1$$

A hydrologic balance is the application of this equation in order to achieve an accounting of physical hydrologic measurements within a particular unit. If the system is composed of many such units (the more units the more faithful the representation of the prototype) the application of appropriate translation or routing functions makes it possible to

describe the movement of water within a system in terms of its occurrence in space and time.

The concept of the hydrologic balance is pictured by the block diagram of figure 1.3. The inputs to the system are precipitation and surface and groundwater inflow, while the output quantity is divided among surface outflow, groundwater outflow, and evapotranspiration. As water passes through this system, storage changes occur on the land surface, in the soil moisture zone, in the groundwater zone, and in the stream channels. These changes occur rapidly in surface locations and more slowly in the subsurface zones.

The hydrologic balance can be applied over any length of time and to a unit or "block" of any size. The space unit might consist of an entire river basin, a particular subbasin, a particular zone, and even an infinitesimal volume. The sizes of both the space unit and the time increment utilized in any model depend upon the answers sought or the problems to be solved.

The ultimate in modeling would utilize continuous time and infinitesimal volumes connected as in the prototype. However, the practical limitations of this approach are obvious. The complexity of a model designed to represent a hydrologic system largely depends upon the magnitudes of the time and spatial increments utilized in the model. In particular, when large increments are applied, the scale magnitude is such that the effects of phenomena which change over relatively small

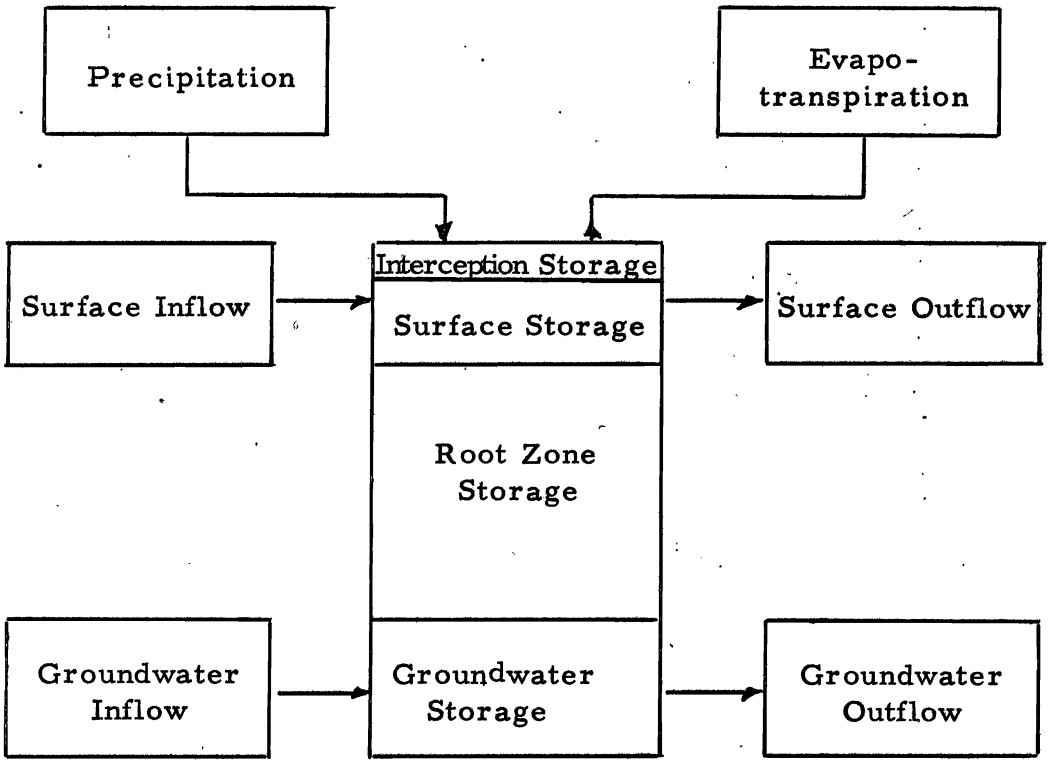

Figure 1.3. A simplified diagram of the hydrologic balance.

increments of space and time are insignificant. For instance, on a monthly time increment interception rates and changing snowpack temperatures are neglected. In addition, sometimes the time increment chosen coincides with the period of cyclic changes in certain hydrologic phenomena. In this event net changes in these phenomena during the time interval are usually negligible. For example, on an annual basis storage changes within a hydrologic system are often insignificant, whereas on a monthly basis the magnitudes of these changes are frequently appreciable and need to be considered. As time and spatial increments decrease, improved definition of the hydrologic processes is required. No longer can short-term transient effects or appreciable variations in space be neglected, and the mathematical model therefore becomes increasingly more complex, with an accompanying increase in the requirements of computer capacity and capability.

The approach to hydrologic simulation at Utah State University has been to first subdivide the river basin into relatively large but meaningful components, describe their operation and fundamental processes as functions of data ordinarily available, verify, and improve definition by using more and smaller control volumes and increments. Each succeeding model then becomes an improvement over its predecessor. While the improved model is capable of solving the same heirarchy of problems as its predecessor, it can be used to solve many additional problems which require more detailed definition.

This report describes the three hydrologic models which have been developed thus far under the simulation research program at Utah State University. Chapter II presents the flow system logic and mathematical relationships which were incorporated into the first model. This model has proved to be entirely satisfactory for the study of inter-basin effects and other hydrologic problems where somewhat gross simulation is sufficient. Since it has already undergone extensive verification and testing in actual operational studies, no verification of this model is included herein. The second model is described in Chapter III. In this model the time increment is still somewhat large (one month, for example), but several of the relationships have been sufficiently improved to justify a smaller space increment (or control volume) than was utilized in the first model. The areal extent of the space increments is selected on the basis that within each zone important characteristics, such as slope, soil type, vegetative cover, and meteorological factors, can be assumed to be reasonably constant. Chapter IV describes briefly a verification of the second model. Because of time limitations, it was necessary to perform this verification study before ongoing analog computer improvements had yet reached the stage where there was enough capacity available to enable the prototype basin to be simulated in smaller space increments than were utilized in the application of the first model to the same area. Thus, a quantitative comparison of the two models is not made in this report. In Chapter V the second model

is expanded so as to incorporate the capability of studying events which occur over small increments of both space and time, such as a single convective storm. A limited testing of this third model is described by Chapter VI. Finally, Chapter VII briefly summarizes the results of this study and reviews future prospects of simulation techniques involving electronic analog computers at Utah State University.

While comprehensive simulation models of hydrologic systems are a recent development, they are, of necessity, broad in scope and thus very dependent upon previous work in hydrology. The works of many authors have influenced the models described by this report, and it is hoped that adequate credit has been given in all cases.

CHAPTER II

HYDROLOGIC MODEL BASED ON LARGE INCREMENTS OF TIME AND SPACE

The design of the first hydrologic model developed at Utah State University was relatively simple. A primary objective was to demonstrate the validity of the analog computer approach to modeling in terms of the basic physical processes which occur in any hydrologic system, and which are not specific to any particular geography. Experimental and analytical results were used wherever possible to assist in establishing the mathematical relationships. The mountainous or watershed area was considered as a single unit or zone, and average values of needed hydrologic quantities, such as soil type and vegetative cover, were established for this area. The hydrologic flow chart developed for this portion of the model is shown by figure 2.1. Each parameter and process depicted by this figure is discussed in the sections which follow.

Precipitation

Average area precipitation. Where sufficient data are available, standard techniques, such as the Thiessen weighting or the isohyetal, are employed to compute average precipitation values for a given area as a function of time. However, for cases where records are available for only the valley floor, isohyetal charts showing average precipitation

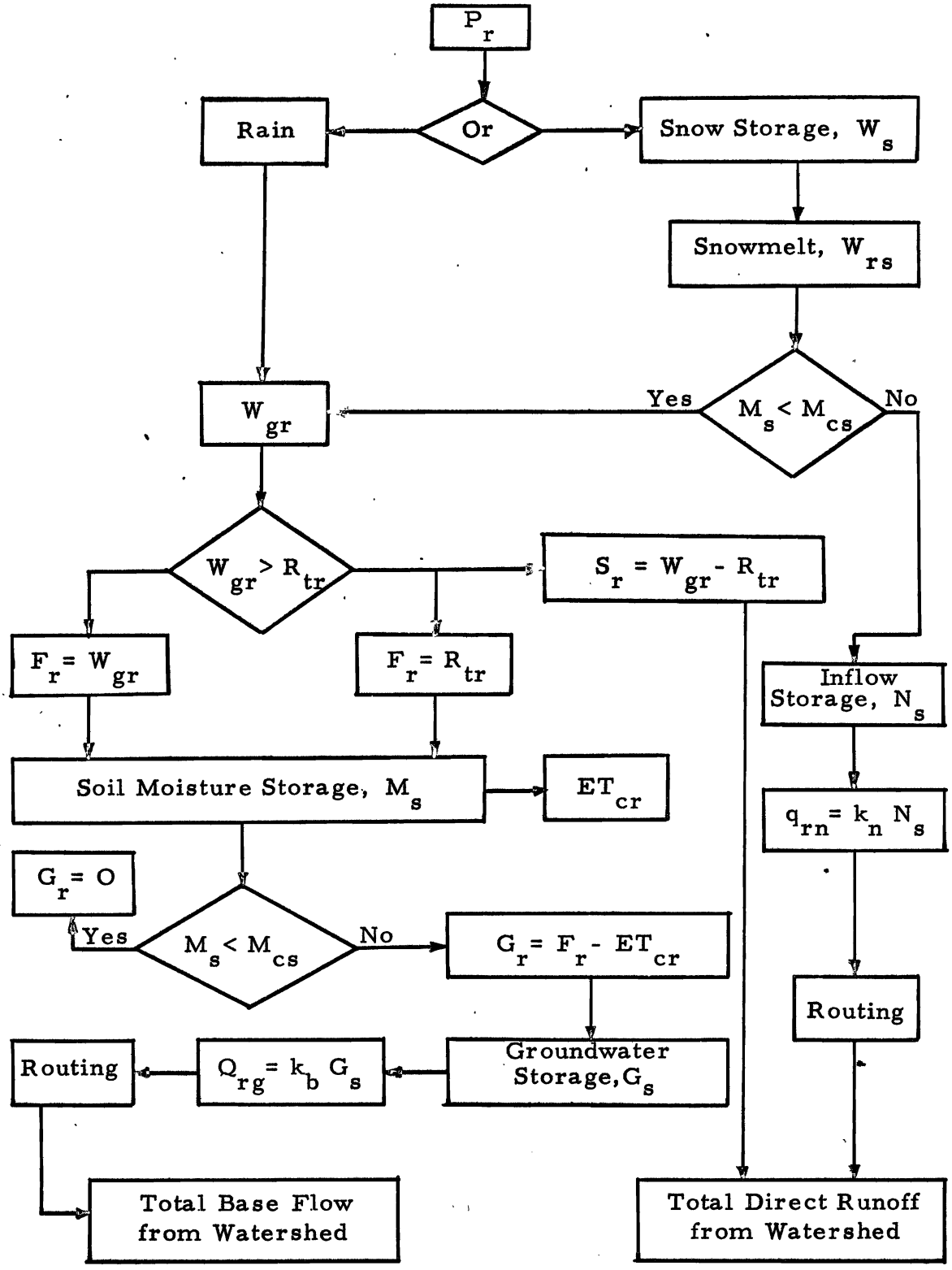

Figure 2.1. Flow diagram for a hydrologic model using large increments of space and time.

values are employed to establish lapse rates between the valley stations and the watershed areas. For Utah, isohyetal charts covering the state have been prepared (54). These indicate lines of equal average precipitation for the two periods, May to September and October to April. Lapse rates can, therefore, be determined for these two periods. Table 2.1 illustrates the application of this procedure for a particular watershed within the Sevier River basin of Utah.

Table 2.1. Precipitation lapse constants, Circleville, Utah

Period	Average watershed precipitation (From isohyetal charts)	Average valley precipitation (From records)	Lapse constant
May to September	5.4	3.2	1.7
October to April	10.3	4.3	2.4

Thus, the multiplication of a particular monthly precipitation quantity recorded at Circleville would yield an estimate of the average precipitation on the adjacent watershed for this same month.

Forms of precipitation. Only two forms of precipitation, rain and snow, are considered in this study, with a temperature criterion being applied to establish the occurrence of these two forms. Temperature is not an ideal index of the form of precipitation since there is no single temperature above which it always rains and below which it

always snows. Unless a better indication as to form of precipitation is present, surface air temperature seems to be the best available index. A chart indicating the probability of the occurrence of snow at various air temperatures is shown by figure 2.2 (49). On the basis of this figure, at a temperature of 35 F there is a 50 percent chance that precipitation will be in the form of snow. When the average temperature elevation lapse rate and the average falling rate of a snowflake are considered, this temperature seems to be a reasonable criterion, and precipitation at surface air temperatures less than this value is considered to be in the form of snow.

Temperature. This variable is introduced into the model not only as a criterion for establishing the form of precipitation, but also as an index of available energy for the snowmelt and evapotranspiration processes. Average temperature values for the area being modeled are required. Integration techniques are necessary in order to utilize point measurements for the estimation of effective or average temperature for an area. For those cases where watershed temperature records are available, this integration is accomplished by preparing area charts showing isothermal lines for particular periods of time. Average zone temperatures are then computed from these charts and a relationship is thus established between these and temperatures at one or more selected index stations. In some cases it is necessary to develop different relationships for different periods of the year.

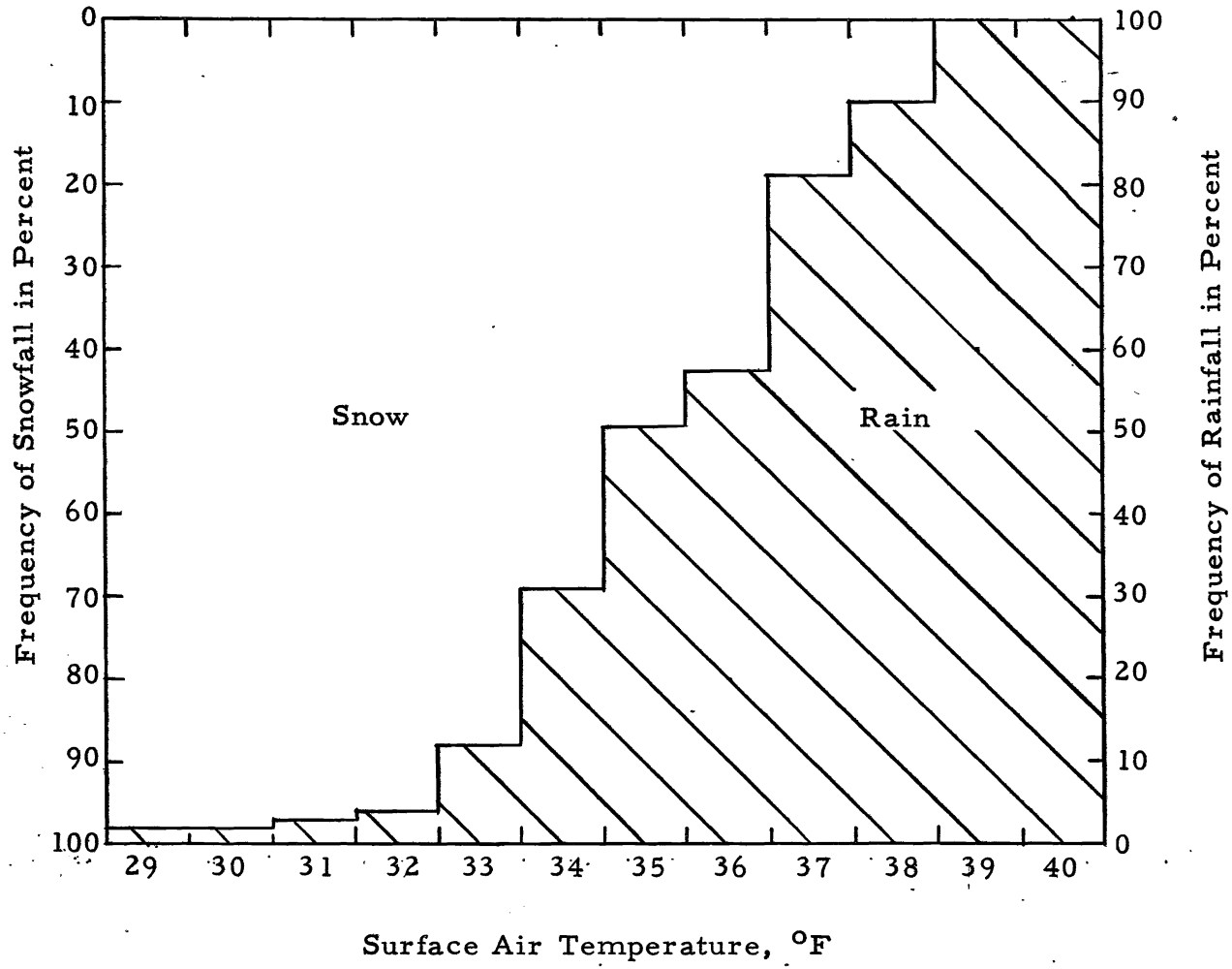

Figure 2.2. Frequency distribution showing rain and snow forms of precipitation.

For watersheds where temperature data are lacking, records from an index station on the valley floor are "lapsed" to the mean elevation of the watershed in accordance with the theoretical atmospheric adiabatic lapse rate of approximately -3.5 F per 1,000 feet elevation increase.

Snowmelt

Both the complex nature of snowmelt and data limitations prevent a strictly analytical approach to this process. In particular, for the computation of melt on the basis of large time increments, such as a month, a rather empirical approach seemed most suitable. Accordingly, a relationship was proposed which states that the rate of melt is proportional to the available energy and the quantity of precipitation stored as snow. Expressed as a differential equation the relationship appears:

$$\frac{d[W_s(t)]}{dt} = -k_s (T_a - 35) W_s(t) \quad . \quad . \quad . \quad . \quad . \quad . \quad . \quad 2.1$$

in which k_s represents a proportionality constant.

From an analysis of snow course data from various parts of Utah, the value of k_s was determined to be approximately 0.10. The independent variables on the right side of equation 2.1 can be expressed either as continuous functions of time or as step functions consisting of mean constant values applicable throughout a particular time increment. In this model a time increment is being utilized with the integration being performed in steps over each successive period. Thus, the final

value of $W_s(t)$ at the end of the period becomes the initial value for the integration process over the following period. On this basis the integral form of equation 2.1 is:

$$\int_{W_s(0)}^{W_s(1)} \frac{dW_s}{W_s} = -0.10\,(T_a - 35) \int_0^1 dt \quad . \quad . \quad . \quad . \quad . \quad 2.2$$

or

$$W_s(1) = W_s(0) \exp\,[\,-0.10\,(T_a - 35)] \quad . \quad . \quad . \quad . \quad . \quad . \quad 2.3$$

Surface runoff

This quantity is provided for by establishing for each watershed zone a limiting rate of surface runoff for any particular period of time. If this value is exceeded by snowmelt, rainfall, or irrigation, or by any combination of these, the surplus becomes surface runoff. Surface runoff records enable the value of the limiting rate to be estimated for each particular watershed or zone during verification of the model. In equation form the rate of surface runoff during a particular period of time, n, is given by:

$$S_r = W_{gr} - R_{tr} \quad , \quad (S_r \geq 0) \quad . \quad . \quad . \quad . \quad . \quad . \quad . \quad . \quad 2.4$$

in which the term R_{tr} represents the limiting or threshold rate of surface supply at which surface runoff begins to occur. For example, if the total water supply available at the ground surface for a given

month exceeds the threshold rate, R_{tr}, surface runoff is assumed to occur during the month.

The values of the threshold surface runoff rate, R_{tr}, are dependent upon variables, such as soil surface conditions, soil moisture, and storm characteristics, which in terms of a long time increment of, for example one month, are very probabilistic in nature. This situation could be accounted for in the model by assuming a normal distribution pattern and generating probability functions about the average values of R_{tr} determined for each particular time period. However, in a sparse data situation and where computing equipment is limited, the deterministic approach or use only of average values of R_{tr} generally should yield satisfactory results.

In this model the term W_{gr} in equation 2.4 includes all water which is available at the soil surface except that portion of the snowmelt which leaves the watershed as "quick seepage" or interflow. As indicated by figure 2.1, interflow is assumed to occur during only the snowmelt periods and when the soil moisture storage is at its capacity level. A soil moisture deficit usually exists at the beginning of the snowmelt period, and under these conditions all available surface waters, including snowmelt, are represented by the term W_{gr}.

Depression storage

Water retained in puddles, ditches, and other depressions in the soil surface is termed depression storage. Outflow from this form of

storage occurs either as direct evaporation or infiltration into the soil where the moisture is subject to use by the plants. In this model where large increments of time are involved, water retained temporarily in depression storage is assumed to be a part of the evapotranspiration loss from the area and thus is not considered as a separate entity.

Available soil moisture storage

The two soil moisture equilibrium points which are of greatest interest to the hydrologist are field capacity and wilting point. The field capacity is the moisture content of soil after gravity drainage is essentially complete, while the wilting point represents the soil moisture content at the time that plants can no longer extract sufficient water from the soil to meet their requirements and permanent wilting occurs. The difference between these two points is termed the available moisture, and it represents the useful storage capacity of the soil or the maximum water available to plants.

Under usual circumstances additions to available soil moisture storage result from infiltration, while abstractive quantities are evapotranspiration losses, deep percolation, and interflow. At this point, several simplifying assumptions were applied in the development of this first model.

1. Evapotranspiration losses occur at the potential or maximum rate under existing conditions as long as any moisture is present in the plant root zone.

2. Deep percolation occurs only when the soil moisture within the plant root zone is at the capacity level.
3. Interflow is the rate at which snowmelt water is available after meeting the demands of any soil moisture deficit.

Under these assumptions the separation of interflow and deep percolation is easily achieved in that neither of these two quantities influences the amount of water in root zone storage.

Available soil moisture as a function of time is, therefore, given by the expression:

$$M_s(t) = \int (F_r - ET_{cr})dt \, , \, (M_s < M_{cs}) \quad . \quad . \quad . \quad . \quad . \quad 2.5$$

Infiltration

Infiltration is the passage of water through the soil surface into the soil. In this model all water which is included within the term W_{gr}, except surface runoff, is assumed to enter the soil, and the rates of infiltration over a particular period of time are therefore given by:

$$F_r = W_{gr} \, , \, (W_{gr} < R_{tr}) \quad . \quad . \quad . \quad . \quad . \quad . \quad . \quad . \quad . \quad . \quad 2.6$$

$$F_r = R_{tr} \, , \, (W_{gr} \geq R_{tr}) \quad . \quad . \quad . \quad . \quad . \quad . \quad . \quad . \quad . \quad . \quad 2.7$$

Evapotranspiration

This process is often defined briefly as the sum of the water

transpired by growing plants and that which evaporates from the soil, snow, and interceptive surfaces. Potential evapotranspiration is that which occurs under conditions of complete crop cover by actively growing plants, and where moisture supplies are not limiting.

A large number of formulas have been developed for estimating evapotranspiration, and many of these were investigated with regard to their application to this study. The rate of evapotranspiration depends on several factors, such as crop, climate, soil moisture supply, salinity, and vegetative cover. Climatic conditions usually considered are solar radiation, precipitation, temperature, daylight hours, humidity, wind velocity, and length of growing season. The quantity of water transpired by plants is also thought to depend upon the availability of moisture within the root zone, the stage of plant development, the foliage cover, and the nature of the leaf surfaces. Many of these various factors are interrelated, and their individual effects on evapotranspiration are difficult to determine.

The methods which have been developed for estimating evapotranspiration can be grouped into three general categories, depending upon the approach employed in their development, namely, vapor transfer, energy balance, and empirical.

A vapor transfer process assumes that the moisture flow through a layer of air near the ground or water surface can be measured. It requires simultaneous measurement of wind velocity, temperature, and

vapor pressure at different heights above the surface. Of the equations reviewed only that proposed by Papadakis (32) can be considered to fall into this category. Working in Argentina he developed the following relationship:

$$E_n = 0.5625 (e_{ma} - e_d) \quad . \quad . \quad . \quad . \quad . \quad . \quad . \quad . \quad . \quad . \quad 2.8$$

in which

E_n = monthly potential evapotranspiration in centimeters

e_{ma} = saturation vapor pressure corresponding to the average daily maximum temperature of the month, in millibars

e_d = vapor pressure that corresponds to dewpoint, in millibars

Under the energy balance technique an attempt is made to establish relationships for the flow of energy which produces evapotranspiration. The assumption is made that the energy received by a surface through radiation must equal 1) the energy used for evaporation, 2) heating the air, 3) heating the soil, and 4) any extraneous or advective energy. It is usually felt that for short periods, such as daily and monthly balances, items 3 and 4 can be neglected without seriously affecting the accuracy of the results. In general, an equation developed under this approach requires parameters which are often not measured at the accuracy of the results. In general, an equation developed under this approach requires parameters which are often not measured at meteorological stations; in addition, calculations tend to be somewhat complicated.

Penman's formula (34), which includes a large number of parameters, is perhaps the best known of these rational relationships.

For many areas his formula yields satisfactory estimates of evapotranspiration, but because the equation does not provide for the advective transfer of energy, results are inclined to be low for regions of high temperatures and low humidity.

The formulas which fall into the category of empirical relationships make up by far the largest group of those which have been proposed to estimate evapotranspiration. The equations were developed from primarily empirical relationships between experimental data and various climatic and water supply measurements. For illustrative purposes the most common equations from among the many reviewed are included in this discussion.

The Lowry-Johnson formula (28) expresses evapotranspiration losses in terms of an effective heat factor.

$$U = 0.8 + 0.156\ F \quad . \ . \ . \ . \ . \ . \ . \ . \ . \ . \ . \quad 2.9$$

in which

U = the "valley" consumptive use or evapotranspiration in acre-feet per acre for the period under consideration

F = "effective heat" for the period in thousands of day degrees. Effective heat is defined as the accumulation, in day degrees, of maximum daily growing season temperatures above 32 F.

This relationship was developed for the purposes of estimating valley consumptive use on an annual basis. However, Criddle (9)

adapted the Lowry-Johnson technique to estimate monthly consumptive use by using the proportion of monthly heat units to annual heat units. Thus, monthly values of consumptive use are given by:

$$u = \left(\frac{f}{F}\right) U \quad . \quad . \quad . \quad . \quad . \quad . \quad . \quad . \quad . \quad . \quad . \quad . \quad . \quad 2.10$$

in which f is the effective heat in thousands of day degrees (above 32 F) for the month.

Thornthwaite (47) developed the following expression:

$$PET_n = 1.6\, L_n \frac{10T_n^{\,a}}{I} \quad , \quad \text{for } T > -1\ C \quad . \quad . \quad . \quad . \quad 2.11$$

in which

PET_n = potential evapotranspiration in inches during the month, n

L_n = mean possible duration of sunlight in the month, n, expressed in units of 30 days of 12 hours each

I = heat index

$$= \sum_{n=1}^{12} i_n \quad , \quad i_n = \left(\frac{T_n}{5}\right)^{1.514} \quad . \quad . \quad . \quad . \quad 2.12$$

$$a = 6.75 \times 10^{-7} I^3 - 7.71 \times 10^{-5} I^2 + 1.792 \times 10^{-2} I + 0.49239$$

T_n = mean monthly temperature in degrees C. $PET_n = 0$ for $T_n \leq -1\ C$

The Blaney-Criddle formula (4) was proposed as follows:

$$U = KF \quad . \quad . \quad . \quad . \quad . \quad . \quad . \quad . \quad . \quad . \quad . \quad . \quad . \quad 2.13$$

in which

U = seasonal crop consumptive use in inches

K = a seasonal coefficient which varies with type of crop and location

F = sum of the monthly consumptive use factors, f, for the growing season

$$f = \frac{tp}{100} \quad . \quad . \quad . \quad . \quad . \quad . \quad . \quad . \quad . \quad . \quad . \quad . \quad . \quad . \quad 2.14$$

in which t is mean monthly temperature in degrees F, and p is monthly percentage of daylight hours of the year.

Phelan and other personnel of the Soil Conservation Service (35, 36) developed a modification of the Blaney-Criddle formula whereby the monthly coefficient, k, is divided into two parts, k_c and k_t. k_t is a function of temperature and is expressed as

$$k_t = (0.0173\ t - 0.314) \quad . \quad . \quad . \quad . \quad . \quad . \quad . \quad . \quad . \quad . \quad 2.15$$

in which t is mean monthly temperature in degrees F. It is considered that k_c is a function mainly of the physiology and stage of growth of the crop, but it is recognized that it no doubt still contains some climatological influences.

This modification has accomplished the following:

1. enabled the application of the formula over a wide area for known values of k_c,
2. largely explained the variation in k for a given month from year to

year, and

3. enabled the establishment of the beginning of the growing season on the basis of mean monthly air temperatures. The growing season for most annual crops is ended before the first 32 F frost in the fall.

Because of its simplicity and wide acceptance, and because through it evapotranspiration losses for individual crops can be estimated, the Blaney-Criddle formula as modified by Phelan and others was selected for this study. The equation is expressed as follows:

$$ET_{cr} = k_c k_t \frac{T_a p}{100} \quad . \quad . \quad . \quad . \quad . \quad . \quad . \quad . \quad . \quad . \quad . \quad 2.16$$

It is again emphasized that the independent variables on the right side of the above relationship can be expressed either as continuous functions or as step functions consisting of constant mean values for a particular time increment. The estimated potential evapotranspiration rate function is established accordingly. For example, if mean monthly values of the independent parameters are used, the relationship yields an estimate of the mean potential evapotranspiration rate during each month.

Plots indicating k_c values as a function of time have been prepared for a number of different agricultural plant varieties. Typical examples are those for alfalfa and spring grain shown by figures 2.3 and 2.4, respectively. In addition, preliminary k_c curves for various

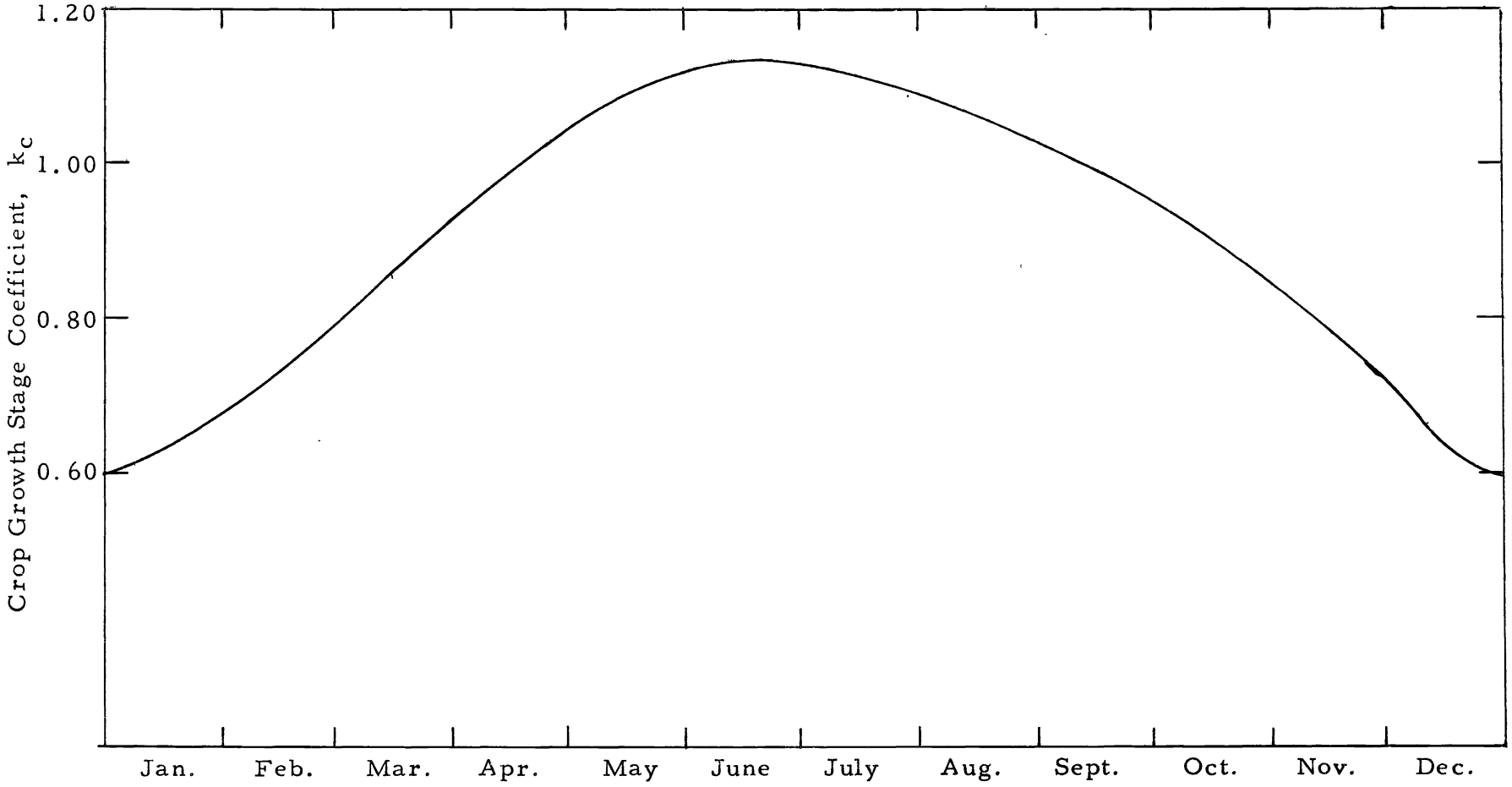

Figure 2.3. Crop growth stage coefficient curve for alfalfa.

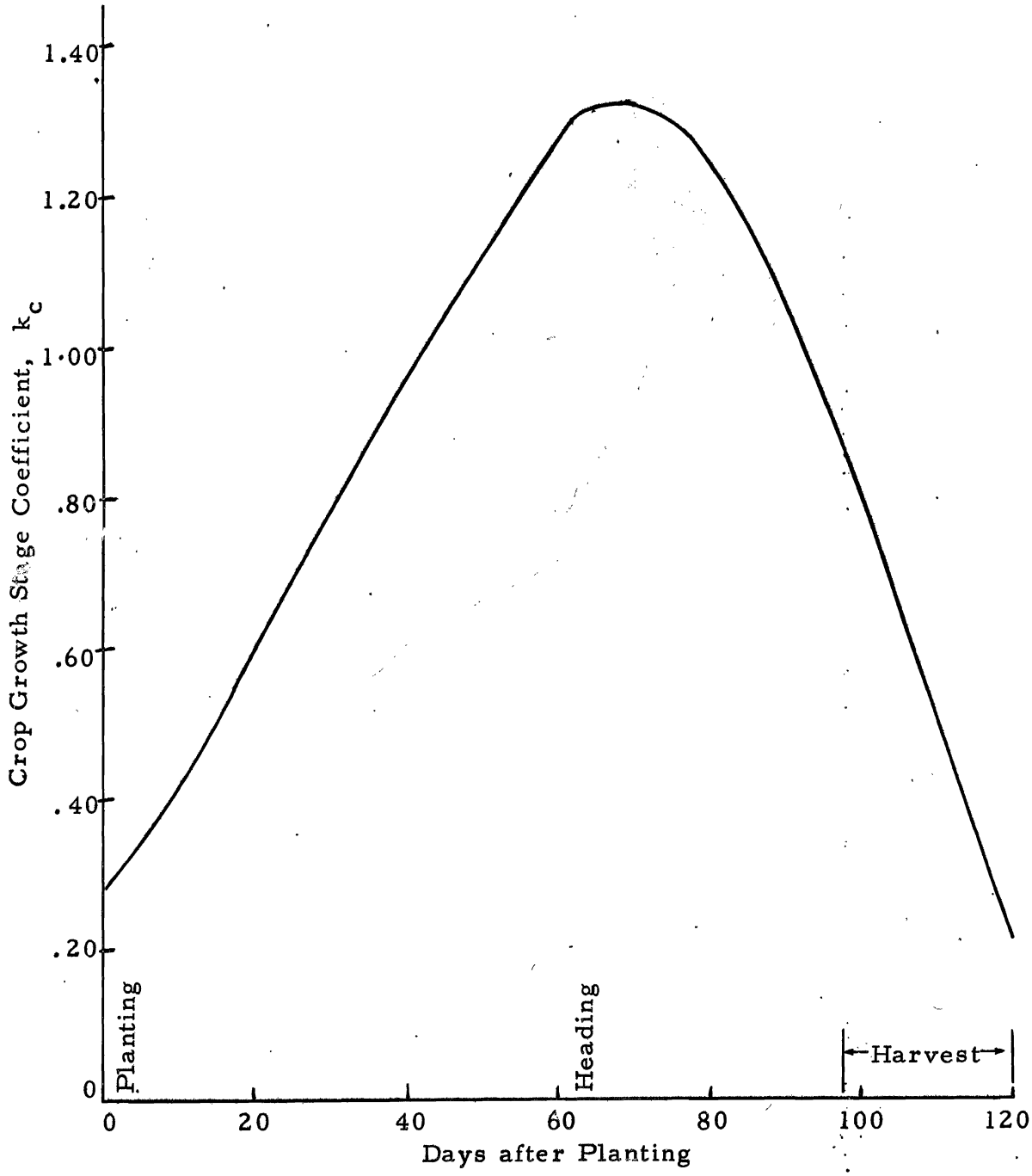

Figure 2.4. Crop growth stage coefficient curve for spring grain.

species of phreatophytic and other forms of native vegetation have been developed from the limited water-use information which is available for these plants (42, 48, 52, 63). The k_c curve for grass pasture shown by figure 2.5 seems applicable to many species of native vegetation. As indicated by figure 2.4, in the case of perennial crops the available curves included only the growing season. Since for any given area evapotranspiration continues throughout the entire year, the k_c curves for all annual varieties have been extended to include the full year (43, 58). During the noncropping season evapotranspiration from bare ground and snow surfaces is estimated.

Deep percolation

Deep percolation is defined as the movement of water through the soil from the plant root zone to the underlying groundwater storage basin. This movement occurs under the influence of both gravity and capillary potential fields. For saturated flow gravity is the dominant force, while in the case of unsaturated flow the capillary field becomes the important potential. Thus, deep percolation exists even though the moisture content of a soil is below field capacity (38, 59). However, as already stated, in this model deep percolation is assumed to occur only at times when the available soil moisture is at its capacity level. Thus:

$$G_r = W_{gr} - ET_{cr} \quad , \quad [M_s(t) = M_{cs}] \quad . \quad . \quad . \quad . \quad . \quad 2.17$$

$$G_r = 0 \quad , \quad [M_s(t) < M_{cs}] \quad . \quad . \quad . \quad . \quad . \quad 2.18$$

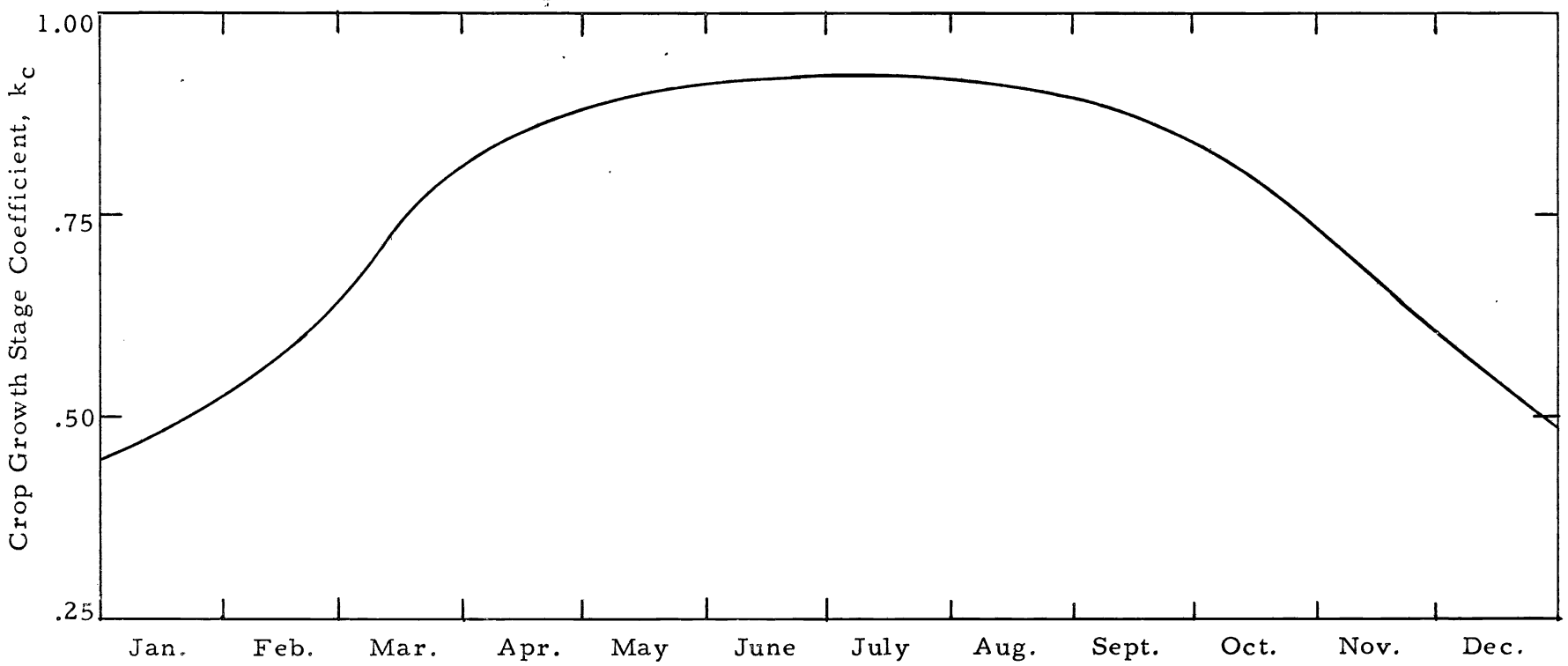

Figure 2.5. Crop growth stage coefficient curve for grass - pasture.

Interflow

Interflow is defined as that portion of the soil seepage water which does not enter the groundwater basin but rather which moves largely in a lateral direction through the upper and more porous portion of the soil profile until it enters a stream channel. It has already been indicated that in this model interflow is assumed to consist of that portion of the snowmelt water not required to satisfy any available soil moisture storage deficit. Interflow is therefore given by the expressions:

$$N_r = 0 \quad , \quad (M_s < M_{cs}) \quad . \quad . \quad . \quad . \quad . \quad . \quad . \quad . \quad 2.19$$

$$N_r = W_{rs} \quad , \quad (M_s = M_{cs}) \quad . \quad . \quad . \quad . \quad . \quad . \quad . \quad . \quad 2.20$$

Routing or translation

The movement of water from one point to another within a hydrologic system is a very complicated process. Some of the characteristics of an area which influence this process are soil porosity, soil depth, surface drainage density, shape, and slope of the watershed or zone. The problem can be simplified, however, by applying a general routing relationship which is based on the premise that the rate of discharge from a storage basin is proportional to the quantity of water in storage (26), namely,

$$q = \frac{d\,s\,(t)}{dt} = - ks(t) \quad . \quad . \quad . \quad . \quad . \quad . \quad . \quad . \quad . \quad . \quad 2.21$$

in which

q = the discharge rate from the basin

s(t) = the storage within the basin at any time, t

k = a constant depending upon the basin characteristics. The value of k is frequently established by model verification studies.

Equation 2.21 is applied to the groundwater basin of the watershed in order to estimate base flow. This same equation with a different value of k is also applied to obtain an estimate of the time distribution of the interflow runoff for each watershed zone. Because interflow moves at relatively shallow depths, it does not usually travel far before emerging in an established surface channel where it combines with surface runoff. In this model where large time increments are involved surface flow is not delayed in any form of storage unless, of course, a surface reservoir exists on the watershed. Thus, in general, this flow appears in the outflow hydrograph as it occurs on the watershed so that the following expression applies:

$$q_{rs} = S_r \quad . \quad . \quad . \quad . \quad . \quad . \quad . \quad . \quad . \quad . \quad . \quad . \quad . \quad . \quad 2.22$$

The following relationships apply where designated:

Base flow.

$$\left[\sum_{i=1}^{m} G_r\right] dt - Q_{rg}\, dt = d\, G_s\,(t) \quad . \quad . \quad . \quad . \quad . \quad . \quad . \quad . \quad 2.23$$

$$Q_{rg} = k_b G_s(t) \quad . \quad . \quad . \quad . \quad . \quad . \quad . \quad . \quad . \quad . \quad . \quad . \quad 2.24$$

in which m is the number of zones into which the watershed is divided, Q_{rg} is the base flow rate from the watershed, and k_b is a constant determined by verification studies.

From equations 2.23 and 2.24

$$G_s(t) = \int_0^t \left[\sum_{i=1}^{m} G_r(i) - Q_{rg} \right] dt$$

$$= \int_0^t \sum_{i=1}^{m} [G_r(i) - k_b G_s(t)] \, dt \quad . \quad . \quad . \quad . \quad . \quad . \quad 2.25$$

Interflow.

$$N_r \, dt - q_{rn} \, dt = d N_s(t) \quad . \quad . \quad . \quad . \quad . \quad . \quad . \quad . \quad . \quad . \quad 2.26$$

$$q_{rn} = k_n N_s(t) \quad . \quad . \quad . \quad . \quad . \quad . \quad . \quad . \quad . \quad . \quad . \quad 2.27$$

in which

$$N_s(t) = \int_0^t (N_r - q_{rn}) \, dt \quad . \quad . \quad . \quad . \quad . \quad . \quad . \quad . \quad . \quad 2.28$$

q_{rn} in these equations represents the interflow rate from a particular watershed zone.

Total outflow

Total outflow from the watershed is given by summing surface

runoff, interflow, and base flow, thus:

$$Q_{rt} = \sum_{i=1}^{m} [\, q_{rs}(i) + q_{rn}(i)] \quad + Q_{rg} \quad . \quad . \quad . \quad . \quad . \quad . \quad . \quad 2.29$$

in which the quantity $\sum_{i=1}^{m} [\, q_{rs}(i) + q_{rn}(i)]$ is designated the direct runoff.

Long transport delay times, such as the average time required for the groundwater or base flow, Q_{rg}, to move off the watershed, are simulated in the model by means of active delay networks. The required delay setting of these networks is established during the model verification studies.

CHAPTER III

HYDROLOGIC MODEL BASED ON LARGE INCREMENTS OF TIME AND SMALL INCREMENTS OF SPACE

The model discussed in this chapter was developed under the second phase of the hydrologic simulation study at Utah State University. In this model the large time increment (monthly) was retained, but capability was provided for considering the simulated area as a series of small and relatively homogeneous zones. This requirement imposed a need for increased space definition by the model, and several relationships were modified to meet this need. For example, radiant energy is applied as a parameter to account for the effect of slope on the snowmelt and evapotranspiration processes. Also, some processes were added, such as interception, which were ommitted from the first model. A diagram showing the flow system logic adopted for the second model is shown by figure 3. 1. The increased complexity of this model is seen by comparing the flow diagram of figure 3. 1 with that of figure 2. 1.

Precipitation

Average area precipitation. As in the first model, precipitation is integrated in terms of space and time by standard techniques. Where required by lack of watershed data, precipitation lapse rates are

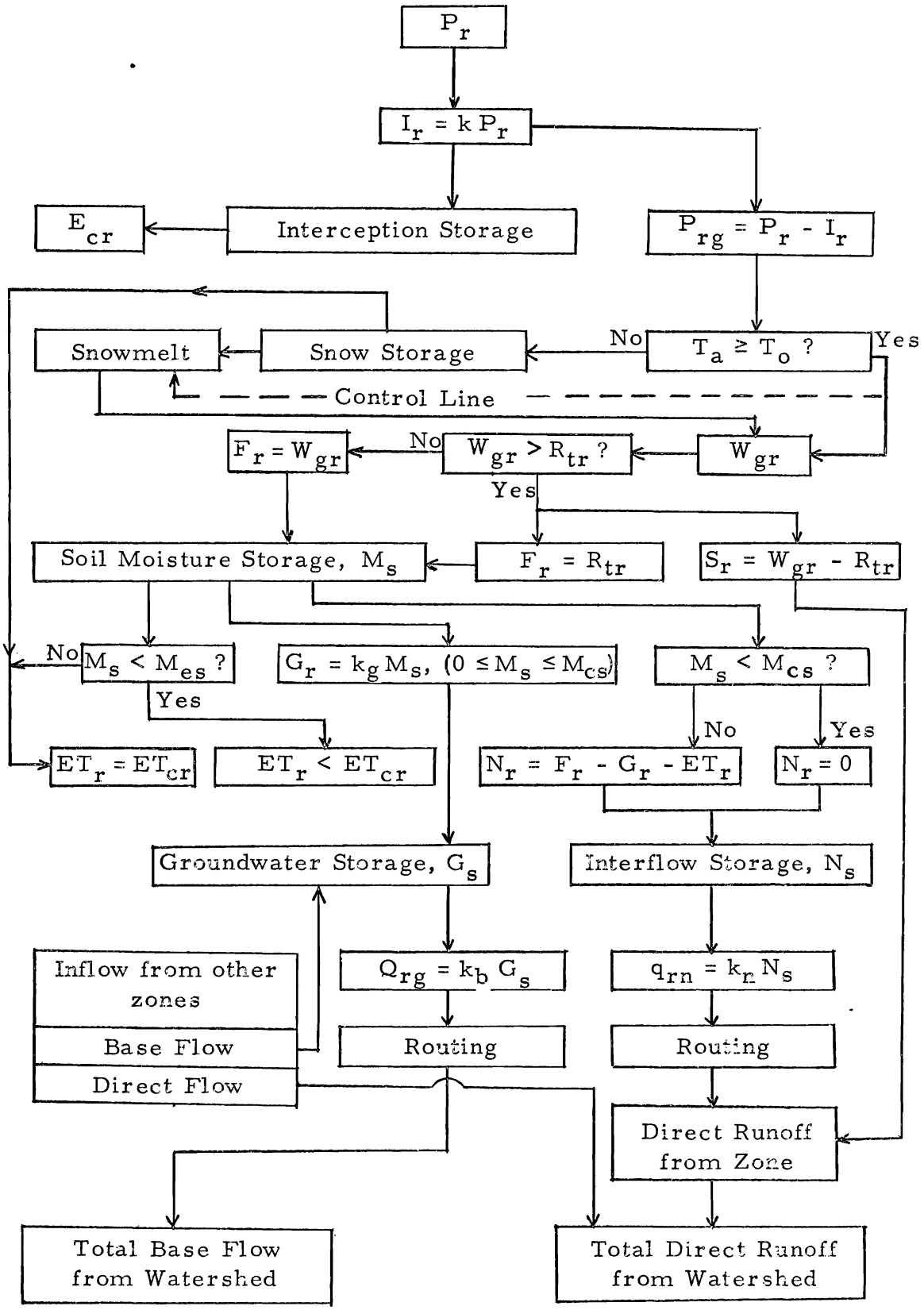

Figure 3.1. Flow diagram for a typical hydrologic model using large time increments.

developed between valley stations and each watershed zone. Thus:

$$P_{iz} = k_{jz} P_{iv} \quad . \quad . \quad . \quad . \quad . \quad . \quad . \quad . \quad . \quad . \quad . \quad . \quad . \quad 3.1$$

in which

P_{iz} = the estimated precipitation in inches of water for zone z and for a particular month, i

P_{iv} = the measured precipitation on the valley floor for the same month

k_{jz} = the lapse rate constant applicable to zone z during a particular period, j

The length of the period j depends upon available information. Obviously, estimates are considerably improved if sufficient information is available to permit the development of lapse rates on at least a monthly basis.

Forms of precipitation. The form of precipitation is established by the same temperature criterion as is applied in the first model (see figure 2.2).

Temperature. Where temperature data are available, the integration techniques discussed in Chapter II are applied. However, for watersheds where these data are not available it is necessary to lapse the temperature to the mean elevation of each zone. The theoretical adiabatic lapse rate applied in the first model of about -3.5 F per 1,000 feet elevation increase varies considerably with both time and location.

In the second model this variation was taken into account by developing monthly lapse rates for a particular location from radiosonde data (53) applied in conjunction with valley temperature records. Figure 3.2 illustrates computed average monthly temperature lapse rates between elevations 6,000 and 10,000 feet for the vicinity of Circleville, Utah. The average annual lapse rate for the 14-year period investigated (1950-1963) was -3.8 F per 1,000 feet.

Interception loss

Interception was not included in the development of the first model. Much of the precipitation falling during the early stages of a storm is stored on the vegetative cover and returned to the atmosphere by evaporation. Evaporation losses from the falling precipitation itself are not considered because these losses are assumed to be uniform over the particular area or zone and, of course, are not measured as an input quantity to the system. The magnitude of the interception loss is dependent largely upon the type and density of forest canopy and the relative extent of the forested land within the area. Interception losses during a large time period of say one month are commonly expressed as a fraction of the precipitation during this same period (49). Thus:

$$I_r = k_i C_d F_d P_r \quad . \quad . \quad . \quad . \quad . \quad . \quad . \quad . \quad . \quad . \quad . \quad . \quad 3.2$$

in which the undefined terms are:

k_i = a constant

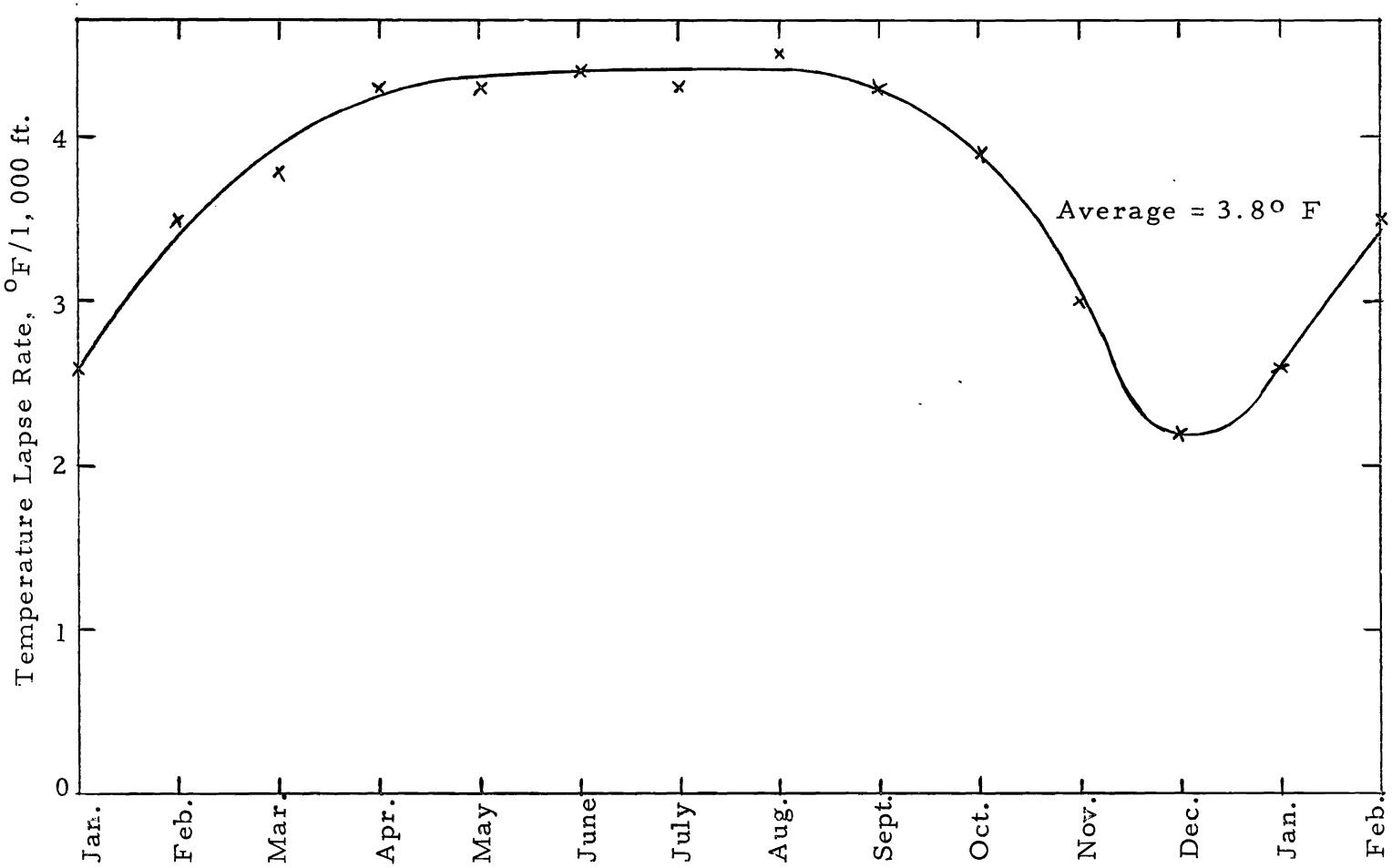

Figure 3.2. Average temperature lapse rate with elevation as a function of time at Circle Valley, Utah.

C_d = canopy density. In the case of deciduous vegetation this value will vary with the season of the year.

F_d = forest cover density within the watershed zone under consideration

Limited studies (19, 49) indicate that the most probable average value of k_i is 0.4 for both rain and snow falling on coniferous trees. This same value is also applicable to deciduous trees during the summer months, but during the winter months interception losses by deciduous vegetation are insignificant. The forest cover density, F_d, is given by:

$$F_d = \frac{A_c}{A_z} \quad . \quad . \quad . \quad . \quad . \quad . \quad . \quad . \quad . \quad . \quad . \quad . \quad . \quad 3.3$$

in which

A_c = area of the watershed zone covered by forest vegetation

A_z = total area of the zone

Thus, for an area containing n types of vegetation

$$I_r = \frac{k_i}{A_z} [a_1 C_d(1) + a_2 C_d(2) + \ldots + a_i C_d(n)] P_r \quad . \quad . \quad 3.4$$

where

$$n$$

where

$$A_c C_d = \sum_{i=1}^{n} a_i C_{di} \quad . \quad . \quad . \quad . \quad . \quad . \quad . \quad . \quad . \quad . \quad . \quad 3.5$$

It follows, therefore, that

$$I_r = k_i C_v P_r \quad . \quad . \quad . \quad . \quad . \quad . \quad . \quad . \quad . \quad . \quad . \quad . \quad 3.6$$

The value of C_v is computed for each zone and represents an input value to the computer. C_d is assumed to equal zero for grasses.

The rate at which precipitation reaches the ground, P_{rg}, is obtained by subtracting interception losses from the precipitation rate. Thus, from equation 3.6:

$$P_{rg} = P_r - k_i C_v P_r$$

$$= P_r (1 - k_i C_v) \quad , \quad (k_i C_v < 1) \quad . \quad . \quad . \quad . \quad . \quad 3.7$$

Snowmelt

In the snowmelt relationship presented in Chapter II (equation 2.1) surface air temperature is applied as an index of available energy for the melting process. On a regional basis, air temperature is a reasonably good index of available energy at particular elevations. However, even if adequate data were available, air temperature does not provide a satisfactory means of comparing the energy flux among the different facets of a landscape. For a particular elevation equation 2.1 would indicate no appreciable differences between melting rates on, for example, easterly and southerly slopes. When large units or areas are considered by a model, the effects of slope differences often tend to average. However, for small zones, slope effects are important and should be considered by a snowmelt relationship.

The potential insolation parameter has been proposed as a means of comparing the energy flux among the different facets of a landscape

(12, 25, 44, 45). In the concept of potential insolation the earth's atmosphere is ignored. Thus, irradiation of a surface by direct sunshine is considered to be only a function of the angle between the surface and the sun's rays. This angle, in turn, is a function only of the geometric relationships between the surface and the sun as expressed by latitude, degree of slope and aspect of the surface, and the declination and hour angle of the sun. For a given site the only variation in instantaneous potential insolation will be perfectly cyclical with time, depending upon the changes in hour angle and declination. Thus, the use of potential insolation as a parameter of a surface is sufficiently simple to make feasible its wide application.

Frequently, potential insolation for a particular surface is expressed as a percentage of the maximum possible radiation rate at the outer limit of the earth's atmosphere. The resulting dimensionless quantity is termed radiation index. Figure 3.3 illustrates a digital computer plot of the radiation index calculated for a particular aspect and expressed as a function of slope inclination and solar declination. The latitude is 40 N. Because direct radiation is equal upon facets that show symmetry with respect to a north-south axis, two aspects are represented by this figure.

The theory involved in computing the radiation index parameter is presented in appendix A of this report. This appendix also includes a digital computer program for determining the variation of radiation index with solar declination for any surface established by latitude,

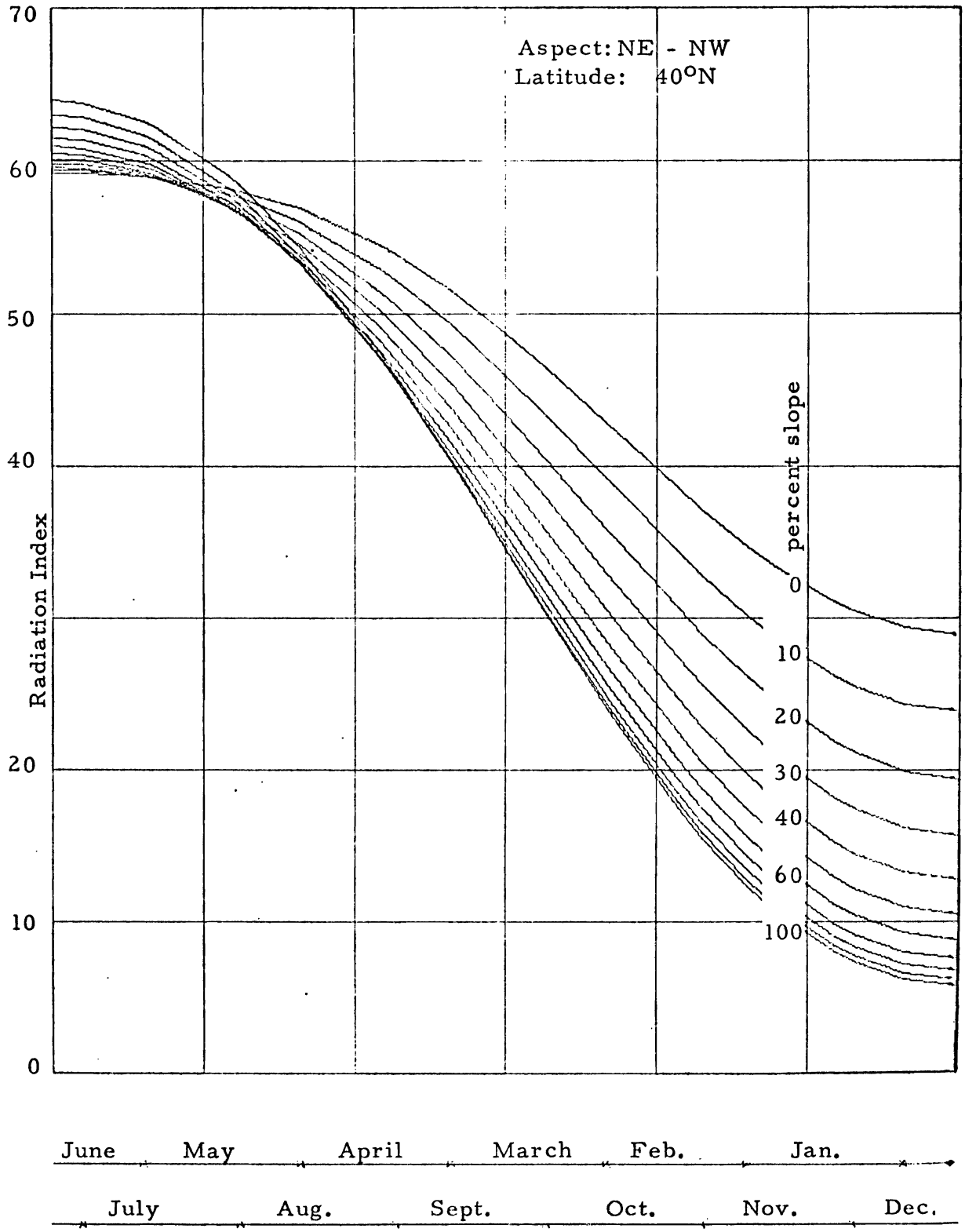

Figure 3.3. Radiation index values as a function of slope inclination and time of year.

aspect, and degree of slope. Some sample output and an additional computer plot (figure A1) are also included in the appendix.

The application of the potential radiation parameter to watershed studies requires that for each zone or area under consideration the orientation and slope of an effective plane surface be defined such that this surface receives as nearly as possible the same potential insolation as is received by the particular zone.

For the second model a term for radiation index is added to equation 2.1 and the result appears as follows:

$$\frac{d[W_s(t)]}{dt} = -k_s (T_a - 35) \frac{RI_s}{RI_h} W_s(t) \quad . \quad . \quad . \quad . \quad . \quad . \quad 3.8$$

in which the undefined terms are:

RI_s = the radiation index on a surface possessing a known degree and aspect of slope

RI_h = the radiation index for a horizontal surface at the same latitude as the particular watershed under study

A test of equation 3.8 is illustrated by figure 3.4 which indicates both predicted and actual rates of snowmelt for a watershed in Montana.

Surface runoff

This quantity is estimated by equation 2.4. However, again, some improvement over the first model is shown in that the term W_{gr} in the second model always represents all water, including snowmelt, which is available at the soil surface. The term for threshold

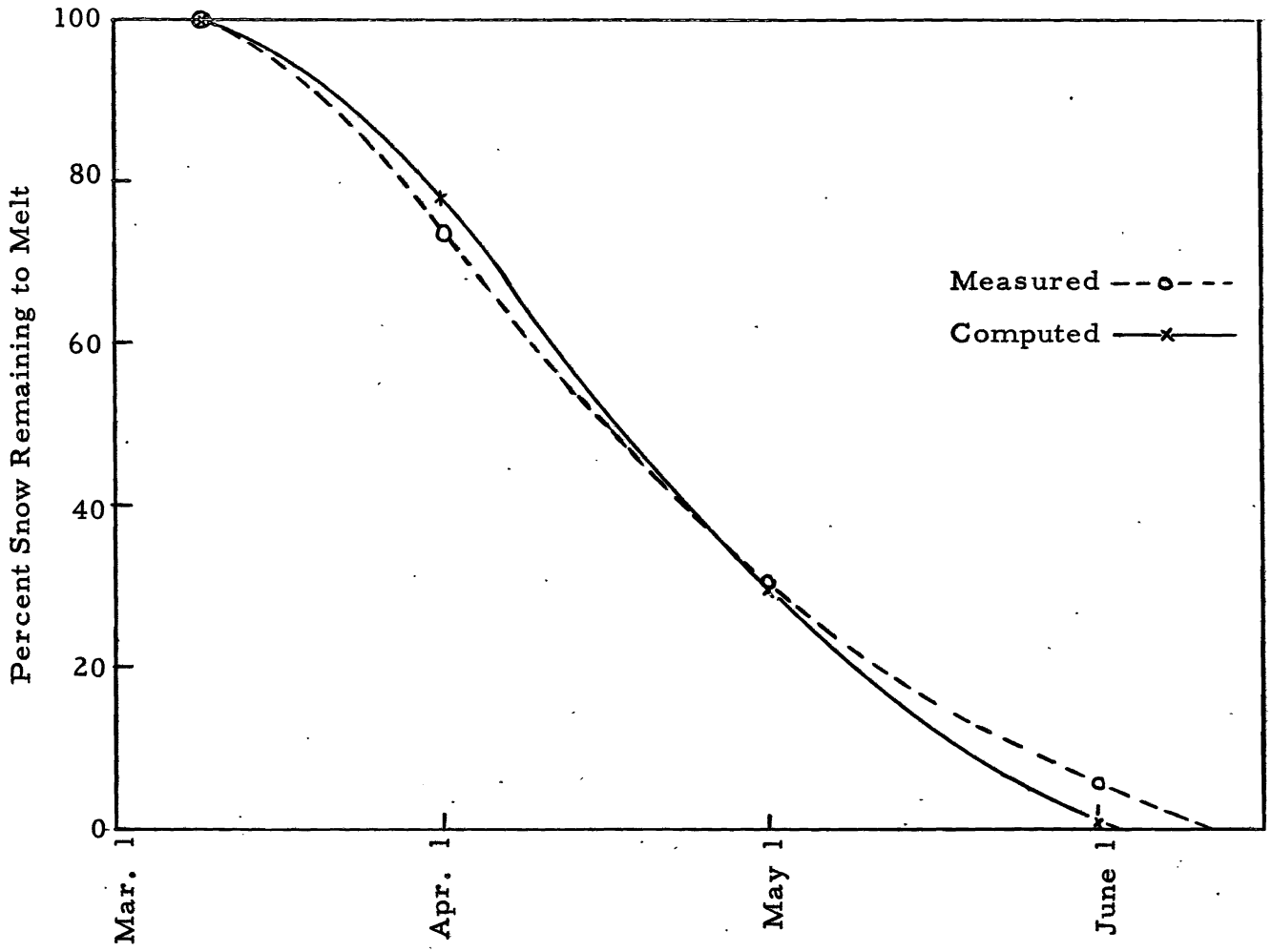

Figure 3.4. Measured and computed snowmelt rate curves for the Middle Fork Flathead River, Montana, 1947.

runoff, R_{tr}, is defined in the same way in both models.

Depression storage

Like the first model, water retained temporarily in depression storage is assumed to be a part of the evapotranspiration loss from the area and thus is not considered as a separate entity.

Available soil moisture storage

In this model soil moisture storage within the plant root zone is represented without the three simplifying assumptions made for the first model. Thus, in the second model, the evapotranspiration and deep percolation rates are assumed to be dependent upon the soil moisture level, and interflow is assumed to occur whenever the available soil moisture storage capacity level is reached. Soil moisture storage as a function of time is, therefore, expressed by:

$$M_s(t) = \int (F_r - ET_r - G_r - N_r)\, dt \quad . \quad . \quad . \quad . \quad . \quad . \quad . \quad 3.9$$

The four flow rates represented by the symbols under the integral signs are infiltration, F_r, evapotranspiration, ET_r, deep percolation, G_r, and interflow, N_r. Each is discussed in the following sections.

Infiltration

Infiltration rates in this model are given by equations 2.6 and 2.7. It is again noted that in the second model the term W_{gr} always includes all water available at the soil surface.

Evapotranspiration

The basic evapotranspiration relationship used in the second model is equation 2.16 of model one. However, in order to make the equation more accurate for describing the process over small geographic units, certain modifications were introduced.

Elevation effects on evapotranspiration. Frequently elevation differences on a watershed are substantial, and it is conceivable that these differences might produce significant effects on the evapotranspiration process. Under this heading only the evaporation portion of the process is considered. The same general principles which govern evaporation apply also to plant transpiration except that in this case plant effects are involved, and these are considered in a subsequent section. It is further pointed out that in this discussion elevation is not regarded as an independent parameter in the evaporation process. The rate at which this process occurs is influenced mainly by solar radiation, air temperature, vapor pressure, and wind (26). However, frequently all of these factors are altered by elevation changes within a watershed. Each factor is subject to independent measurement, but in many areas data are inadequate or entirely lacking. Air temperature, a commonly measured parameter, is utilized in several relationships which have been developed for predicting evaporation and evapotranspiration. The dependency of evaporation upon vapor pressure is demonstrated by the Dalton mass transfer equation (11). In turn, vapor pressures are a

function of temperature (26). Air temperatures are not directly related to wind or air movement, a parameter which can substantially influence the vapor pressure gradient above an evaporating surface. However, in general, the importance of wind is greatly lessened under regional considerations of evaporation rates as opposed to local or point rates (29). Evaporation is profoundly influenced by total insolation since this energy represents the driving function in the process (6, 18, 22). Particularly within the region of a continental climate, there exists a high degree of correlation between total insolation and air temperature (40). However, under stable and equilibrium air-mass conditions an increase in elevation, on a watershed for example, causes a reduction in air temperature due to adiabatic cooling, and, on the other hand, produces an increase in insolation because of the reduced atmospheric transmission losses (26, 27). Thus, within the local area, air temperatures cease to be entirely indicative of the incoming energy supply available for the evapotranspiration process on the watershed. For this reason, a correction or adjustment seems appropriate to evaporation equations based primarily on the temperature parameter. Theoretically this adjustment should compensate for the joint effects of adiabatic cooling of the air and increasing total insolation with height above the base elevation of the land surface or valley floor. The following discussion develops a basis for a correction factor of this nature.

For a given set of equilibrium conditions within the air mass, it can be shown by means of the energy budget equation that a change in

energy available for evaporation is a direct function of the change in insolation being received by the evaporating surface. Thus:

$$\Delta Q_e = \Delta Q_s \quad . \quad . \quad . \quad . \quad . \quad . \quad . \quad . \quad . \quad . \quad . \quad . \quad . \quad 3.10$$

in which

Q_e = the energy used for evaporation

Q_s = solar and sky radiation reaching the surface

Letting H_v represent the latent heat of vaporization of water and ρ its density, equation 3.10 can be written

$$\Delta E = \frac{\Delta Q_s}{H_v \rho} = K \Delta Q_s \quad . \quad . \quad . \quad . \quad . \quad . \quad . \quad . \quad . \quad . \quad 3.11$$

in which E is the evaporation in depth units.

For particular conditions the quantity of solar and sky radiation reaching a surface is dependent upon the length of the atmospheric path traversed by the sun's rays in reaching that surface. A parameter termed optical air mass is a measure of this distance. Figure 3.5 illustrates the radiation intensity reaching a horizontal surface at sea level for cloudless conditions as a function of the optical air mass. Because the optical air mass is a function of the zenith angle of the sun (27), the terrestrial radiation intensity at a particular latitude and Because the optical air mass is a function of the zenith angle of the sun (27), the terrestrial radiation intensity at a particular latitude and solar declination can be related to the hour angle as shown by figure 3.6. It will be noted that for a given latitude (in this case 40 N) the intensity of radiation is dependent upon not only the hour angle and

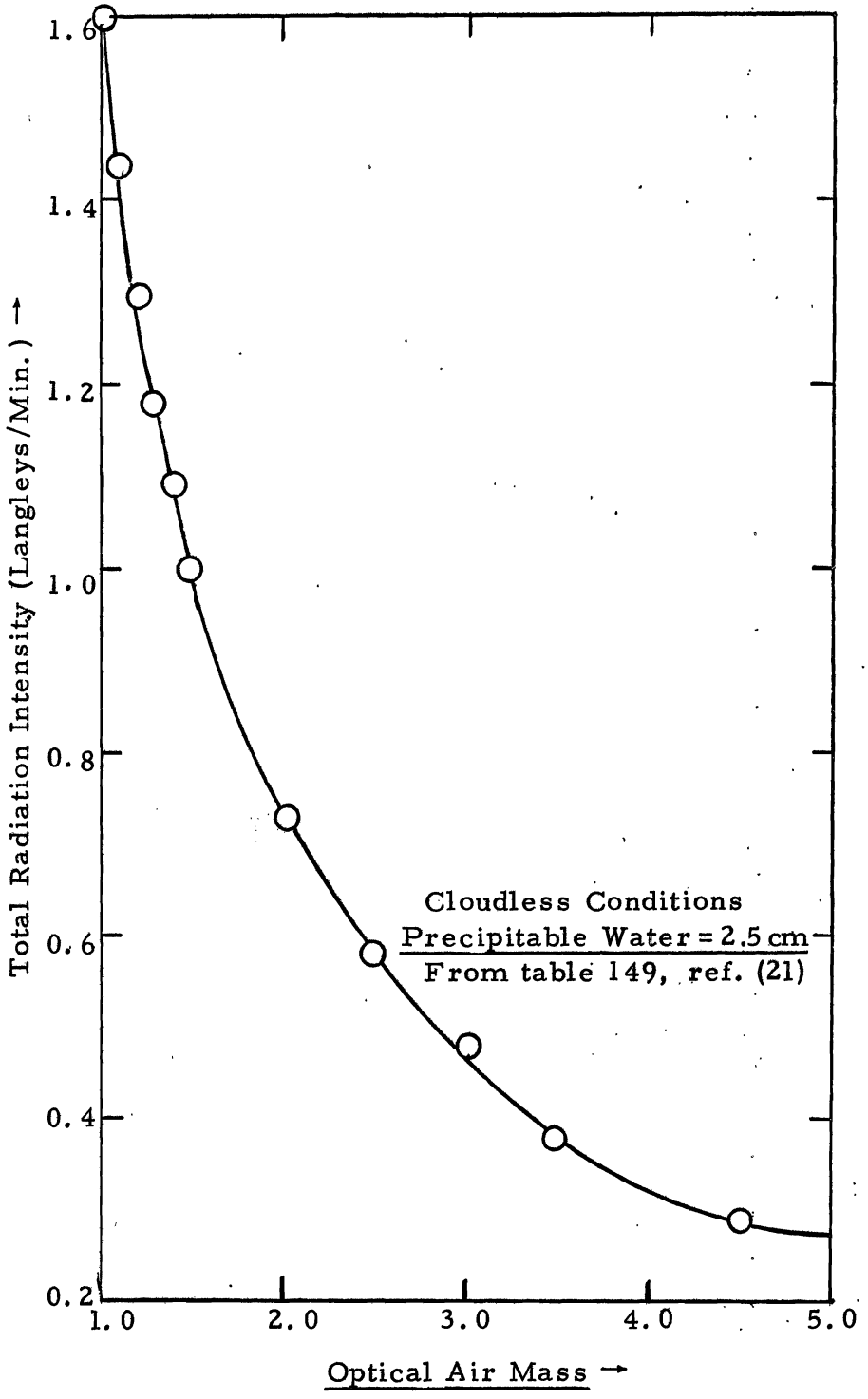

Figure 3.5. Total solar and sky radiation on a horizontal surface at sea level during cloudless conditions as a function of the optical air mass.

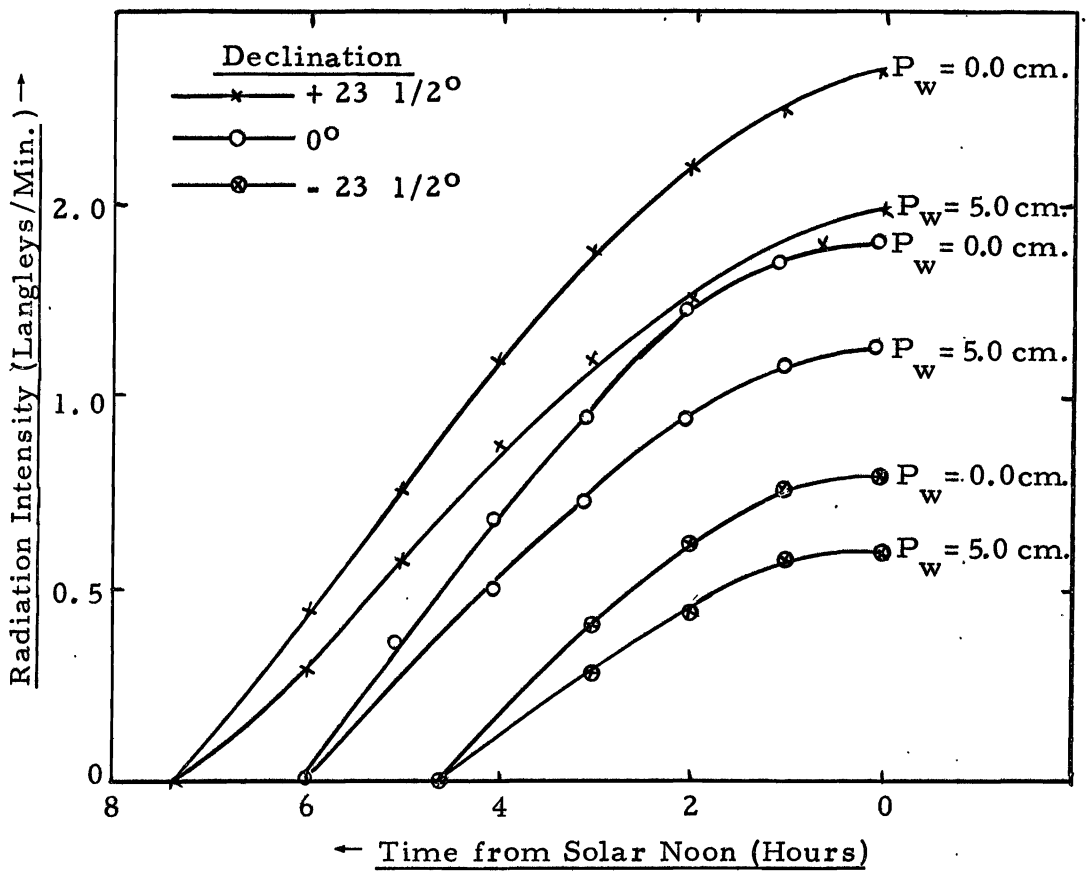

Figure 3.6. Total radiation intensity upon a horizontal surface at sea level under cloudless conditions as a function of time at a latitude of 40°N.

declination of the sun, but also the precipitable moisture content of the atmosphere. The variation in total daily insolation received on a horizontal surface at sea level as a function of atmospheric moisture content and solar declination is illustrated by figure 3.7. Also shown for comparison is a plot of the extraterrestrial radiation received on a horizontal surface. For the same three levels of precipitable atmospheric moisture, namely 0, 2.0, and 5.0 centimeters, and a latitude of 40 N, figure 3.8 indicates the mean monthly losses of radiant energy by transmission through a cloudless atmosphere expressed as a percentage of the total radiation received on a horizontal surface at sea level. Transmission losses expressed as a function of precipitable moisture are shown by figure 3.9. It will be noted that for a precipitable moisture content of 2.5 centimeters (approximately one inch) the average annual atmospheric transmission loss at a latitude of 40 N is approximately 33 percent of the total received at sea level.

For stations at elevations greater than sea level the values of optical air mass corresponding to a particular zenith angle are multiplied by the ratio P_i/P_o, where P_i represents the barometric pressure at the station in question and P_o indicates the barometric pressure at a base elevation, such as sea level (27). Thus, for a particular latitude and precipitable moisture content, the time variation in total radiation intensity on a horizontal surface can be estimated for any desired elevation. Figure 3.10 illustrates this variation for an elevation

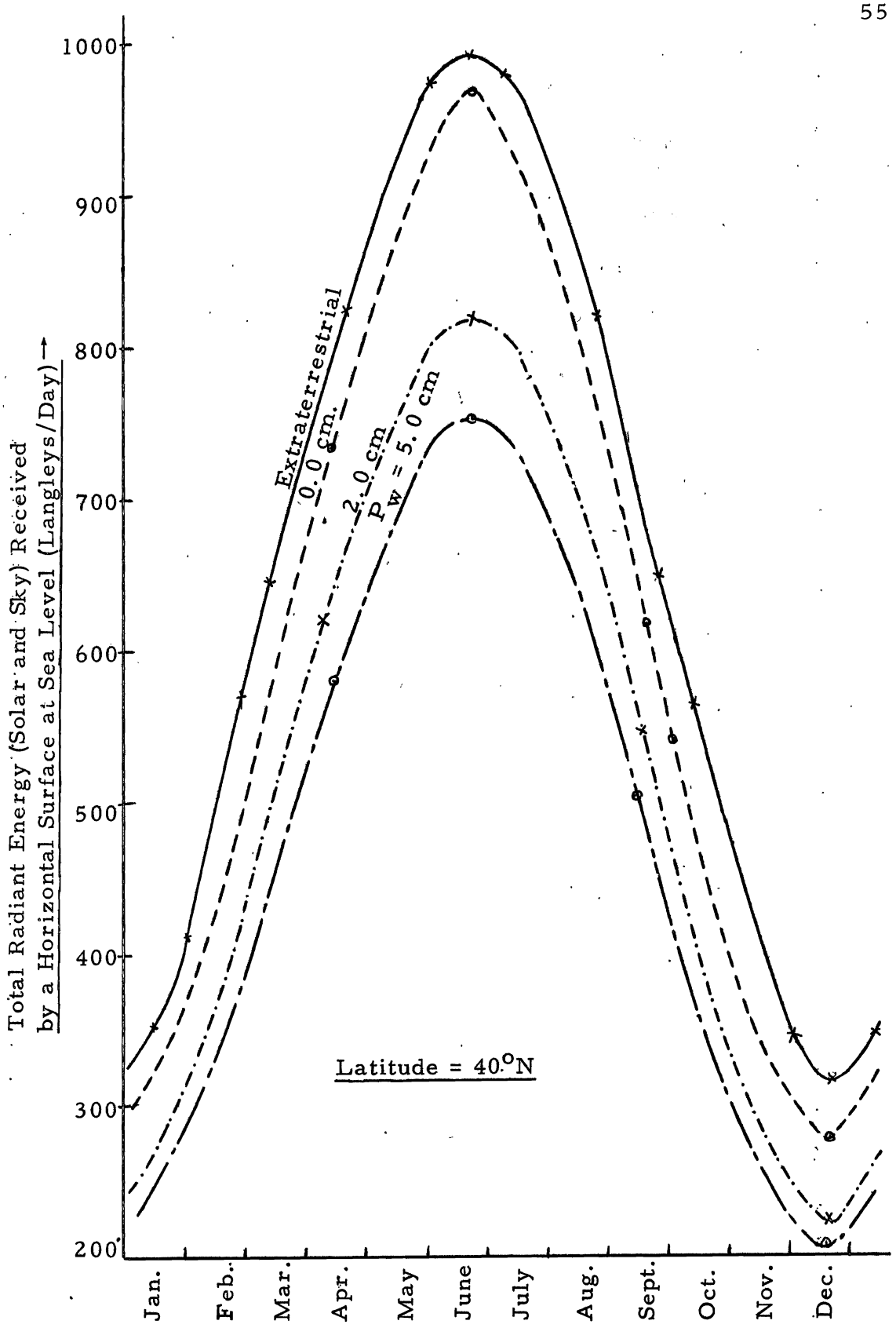

Figure 3.7. Radiation intensity as a function of time and atmospheric precipitable water content.

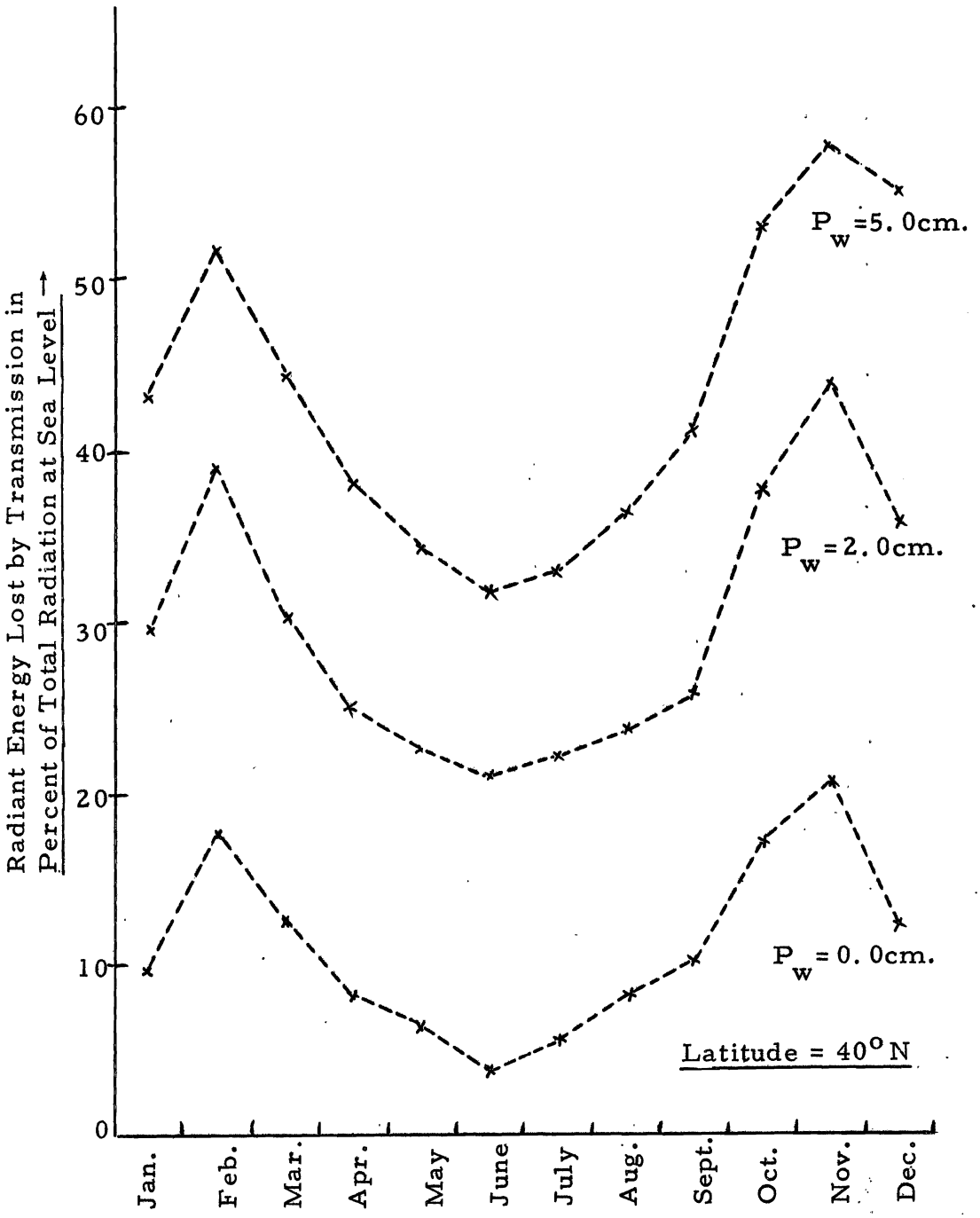

Figure 3.8. Radiation transmission losses as a function of time and atmospheric precipitable water content.

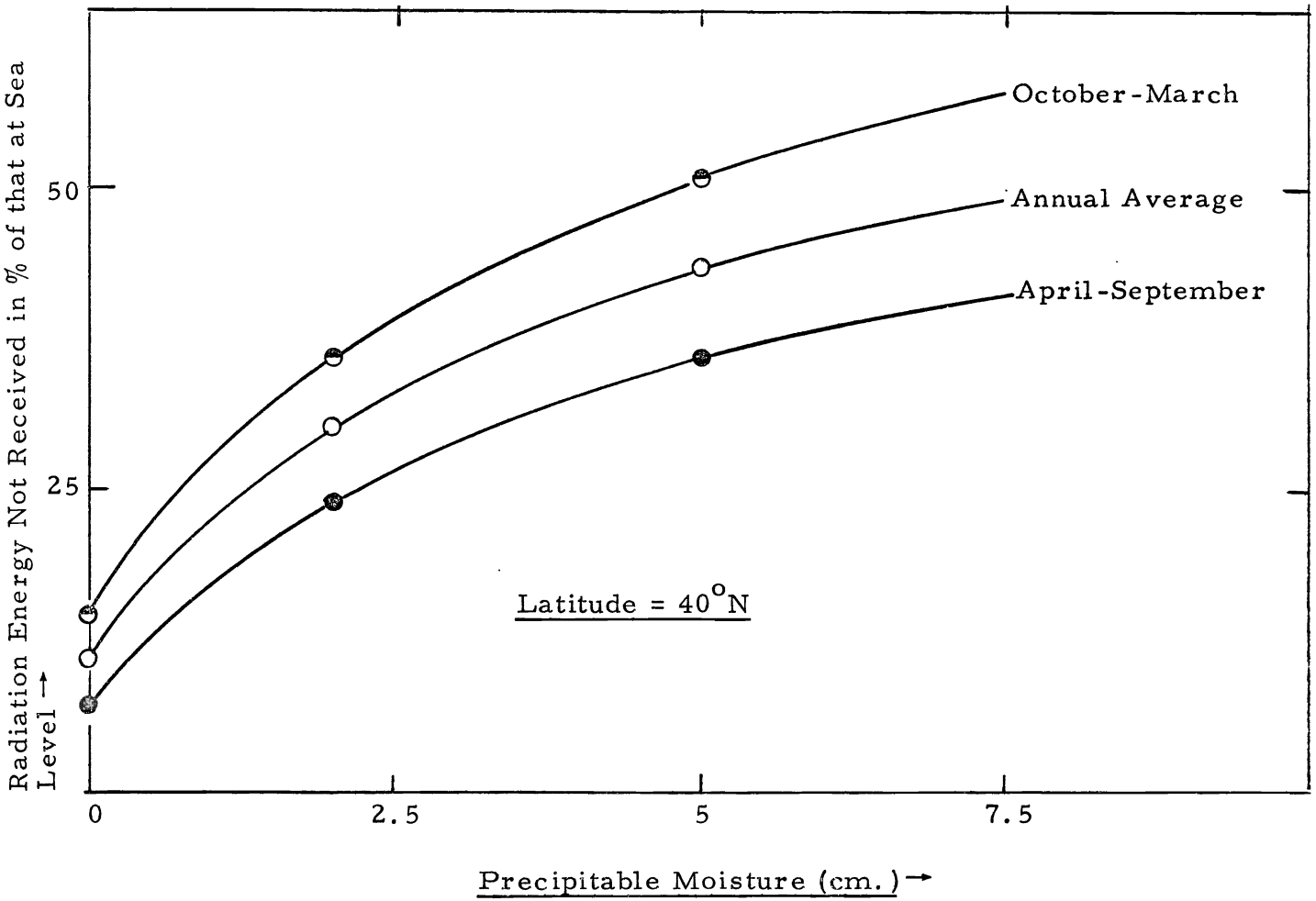

Figure 3.9. Seasonal and annual radiation transmission losses as a function of atmospheric precipitable water content.

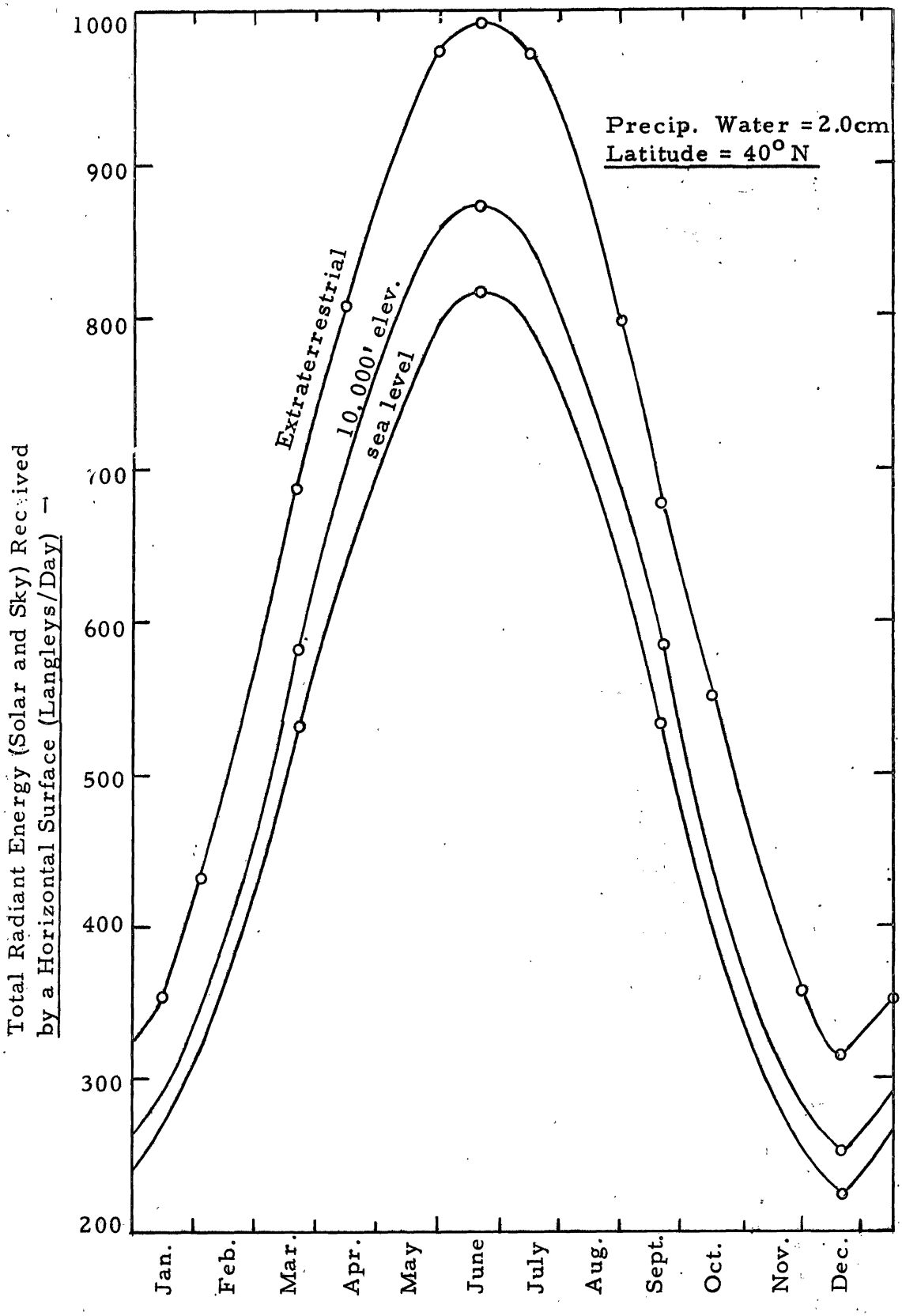

Figure 3.10. Total radiant energy as a function of elevation.

of 10,000 feet, a latitude of 40 N, and a precipitable moisture content of 2.0 centimeters.

On the basis of the relationship between barometric pressure and insolation received, equation 3.11 can be modified to read:

$$\Delta E = \frac{Q_E - Q_o}{H_v \rho} \left[1 - \frac{P_i}{P_o} \right] \quad . \quad . \quad . \quad . \quad . \quad . \quad . \quad . \quad . \quad 3.12$$

in which

ΔE = the evaporation increase in centimeters per day

Q_E = the extraterrestrial radiation in langleys per day

Q_o = radiation in langleys per day on a horizontal surface at a given base

and the other variables have been defined previously.

Within the elevation range between sea level and 12,000 feet the ratio P_i/P_o is fairly linear with elevation so that a good estimate of ΔE expressed in inches per day per 1,000 feet elevation increase can be determined from equation 3.12 and expressed in the following relationship:

$$\Delta E = \frac{Q_E - Q_o}{(12)(2.54) H_v \rho} \left(1 - \frac{P_{12}}{P_o} \right)$$

$$= (Q_E - Q_o) \, 2.23 \times 10^{-5} \quad . \quad . \quad . \quad . \quad . \quad . \quad . \quad . \quad 3.13$$

From equation 3.13 and figure 3.7, monthly values of ΔE were computed for three levels of precipitable moisture. These computations are shown by table 3.1.

Table 3.1. Evaporation rate as a function of elevation and atmospheric precipitable moisture.[1]

Month	Monthly avg. rad. on horiz. surface (l/day)				$Q_E - Q_o$ (langleys/day)			$\Delta E \times 10^{-4}$ (in./day/1000')		
	Q_E (Extra-terrestrial)	Q_o at sea level								
		P_w = 0.0 cm	P_w = 2.0 cm	P_w = 5.0 cm	P_w = 0.0cm	P_w = 2.0 cm	P_w = 5.0 cm	P_w = 0.0 cm	P_w = 2.0 cm	P_w = 5.0cm
January	350	320	270	245	30	80	105	6.7	17.8	23.4
February	500	425	360	330	75	140	170	16.7	31.2	37.9
March	665	590	510	460	75	155	205	16.7	34.5	45.7
April	800	740	640	580	60	160	220	13.4	35.6	49.0
May	920	865	750	685	55	170	235	12.3	37.8	52.4
June	980	945	810	745	35	170	235	7.8	37.8	52.4
July	970	920	795	730	50	175	240	11.1	39.0	53.5
August	865	800	700	635	65	165	230	14.5	36.8	51.2
September	705	640	560	500	65	145	205	14.5	32.3	45.7
October	550	470	400	360	80	150	190	17.8	33.4	42.3
November	410	340	285	260	70	125	150	15.6	27.8	33.4
December	325	290	240	210	35	85	115	7.8	19.0	25.6
Averages										
Annual								13.0	31.9	42.8
Ap.-Sept.								12.3	36.5	50.8
Oct.-Mar.								13.6	27.3	34.7

[1] Notes: (1) Cloudless conditions.
(2) Latitude = 40°N.
(3) P_w = precipitable water within the atmosphere in centimeters.
(4) Table applicable between sea level and an elevation of 12,000 feet.

From the average values shown at the bottom of table 3.1, figure 3.11 was plotted. A comparison of figures 3.9 and 3.11 indicates that on a percentage basis energy transmission losses during the winter months exceed those of the summer months. On the other hand, the magnitudes of the summer losses are considerably higher than those of the winter months. In both cases seasonal differences become more pronounced with increasing levels of precipitable moisture. For a given moisture level, magnitudes of transmission losses and seasonal differences both decrease with decreasing latitude. However, even at the 40 N latitude the magnitude of the incremental evaporation with increasing elevation is rather small. For example, at a precipitable moisture level of 2.54 centimeters (one inch), figure 3.11 indicates the average annual value of ΔE to be approximately 0.0035 inch per day per 1,000 feet, or about 0.10 inch per month per 1,000 feet elevation increase above the floor of the valley. In terms of absolute magnitude, variations from this figure on both a seasonal basis and with precipitable moisture are small.

Average monthly values of the precipitable water content of the atmosphere over the continental United States are shown by table 3.2 (55). These figures apply to a vertical column of air extending eight kilometers (26,300 feet) above the earth's surface. The annual average for the United States is 0.78 inch, with seasonal values of 0.54 inch for the winter months and 1.03 inches for the summer. Included in table

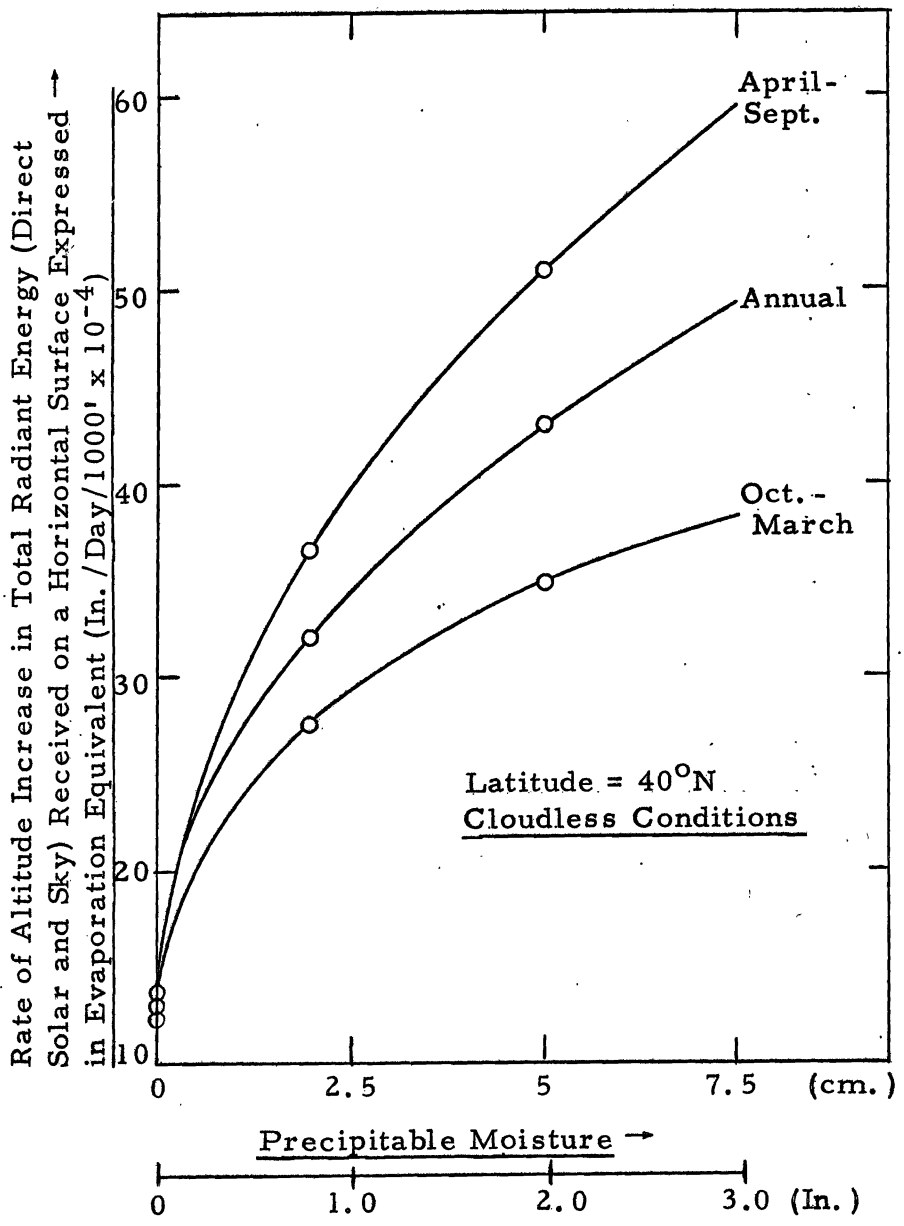

Figure 3.11. Seasonal and annual values of radiant energy as a function of atmospheric precipitable moisture and elevation.

Table 3.2. Average values of precipitable water, surface to eight kilometers [1]

Month	Total precipitable water in inches		
	Average for continental U. S.	Ely, Nevada	Average for Intermountain Region
January	0.44	0.275	0.32
February	0.45	0.277	0.32
March	0.49	0.282	0.33
April	0.64	0.351	0.41
May	0.84	0.378	0.45
June	1.11	0.441	0.52
July	1.26	0.580	0.69
August	1.26	0.563	0.66
September	1.05	0.479	0.57
October	0.79	0.387	0.45
November	0.57	0.285	0.33
December	0.51	0.290	0.34
Annual	0.78	0.382	0.45
Winter	0.54	0.300	0.35
Summer	1.03	0.465	0.55

[1] Data taken from reference (55)

3.2 are corresponding average monthly values of the precipitable water within the atmosphere at Ely, Nevada, where the annual average figure is 0.382 inch, with seasonal averages of 0.30 inch during the winter period and 0.465 inch for the summer. Corresponding average values of precipitable water for the intermountain region, including eastern Nevada, Utah, and southern Idaho, were estimated from constant moisture charts (55) as being 0.45 inch, 0.35 inch, and 0.55 inch, respectively (table 3.2). On the basis of these values, within the intermountain region incremental evaporation per 1,000 feet elevation increase varies from an annual average of 0.0027 inch per day (0.081 inch per month) to 0.0026 inch per day during the winter and 0.0029 inch per day during the summer months. These figures indicate that for most applications within this region use of the average annual value throughout the entire year would yield satisfactory results.

On the basis of the foregoing discussion, equation 2.16 can be modified to include an elevation correction. In order to consider the plant influences the elevation correction is multiplied by the crop coefficient parameter, k_c. Thus, equation 2.16 becomes:

$$ET_{cr} = k_c \left[k_t \frac{T_a p}{100} + C_e (E_s - E_v) \right] \quad . \quad . \quad . \quad . \quad . \quad 3.14$$

in which

C_e = the elevation correction factor applicable to the particular time increment

E_s = the mean elevation of the watershed zone in thousands of feet

E_v = the mean elevation of the valley floor in thousands of feet

In this study an average annual elevation correction factor of 0.0027 inch per day per thousand feet was applied.

Slope effects on evapotranspiration. The two parameters of temperature and percent daylight hours which appear in equations 2.16 and 3.14 are indices of the total energy available to surfaces subject to the evapotranspiration process. Values of p on a monthly basis are available in a number of references, one of which is cited (10). These indices integrate total energy received on a regional basis and the equation is applicable to horizontal surfaces. In order to provide an adjustment for sloping land surfaces, such as occur on a watershed, the potential insolation parameter was introduced into equation 3.14, thus:

$$ET_{cr} = \frac{RI_s}{RI_h} k_c \left[k_t \frac{T_a p}{100} + C_e (E_s - E_v) \right] \quad . \quad . \quad . \quad . \quad 3.15$$

in which all parameters, whether continuously variable functions or finite mean values, are applicable to the same time increment, and

RI_s = the radiation index for a particular watershed zone possessing a known degree and aspect of slope

RI_h = the radiation index for a horizontal surface at the same latitude as the particular watershed under study

It is interesting to note that in the northern hemisphere and for northerly

slopes the ratio RI_s/RI_h decreases with a declination decrease, while for southerly slopes the ratio increases with decreasing declination (figure 3.3). Thus, for given values of p and T, the evapotranspiration rate on northerly slopes is less during the winter months than the summer months. For southerly slopes the reverse is true. It might be further noted from the definition of the radiation index parameter that the ratio RI_s/RI_h is equivalent to the ratio I_s/I_h in which the terms I_s and I_h refer to total potential insolation received on the sloping and horizontal surfaces respectively during a particular day.

Soil moisture effects on evapotranspiration. The influence of soil water on evapotranspiration has been the subject of much research and discussion (56, 57). It it now generally conceded that there is some reduction in the evapotranspiration rate as the quantity of water available to plants within the root zone decreases. Thornthwaite (47) contends that this rate is proportional to the amount of water remaining in the soil. This criterion has been somewhat modified by recent studies at the U. S. Salinity Laboratory in Riverside, California (13). These indicate that transpiration occurs at the potential rate through approximately two-thirds of the range of available moisture within the rooting depth. A critical point is then reached when actual transpiration begins
mately two-thirds of the range of available moisture within the rooting depth. A critical point is then reached when actual transpiration begins
to lag behind the potential rate. Because soil moisture becomes a limiting factor at this point, plants begin to wilt. Thereafter, the relationship between available water content and transpiration rate is

virtually linear. Average daily transpiration rates plotted as a function of water content (weight basis) for three soil types are shown by figure 3.12. Typical values of the soil moisture content at various points on these curves are shown by table 3.3. It should be noted that the soil moisture content at the point of discontinuity on the curve, M_{es}, is a function of the average soil moisture tension within the plant root zone, and is, therefore, dependent upon not only the soil type but also the extent and distribution of the root system of the transpiring plants.

Table 3.3. Typical soil moisture values, in inches per foot of soil depth, for three characteristic soil types

Soil type	Total soil moisture of field capacity	Approx. lower limit of available water for plants	Total soil moisture available to plants	Available moisture at the critical value, M_{es}
Clay	6.0	2.0	4.0	1.3
Loam	3.5	0.8	2.7	0.9
Sand	1.2	0.3	0.9	0.3

On the basis of the preceding discussion, actual evapotranspiration is expressed as follows:

On the basis of the preceding discussion, actual evapotranspiration is expressed as follows:

$$ET_r = ET_{cr} \quad , \quad [M_{es} < M_s(t) \leq M_{cs}] \quad . \quad . \quad . \quad . \quad 3.16$$

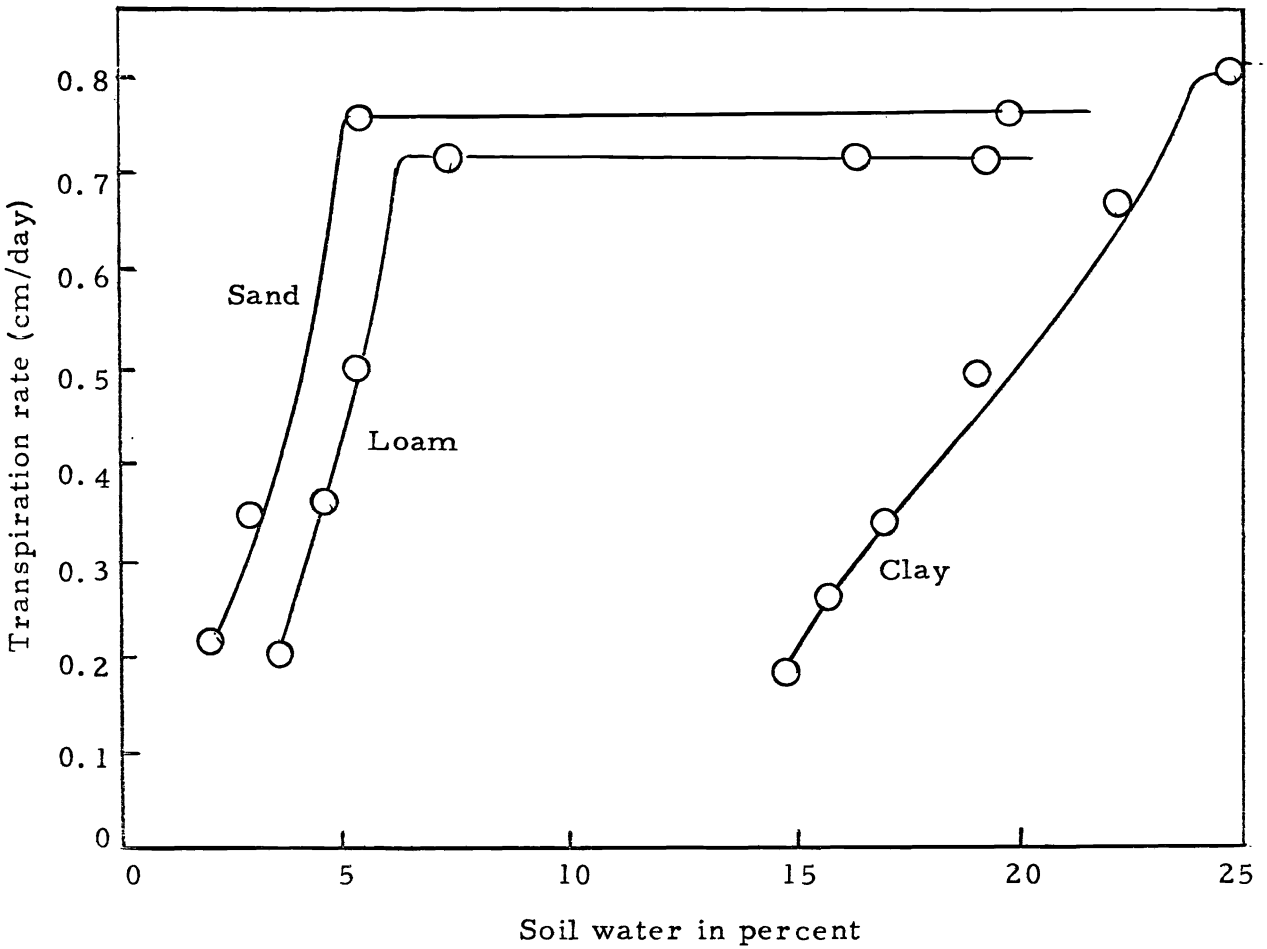

Figure 3. 12 Average daily transpiration rates as functions of water content for birdsfoot trefoil in shallow containers.

From equation 3.16 it is apparent that when the available moisture in the plant root zone is greater than a critical value, M_{es}, the actual evapotranspiration can be estimated by equation 3.15. For available soil moisture levels less than M_{es} actual evapotranspiration is given by

$$ET_r = ET_{cr} \frac{M_s(t)}{M_{es}} \quad , \quad (0 \leq M_s(t) \leq M_{es}) \quad . \quad . \quad . \quad 3.17$$

This equation when integrated is exponential in nature. To demonstrate this statement, the integration is simplified by assuming that changes in soil moisture are due entirely to evapotranspiration and further that the potential evapotranspiration rate, ET_{cr}, is a constant throughout the time increment or integration period. Actually, neither of these assumptions is necessary in the analog computer program. Equation 3.17 can then be written in the form:

$$ET_r = \frac{dM_s}{dt} = -ET_{cr} \frac{M_s(t)}{M_{es}} \quad . \quad . \quad . \quad . \quad . \quad . \quad . \quad . \quad 3.18$$

with the negative sign indicating abstraction from storage. Integrated between times t_1 and t_2 equation 3.18 appears as:

$$M_s(2) = M_s(1) \exp \left[- \frac{ET_{cr}}{M_{es}} (t_2 - t_1) \right] \quad . \quad . \quad . \quad . \quad . \quad 3.19$$

$$M_s(2) = M_s(1) \exp \left[- \frac{ET_{cr}}{M_{es}} (t_2 - t_1) \right] \quad . \quad . \quad . \quad . \quad . \quad 3.19$$

in which $M_s(1)$ and $M_s(2)$ are the soil moisture storage values at times t_1 and t_2, respectively.

From equation 3.17, equation 3.15 can now be modified to read:

$$ET_r = \frac{M_s}{M_{es}} \frac{RI_s}{RI_h} k_c \left[k_t \frac{T_a p}{100} + C_e (E_s - E_v) \right] ,$$

$$(0 \leq M_s \leq M_{es}) \quad . \quad . \quad . \quad . \quad . \quad 3.20$$

Equation 3.20 is the general equation used in the second model for estimating evapotranspiration rates. Under the particular conditions when $M_s > M_{es}$, $ET_r = ET_{cr}$ and equation 3.20 is of the particular form shown as equation 3.15. Thus, the evapotranspiration equation of model one (equation 2.16) has been improved to reflect the effects of available soil moisture, land surface slope, and elevation changes upon the evapotranspiration process.

Computation of evaporation from water surfaces. Evaporation rates, E_{cr}, from interception and surface depression storage within the watershed zone are estimated by equation 3.15. In the case of water surfaces a k_c factor of 1.0 is applied (33, 34) whereas for snow and bare ground this factor is assumed to equal 0.25 (14, 43). Evaporation losses from interception and surface depression are assumed to occur concurrently. During snow accumulation periods as indicated by an air temperature of less than 35 F, soil moisture content is assumed not concurrently. During snow accumulation periods as indicated by an air temperature of less than 35 F, soil moisture content is assumed not to influence evapotranspiration rates. During these periods equation 3.15 applies regardless of the soil moisture level within the plant root zone. Thus:

$$ET_r = ET_{cr} \quad , \quad (T < 35\ F) \quad . \quad . \quad . \quad . \quad . \quad . \quad . \quad . \quad 3.21$$

Several studies have been carried out in which the evaporation loss from the top surface of a snow pack was investigated (14, 49, 58, 60, 61). Typical rates vary from 0.01 inch per day to 0.03 inch per day, depending upon the degree of exposure of the snow surface. In cases where lake or pan evaporation data are available, close estimates of snow surface evaporation rates are obtained by assuming about one-third those of the lake or one-fifth the pan rates.

Deep percolation

In the first model deep percolation is assumed to exist only at times when the available moisture storage is at the capacity level (equations 2.17 and 2.18). However, these losses continue when the available soil moisture level is less than field capacity. In general terms, the relationships for deep percolation losses in the saturated and unsaturated states are expressed as follows:

$$G_{rs} = f(k_h) \quad . \quad . \quad . \quad . \quad . \quad . \quad . \quad . \quad . \quad . \quad . \quad . \quad 3.22$$

$$G_{ru} = f(k_u, \theta) \quad . \quad . \quad . \quad . \quad . \quad . \quad . \quad . \quad . \quad . \quad . \quad . \quad 3.23$$

$$G_{ru} = f(k_u, \theta) \quad . \quad . \quad . \quad . \quad . \quad . \quad . \quad . \quad . \quad . \quad . \quad . \quad 3.23$$

in which

G_{rs} and G_{ru} = the saturated and unsaturated rates of deep percolation losses, respectively

k_h = the hydraulic conductivity or permeability of the soil

k_u = the capillary conductivity of the soil

θ = the soil moisture content

Equations 3.22 and 3.23 can be aproximated by the empirical expression:

$$G_r = -k_g M_s(t) \quad , \quad [0 \leq M_s(t) \leq M_{cs}] \quad . \quad . \quad . \quad . \quad . \quad 3.24$$

in which the negative sign indicates outflow or storage loss and k_g is a constant of proportionality, depending upon the porosity of the soil. $M_s(t)$ is given by equation 3.9. At field capacity $M_s(t) = M_{cs}$, and if deep percolation is assumed to be vertical (gradient = 1), equation 3.22 can be written in the form $G_{rs} = k_h$. Now, if the capillary component of flow is neglected at field capacity, this expression can be combined with equation 3.24 to yield

$$k_g M_{cs} = k_h$$

or

$$k_g = \frac{k_h}{M_{cs}} \quad . \quad . \quad . \quad . \quad . \quad . \quad . \quad . \quad . \quad . \quad . \quad . \quad . \quad 3.25$$

Interflow

In model one interflow was somewhat arbitrarily established as being that portion of snowmelt not required to satisfy any deficit of available soil moisture storage. In the second model interflow is

expressed as a surplus water quantity within the soil root zone. Thus, it is assumed that no interflow occurs until the available moisture holding capacity of the soil root zone has been satisfied. Once this point is reached storage changes within the root zone are insignificant, so that interflow rate is given by the following expressions:

$$N_r = 0 \quad , \quad (M_s < M_{cs}) \quad . \quad . \quad . \quad . \quad . \quad . \quad . \quad . \quad . \quad 3.26$$

$$N_r = F_r - G_r - ET_{cr} \quad , \quad (M_s = M_{cs}) \quad . \quad . \quad . \quad . \quad . \quad 3.27$$

Equations 3.24 and 3.27 can be combined to yield:

$$N_r = F_r - k_g M_{cs} - ET_{cr} \quad . \quad . \quad . \quad . \quad . \quad . \quad . \quad . \quad . \quad 3.28$$

The total interflow quantity which is available during a time period, n, is given by the integration of equation 3.28.

$$\int_{t_{cr}}^{t_n} N_r \, dt = \int_{t_{cr}}^{t_n} (F_r - k_g M_{cs} - ET_{cr}) \, dt \quad . \quad . \quad . \quad . \quad . \quad 3.29$$

in which t_{cr} represents the time at which $M_s = M_{cs}$ and is bounded as follows: $(t_o \leq t_{cr} \leq t_n)$.

Routing or translation

The routing or translation relationships of the first model (equations 2.21 to 2.28) are also applied to model two.

Total outflow

As expressed by equation 2.29 of model one, the total outflow from the watershed is obtained by summing the various runoff components from each zone within the model.

CHAPTER IV

TESTING AND VERIFICATION OF THE SECOND MODEL

In order to test and verify a hydrologic model, it is necessary to simulate an actual hydrologic unit. Of major importance in this analysis is the accuracy with which the known input and output data actually represent the various hydrologic quantities as they occur on the watershed. Frequently, the accuracy of available data is the limiting criterion which establishes the simulation accuracy for a particular watershed.

The first test of the model presented by Chapter III was made before ongoing computer modifications and improvements had yet reached the stage where there were enough amplifiers available to simulate the watershed area as more than a single zone. This restriction limited the usefulness of the test since it was then not possible to quantitatively evaluate improvements resulting from the use of a small space increment in the model. Models one and two will be quantitatively compared in subsequent studies carried out for the highly instrumented Reynolds Creek watershed near Boise, Idaho. The first test, briefly described in this chapter, was, however, useful because it demonstrated that the equations developed for the second model can be synthesized into a computer model of a hydrologic system. Preliminary tests of the second model were made by simulating a subbasin of

the Sevier River drainage in central Utah. This subbasin, which is referred to as Circle Valley, contains approximately 93,000 acres. It is situated at a latitude of about 40 N, and is formed by a widening of the Sevier River valley at a point immediately upstream from its point of confluence with the drainage of the East Fork of the Sevier River. Figure 4.1 shows a general outline of the subbasin. The average elevation of the valley floor is approximately 6,000 feet above sea level. On the west side of the valley the mountains rise to a peak elevation of 11,440 feet, while on the east side 11,036 feet is the maximum elevation. Circle Valley was selected for the study because its hydrologic system is relatively uncomplicated and yet contains many of the characteristic hydrologic phenomena. In addition, there are sufficient physical data available in the subbasin to guide the formulation of a model and to provide an evaulation of its performance.

An area-elevation curve for the mountainous or watershed area of Circle Valley is shown by figure 4.2. This curve indicates the mean watershed elevation to be about 7,400 feet. The total area of the watershed or land above the elevation of the valley floor is 84,700 acres. If the watershed is considered as consisting of two general facets, that on the west side of the Sevier River has a south-east aspect and an ap-
the watershed is considered as consisting of two general facets, that on the west side of the Sevier River has a south-east aspect and an ap-proximate average slope of 60 percent, while corresponding values for the facet on the east side of the river are north-west and also 60 percent. The various types of watershed cover were grouped into very broad

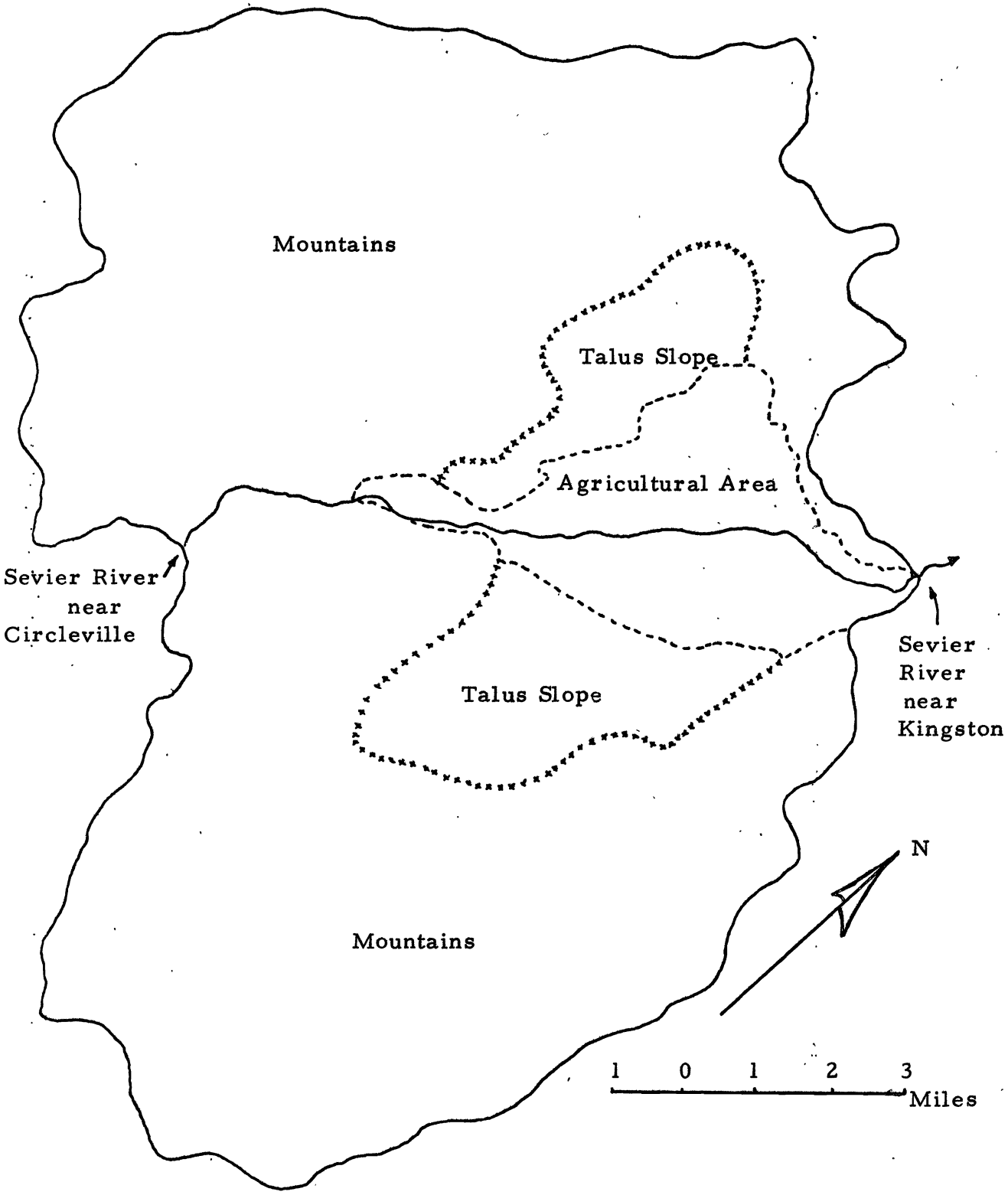

Figure 4. 1. General outline of Circle Valley subbasin, Sevier River, Utah.

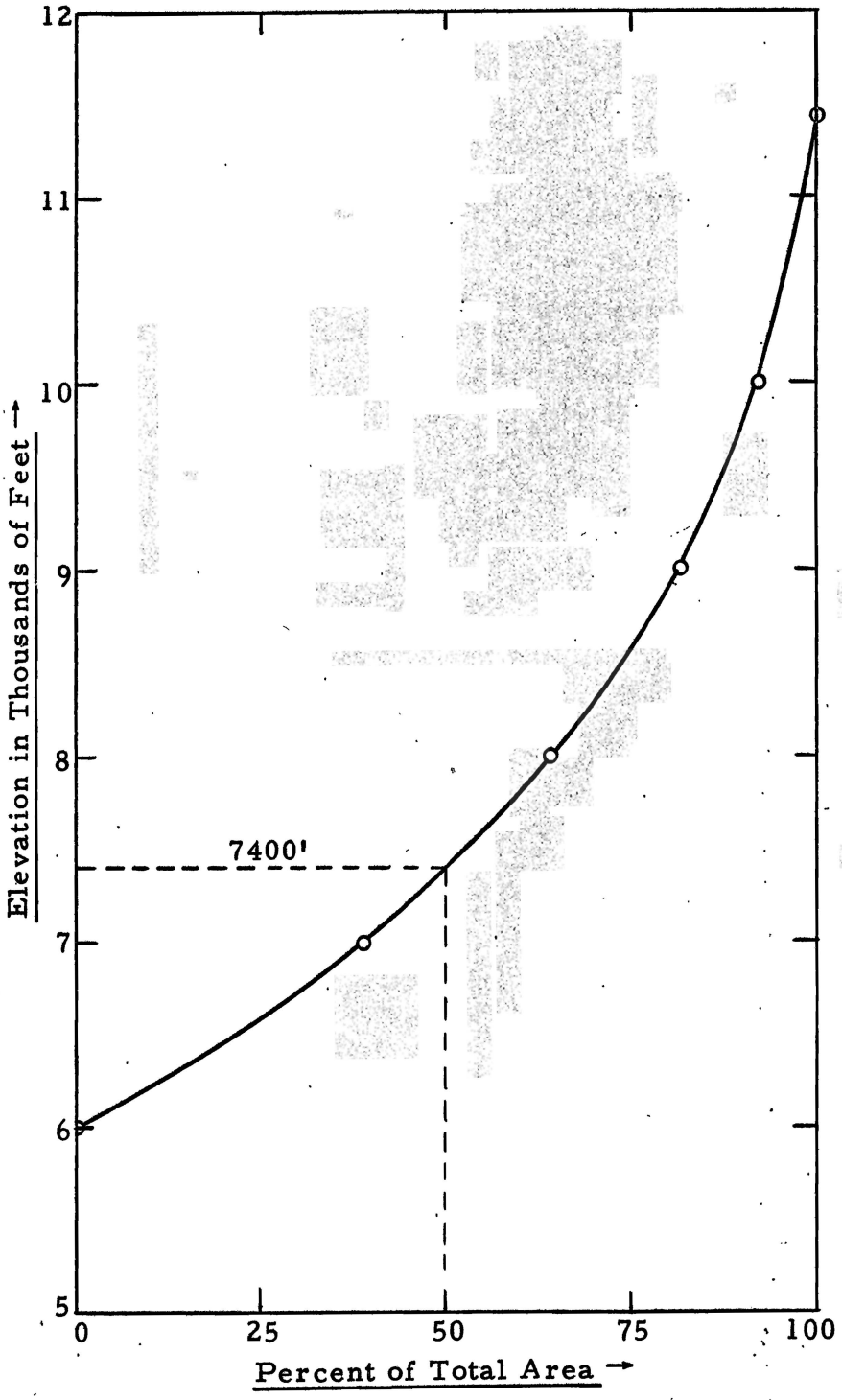

Figure 4.2. Area-elevation curve for the mountainous portion of Circle Valley basin.

categories. The approximate areas included within each of these categories are shown by table 4.1.

Table 4.1. Watershed cover, in acres, Circle Valley, Utah

Facet	Brush & sage	Coniferous	Deciduous	Barren	Total
West	28,428	4,732	1,085	4,250	38,495
East	30,160	14,140	1,140	765	46,205
Totals	58,588	18,872	2,225	5,015	84,700

The dominant soil type on the watershed is a course-textured loam which in many cases contains a large number of stones. The average available soil moisture holding capacity is about 0.83 inches per foot of soil.

The flat or bottom land area within Circle Valley is shown by figure 4.3. This sketch shows the locations of the irrigation canals and the single irrigation well within the valley. Also shown is the cropland area which contains some 4,580 acres, and a wet or swampy area of about 3,430 acres at the lower end of the valley. The primary agricultural crops within the cultivated area are grain (820 acres), potatoes (370 acres), corn (180 acres), and alfalfa (3,210 acres).

The wet area is formed by a natural subsurface barrier of low permeability material which extends across the mouth of the valley. Geologic investigations (5) have indicated that this barrier prevents any appreciable subsurface outflow from Circle Valley so that

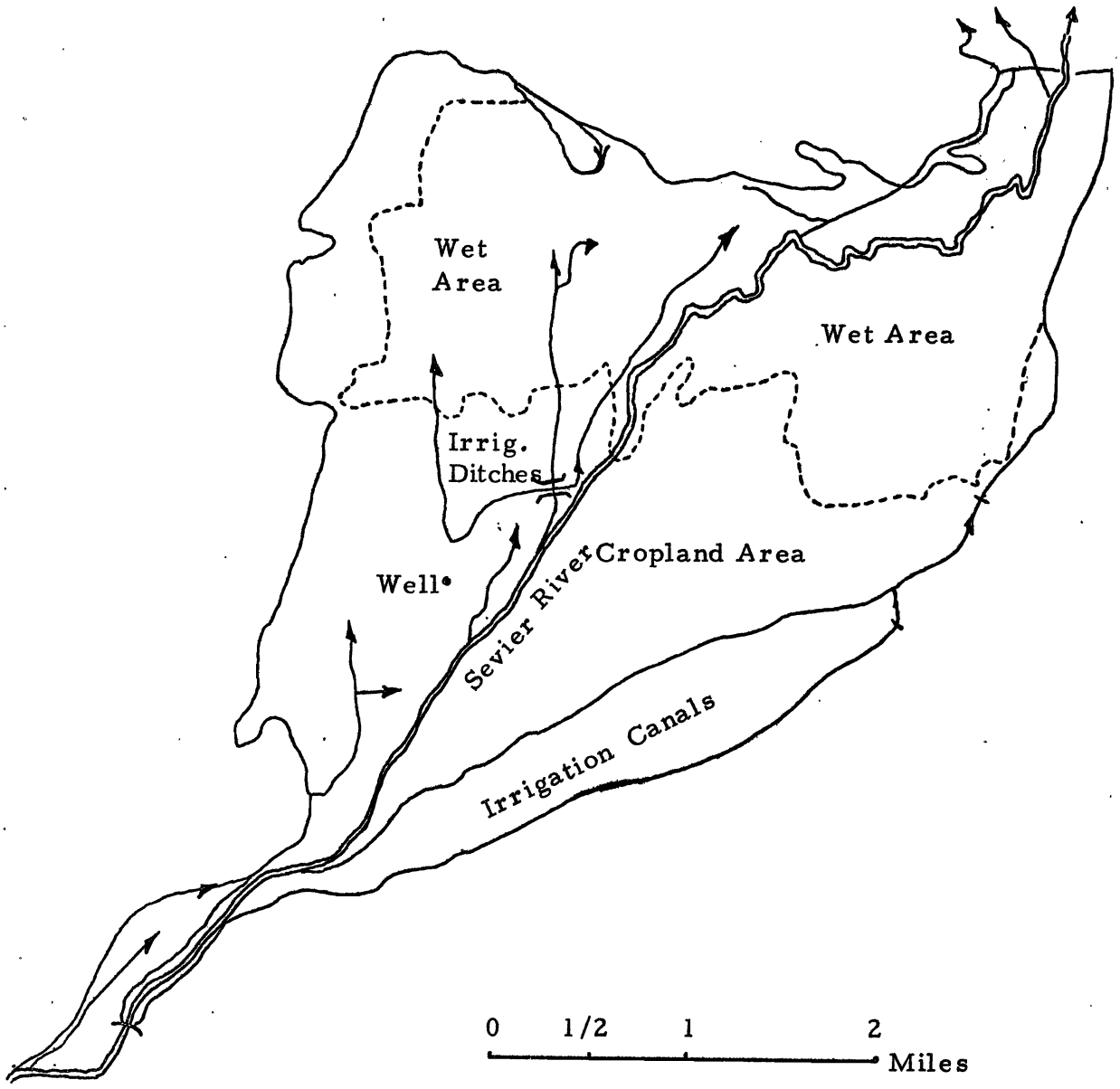

Figure 4.3. Agricultural area of Circle Valley.

essentially all outflow is accounted for by surface measurements. The boundary between the cropland area and the wet area approximates the division between the confined and the unconfined groundwater conditions. The groundwater underlying the cropped land is unconfined, while the underground reservoir beneath the wet area is confined and subject to a hydrostatic pressure.

In formulating a model for Circle Valley, the basin was divided into four basic hydrologic subunits; namely, the watershed, the cropland, the groundwater basin beneath the cropland, and the wet area. Average values of input parameters, such as in temperature, precipitation, radiation index, and soil type, were developed for the entire watershed.

Figure 4.4 is a hydrologic block flow diagram for Circle Valley. The four hydrologic subunits mentioned in the previous paragraph are shown by this diagram. Figure 4.5 is the analog flow diagram representing the simulation model of Circle Valley. This diagram represents a synthesis of the mathematical equations presented in Chapter III into the flow system depicted by figure 4.4.

Temperature and precipitation data are available from one U. S. Weather Bureau station within Circle Valley. This station is situated

Temperature and precipitation data are available from one U. S. Weather Bureau station within Circle Valley. This station is situated on the valley floor near the small town of Circleville. Because no meteorological data are available on the watershed, temperature and precipitation were lapsed from the valley station in accordance with

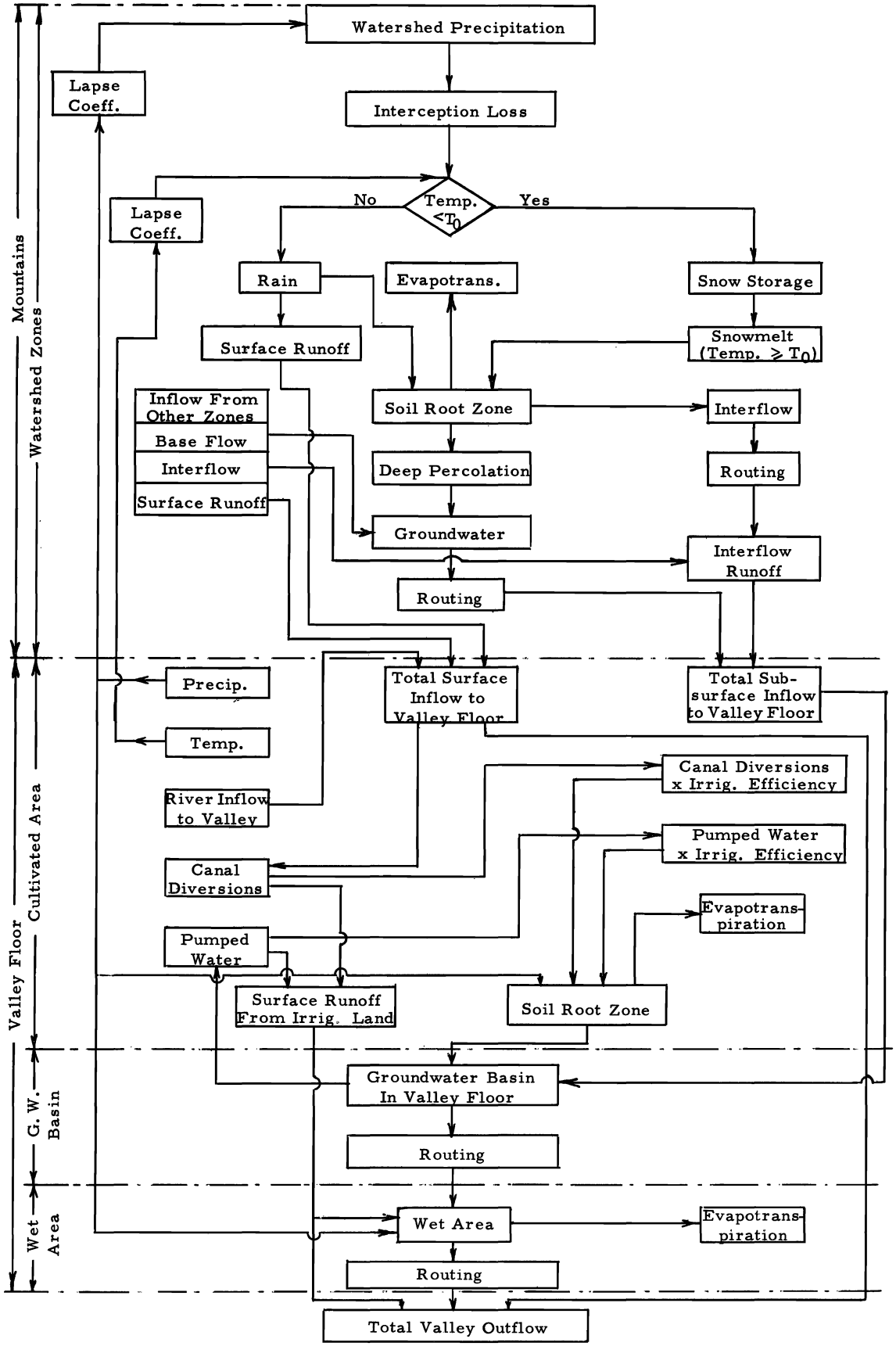

Figure 4.4. Hydrologic flow chart for the Circle Valley subbasin, Sevier River, Utah.

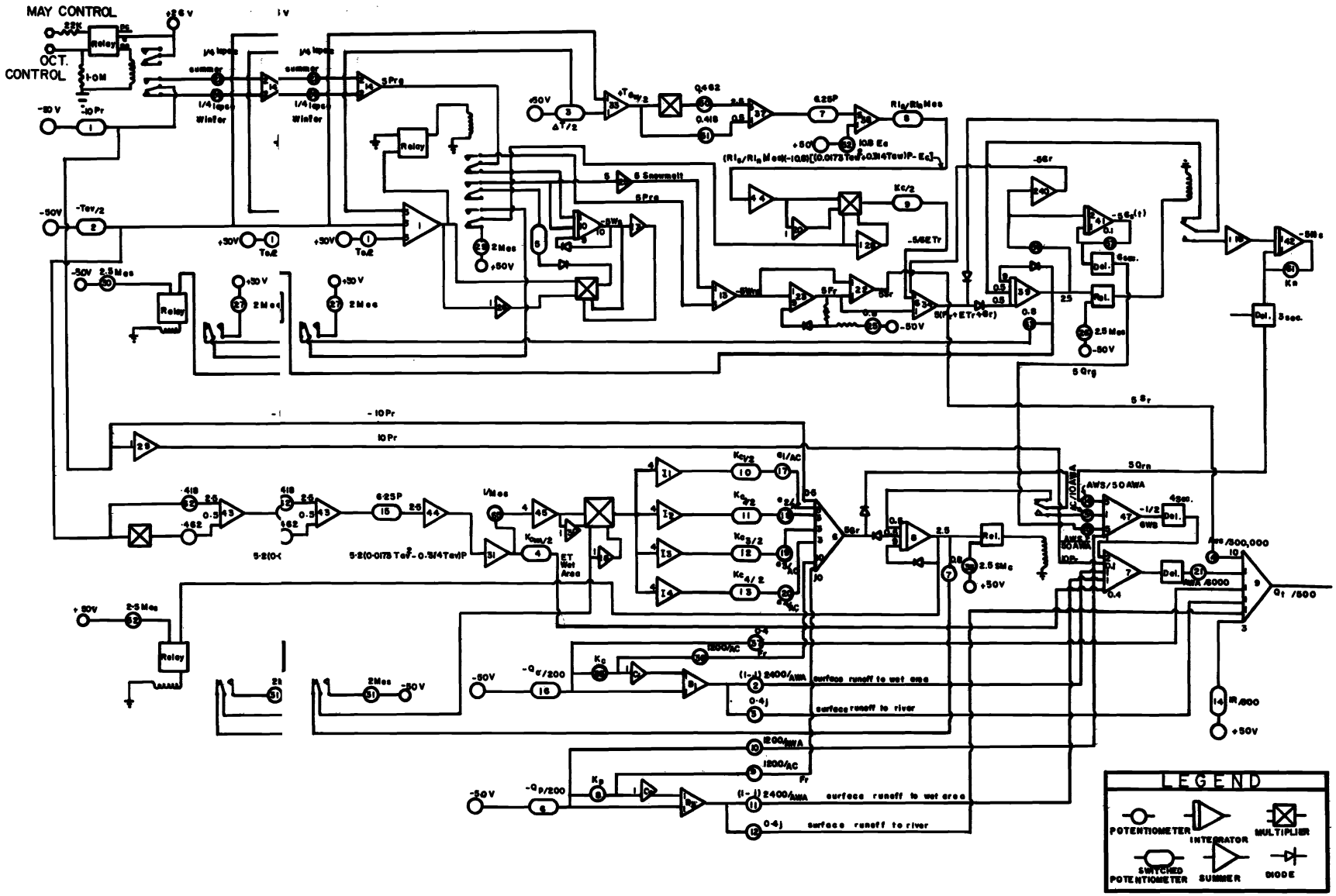

Figure 4.5. Analb. Analog flow diagram for the Circle Valley subbasin, Sevier River, Utah.

the relationships of figure 3.2 and table 3.1, respectively. Interception losses were computed from equation 3.2, using a value of 0.4 for k_i and a canopy density of 0.5. Calculations were also based on the assumptions that only coniferous vegetation contributes to interception losses during the winter months, whereas during the summer period these losses occur on both coniferous and deciduous types. Monthly interception losses for the west facet of the watershed were estimated at 0.025 P_r and 0.030 P_r during the winter and summer periods, respectively. Corresponding estimates for the east facet were 0.060 P_r and 0.070 P_r, respectively. Weighted on an area basis, monthly interception losses over the entire watershed were calculated as 0.044 P_r (winter) and 0.052 P_r (summer).

An estimate of monthly values of the radiation index applicable to the entire watershed was reached by first computing the radiation indexes for each of the two major facets into which the watershed had been divided. Since the area of each facet was approximately the same, composite values of the radiation index were obtained by a simple average of the corresponding monthly values for each of the two facets. The computations outlined in this paragraph are shown by figure B1 and table B1.

Other input values for Circle Valley are included within tables B2 and B3. Parameters which are applicable only to a particular year, such as temperature, precipitation, and flow measurements, are shown

by table B4. It will be noted that the data within this table are for the calendar years 1962 and 1963.

The computed and observed mean monthly outflow values for the year 1962 are shown by figure 4.6. This figure and all other graphs showing computer output in this chapter were plotted directly on the x-y variplotter which is connected to the analog computer. Points of discontinuity on many of the curves resulted from the input of information to the computer in digital format. Plots of the accumulated outflow quantities occurring in 1962, both computed and observed, are shown by figure 4.7. For this year output values were also plotted at various intermediate points within the system. These plots are shown as figures B2 to B9, inclusive. Because of the absence of data, a quantitative evaluation of this model at intermediate points was not possible. The figures included within appendix B do, however, illustrate that the model simulated on a continuous basis the major hydrologic processes which occur within the prototype basin. Therefore, the operation of these processes could be examined in detail. In cases where sufficient data exist, qualitative evaluations of simulation accuracy is possible for individual processes within the system.

Conditions existing at the end of 1962, such as accumulated snow,
curacy is possible for individual processes within the system.

Conditions existing at the end of 1962, such as accumulated snow, soil moisture, and groundwater flow, were applied as initial or antecedent conditions for operation of the model over the twelve months of 1963. Monthly and accumulated plots of the computed and observed

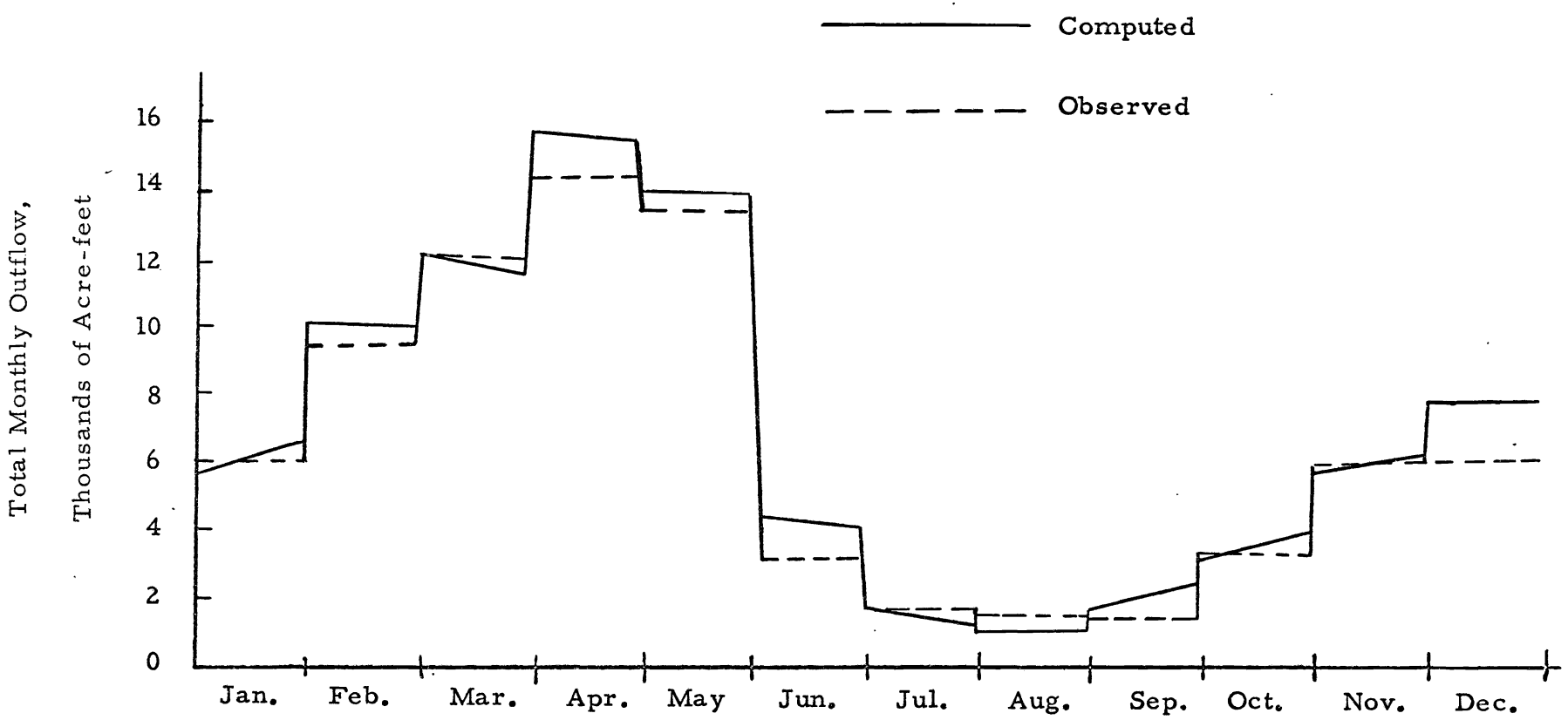

Figure 4. 6. Comparison between computed and observed monthly outflow from Circle Valley during 1962.

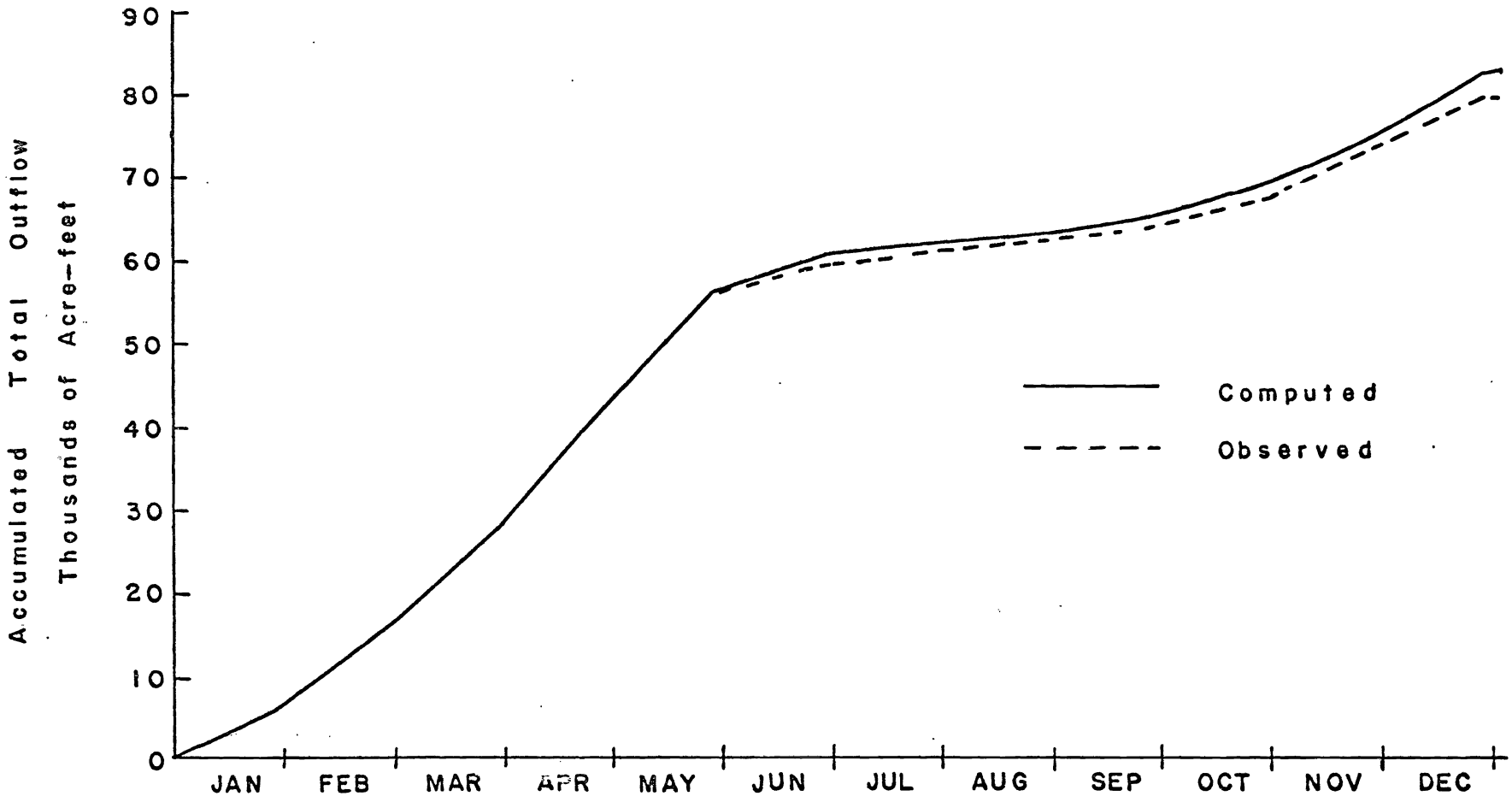

Figure 4.7. Comparison between computed and observed accumulated outflow from Circle Valley during 1962.

outflow values for that year are shown by figures 4.8 and 4.9, respectively. Values of computed snow storage equivalent on the watershed area during 1963 are shown by figure B10. It will be noted that during April there was no appreciable change in snow-water storage. This occurrence is explained on the basis that the mean temperature on the watershed for April was 41.2 F less a lapse of 5.9 F, or 35.3 F. Since the rate of snowmelt, as given by equation 3. 8 , is directly proportional to the difference $(T_a - T_0)$, a critical temperature, T_0, of 35 F yielded a negligible melt during this particular month. On the other hand, within the program precipitation during the month occurred in the form of rain.

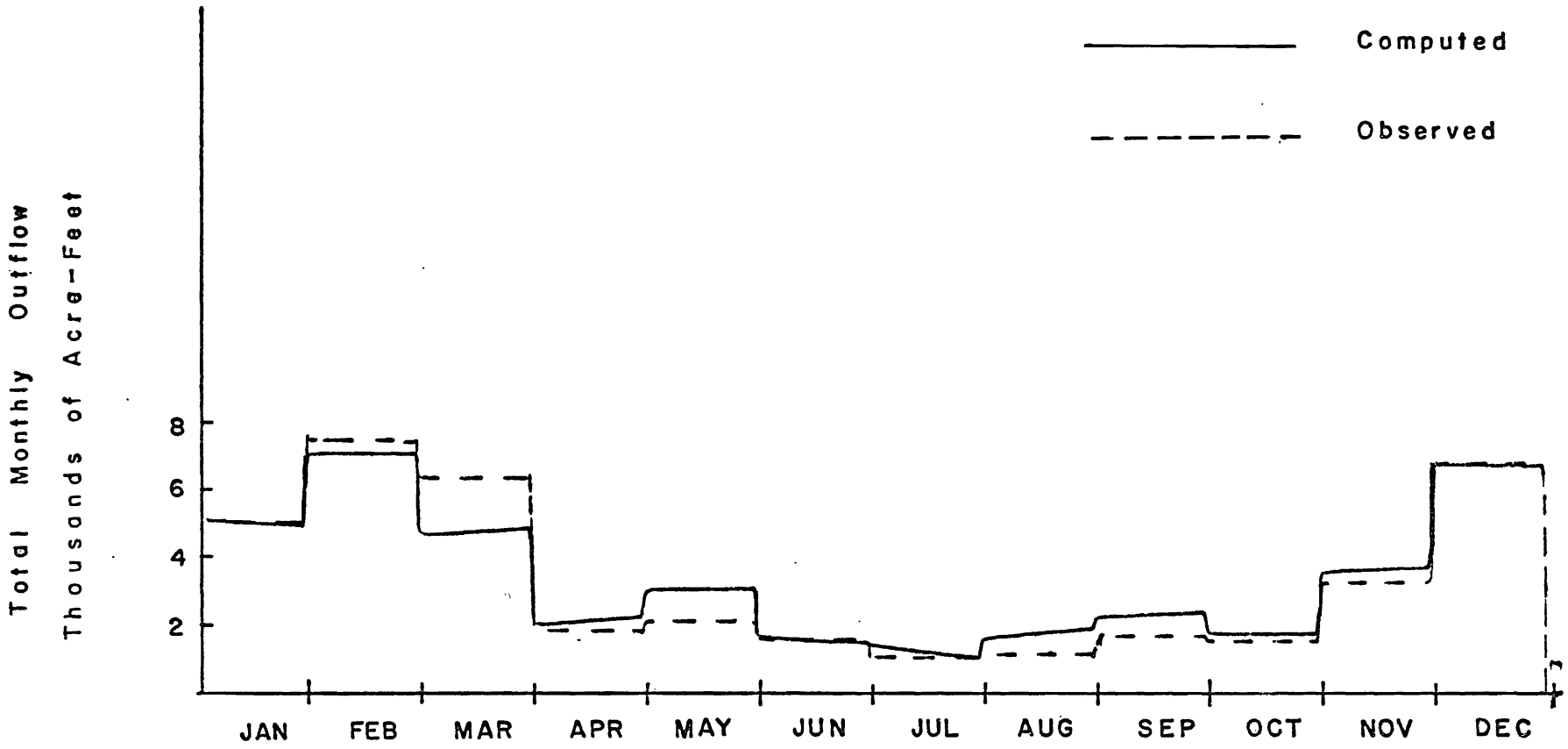

Figure 4. 8. Comparison between computed and observed monthly outflow from Circle Valley during 1963.

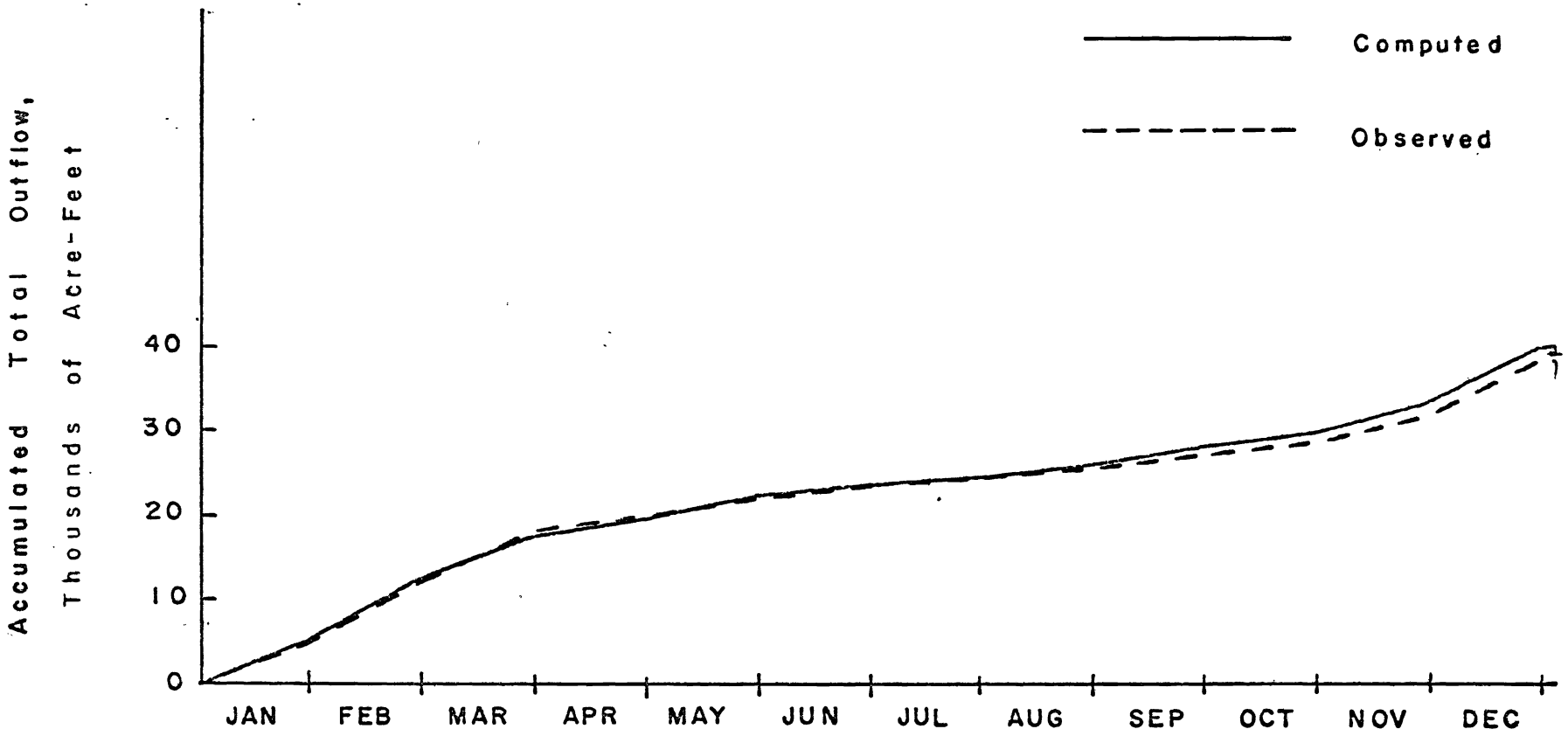

Figure 4.9. Comparison between computed and observed accumulated outflow from Circle Valley during 1963.

CHAPTER V

HYDROLOGIC MODEL BASED ON SMALL INCREMENTS OF TIME AND SPACE

The model discussed in this chapter represents the third phase of the hydrologic simulation program at Utah State University. A further increase in definition is achieved by considering small increments of both time and space. In the first and second models the time interval is in the order of one month or more, while in the third model this increment is taken to be in terms of a day, an hour, and even a few minutes. A chart showing the flow system logic of a model based on small increments of time and space is shown by figure 5.1.

Precipitation and temperature

In this model the problems involving input values of precipitation and temperature are similar to those of the first and second models. In each model the two parameters vary with respect to time and space. However, the variabilities of the parameters bear an inverse relation to the increment sizes utilized in the time and space dimensions, and the value of lapsing techniques is often somewhat doubtful for studies involving short increments of time and space. In these cases it is usually necessary to establish a network of temperature and precipitation recording stations within the area under study. Point information obtained from this network is then integrated using either the Thiessen weighting or the isograph technique (26).

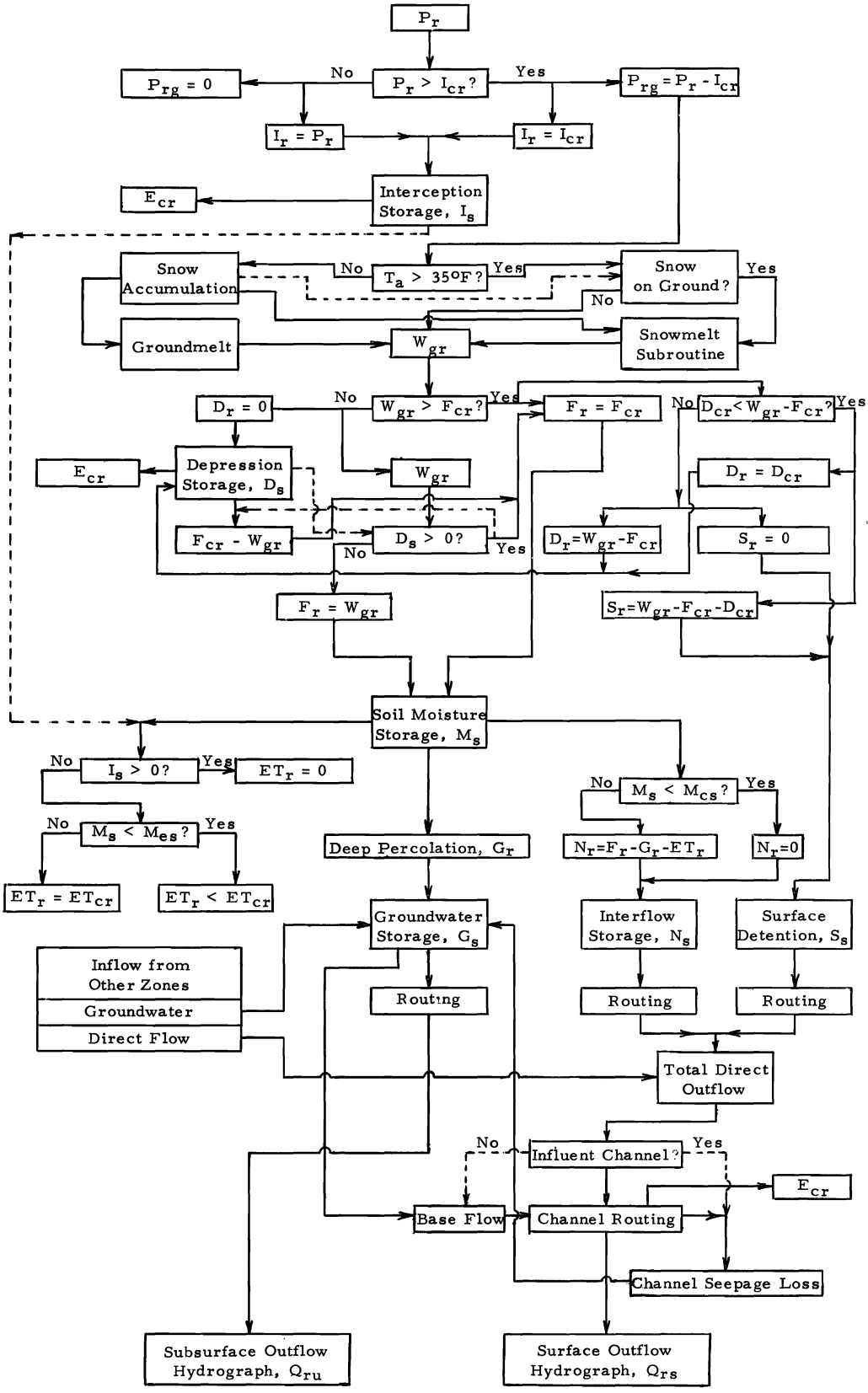

Figure 5.1. Flow diagram for a typical hydrologic model using small increments of time and space.

Interception loss

For a particular storm the magnitude of the interception loss is dependent upon both the interception storage capacity of the vegetative cover and the rate at which precipitation enters this form of storage. Interception storage capacity for a given area is dependent largely upon the type and density of vegetative cover and the relative extent of the vegetated land within the area. To a large degree these same factors also govern the rate at which precipitation enters this form of storage (49). For instance, in general terms, rather a small quantity of precipitation reaches the ground surface beneath a coniferous forest during the period of a storm before the interception storage capacity is filled. On the other hand, under a deciduous canopy the quantity of precipitation reaching the ground is usually appreciable during the initial interception period.

The total interception storage capacity of the forest cover on an area can be estimated by the following relationship:

$$I_{cs} = k_{is} C_d F_d \quad . \quad . \quad . \quad . \quad . \quad . \quad . \quad . \quad . \quad . \quad . \quad . \quad 5.1$$

in which

I_{cs} = total interception storage capacity of the vegetation expressed in terms of depth units, or water equivalent in the case of snow

k_{is} = a constant equal to the interception storage capacity under complete canopy cover

C_d and F_d are as defined for equation 3.2 . The value of F_d is given by equation 3.3 .

Experimental results (19, 49) indicate that an average value of k_{is} is 0.1 for both rain and snow falling on a coniferous cover, and also on deciduous vegetation during the summer months. The value of I_{cs} is computed for each zone and represents an input constant to the computer.

A likely form of the relationship between the quantity of precipitation stored as interception and time is shown by figure 5.2(a). Figure 5.2(b) is a plot of interception storage versus the slope of the curve of figure 5.2(a). This curve represents the maximum rate at which precipitation is able to enter interception storage, and therefore might be considered the interception capacity curve. Because the maximum rate of interception is a function of the interception storage at any time, t, it is expressed as follows:

$$I_{cr} = \frac{d[I_s(t)]}{dt} = k_i [I_{cs} - I_s(t)] \quad . \quad . \quad . \quad . \quad . \quad . \quad . \quad 5.2$$

in which all variables have been defined and k_i is a constant depending upon the type of vegetative canopy.

Some indication of the relative magnitude of k_i can be obtained by assuming a maximum interception capacity [obtained at $I_s(0) = 0$] of 0.05 inch per hour. If I_{cs} is assumed equal to 0.10 inch, equation 5.2 will yield a value of k_i equal to 2.0.

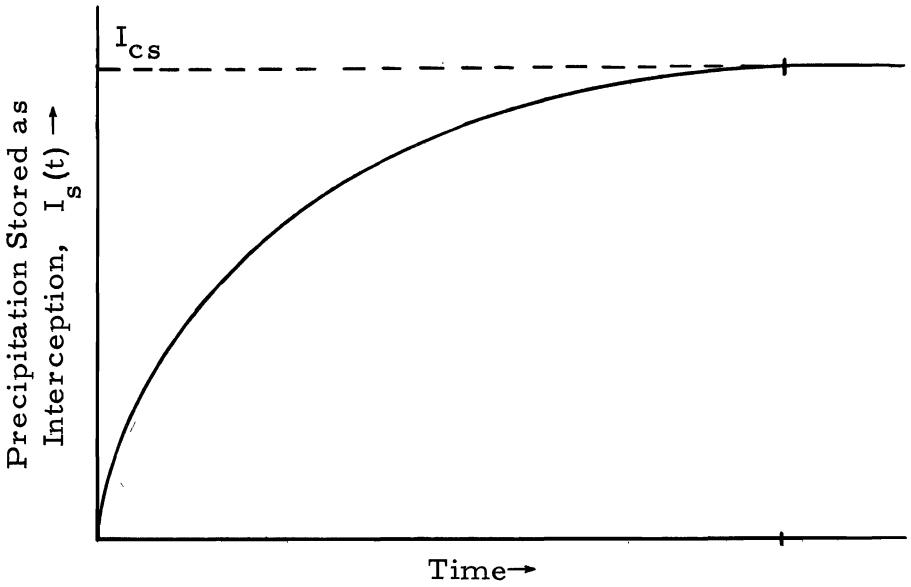

Figure 5.2(a). A qualitative plot of precipitation stored as interception as a function of time during a storm.

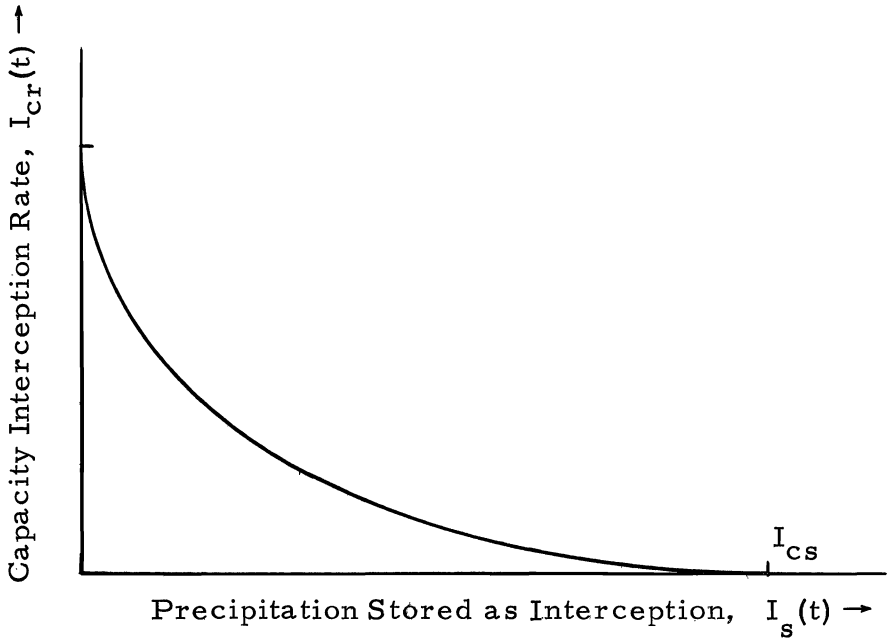

Figure 5.2(b). A qualitative plot of capacity interception rate as a function of the quantity of precipitation stored as interception.

Integration of equation 5.2 over a period of time, n, yields the expression:

$$I_s(n) = I_{cs} - (I_{cs} - I_o) \exp [-k_i(t_n - t_0)] \quad . \quad . \quad . \quad . \quad . \quad 5.3$$

in which I_o is the interception storage existing at time, t_0. It is emphasized, however, that $I_s(n)$ is not necessarily the quantity of precipitation actually added to interception storage during the period n. Equation 5.2 expresses the limiting or capacity rate at which precipitation is able to enter interception storage. Thus, the actual interception rate, I_r, is equal to this limiting value, I_{cr}, only at times when the rate of precipitation equals or exceeds I_{cr}. When this condition is not satisfied, the actual interception rate is equal to the coincident precipitation rate. Abstraction from interception storage occurs by evaporation, and because this is a continuous process it is possible that the total of interception losses during the entire period of a storm might considerably exceed the interception storage capacity, I_{cs}. Computation of the evaporation rate, E_{cr}, is discussed in a later section under the heading of "Evapotranspiration." It is noted here that withdrawal of moisture from the plant root zone by the process of transpiration is assumed not to occur during periods when any precipitation exists in interception storage.

In mathematical terms the foregoing discussion can be represented as follows:

$$I_s(t) = \int_0^t (I_r - E_{cr})dt + I_s(0) \quad . \quad . \quad . \quad . \quad . \quad . \quad . \quad . \quad 5.4$$

in which

$I_s(t)$ = the quantity of precipitation in interception storage at any time, t

$I_s(0)$ = the initial value of interception storage, or the quantity stored at $t = 0$

The value of I_r in equation 5.4 is established by the following two limiting relationships:

$$I_r = P_r \quad , \quad (P_r < I_{cr}) \quad . \quad . \quad . \quad . \quad . \quad . \quad . \quad . \quad 5.5$$

$$I_r = I_{cr} \quad , \quad (P_r \geq I_{cr}) \quad . \quad . \quad . \quad . \quad . \quad . \quad . \quad . \quad 5.6$$

in which I_{cr} is given by equation 5.2. During periods when the rate of precipitation is less than the evaporation rate, equation 5.4 indicates a loss from interception storage. This loss continues at a rate established by the difference $(I_r - E_{cr})$ until either this value again becomes positive or the interception storage is depleted.

It is obvious that at all times when P_r exceeds I_{cr} some precipitation reaches the ground in the form of either stemflow or throughfall or both. The net rate at which precipitation reaches the precipitation reaches the ground in the form of either stemflow or throughfall or both. The net rate at which precipitation reaches the ground surface is therefore expressed as follows:

$$P_{rg} = (P_r - I_{cr}) \quad , \quad (P_r > I_{cr}) \quad . \quad . \quad . \quad . \quad . \quad . \quad 5.7$$

$$P_{rg} = 0 \quad , \quad (P_r \leq I_{cr}) \quad . \quad . \quad . \quad . \quad . \quad . \quad . \quad . \quad . \quad 5.8$$

Ablation of the snowpack

For this model an attempt has been made to represent the various segments of the snow ablation process in a somewhat rational manner. A thoroughly rational approach to the problem of evaluating snowmelt involves a consideration of all three processes of heat transfer, namely radiation, convection, and conduction. The relative importance of each of these processes is highly variable, depending upon conditions of weather and local environment. For example, in late spring, given a clear day and fairly open terrain, radiation is the prime factor in the melting of snow. However, under conditions of heavy cloud cover or heavily forested terrain, radiation becomes a minor element. In the exposed areas wind is an important element in the convection process, while in heavily forested areas wind becomes a minor factor.

The sources of heat involved in the melting of snow are as follows (37, 49):

1. adsorbed solar radiation
2. net long wave (terrestrial) radiation
3. convection heat transfer from the air
2. net long wave (terrestrial) radiation
3. convection heat transfer from the air
4. latent heat of water vaporization by condensation from the air
5. conduction of heat from the ground
6. heat content of rain water

Rational formulas based upon the various factors listed in the preceding paragraph have been developed for snowmelt at a point. However, data required for the solution of these relationships are frequently lacking. For this reason and because of the complex nature of the process, in this model much reliance is still placed upon the empirical approach in the development of relations for predicting snowmelt. Many of the equations contained in this section were developed from published charts and other available sources of information, and heavy reliance was placed upon the sources of information cited. While these equations have not as yet been extensively tested, it is considered that they are sufficiently general in nature to permit their broad geographic application with perhaps appropriate adjustments in certain of the constants.

The two primary causes of snowpack ablation are net evaporation from the top surface of the pack and melting of the snow. Evaporation losses from snow surfaces have already been briefly discussed in Chapter III. Equation 3.15 is applied with a k_c value of 0.25. Values of the independent variables in this equation are, of course, those which apply to the particular time increment being utilized in the model. For short-term melt estimates, such as on a daily basis, it is necessary to take into account the temperature of the snowpack. Significant melt will not appear at the bottom of the pack until it has reached an isothermal temperature of 32F and its free water holding capacity has

been satisfied (49). Thus, it is necessary to predict at any time, t, both the temperature profile within the pack and its average free water holding capacity.

A flow chart of the snow accumulation and ablation processes is shown by figure 5.3. A very brief discussion of each segment of this process is presented herein. Consider first the following symbols:

A = albedo of the top surface of a snowpack

C_r = average rate of settlement of a snowpack

D = actual depth of the snowpack taking into account settlement, evaporation, and melt losses

D_a = depth of the snowpack taking into account settlement but neglecting evaporation and melt losses

D_{ao} = initial value of D_a or $D_a(o)$

D_m = minimum settled depth of the snowpack

L_c = free water holding capacity of the snowpack expressed as a fraction of its water equivalent

M_r = total melt rate of a snowpack, including both surface and ground melting

M_{rg} = groundmelt rate beneath the pack

M_{rs} = melt rate at the surface of the pack

M_{rg} = groundmelt rate beneath the pack

M_{rs} = melt rate at the surface of the pack

Q_f = quantity of free water held within a snowpack

ρ_i = initial density of newly fallen snow

ρ = average density, or average water equivalent per unit depth of the snowpack

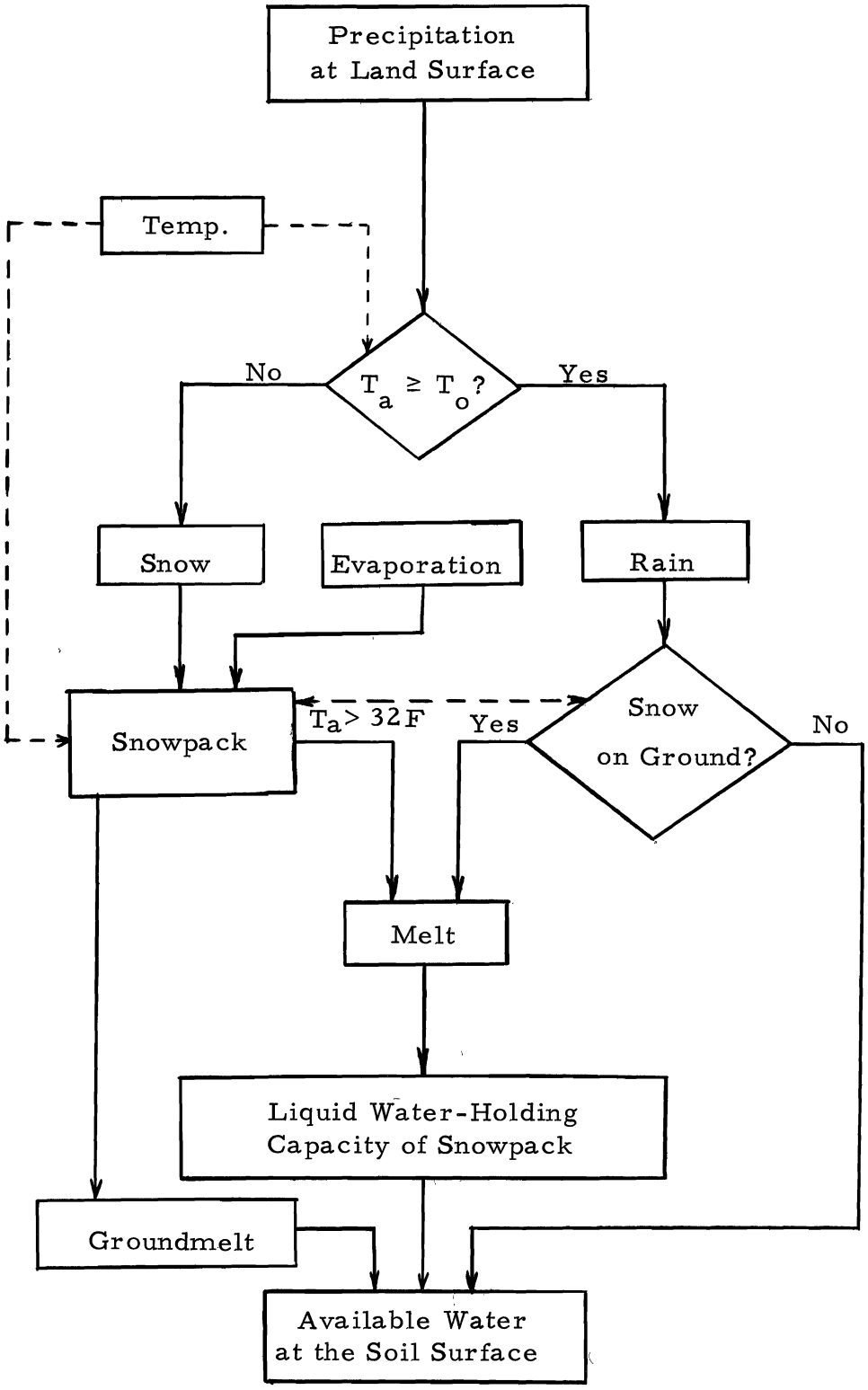

Figure 5.3. A flow chart of the snow accumulation and ablation process.

T = snow temperature at any point within the pack

W_s = actual water equivalent of the snowpack

W_a = total accumulated water equivalent of the snowpack neglecting evaporation and melt losses

W_{ao} = initial value of the total accumulated water equivalent of the snowpack, or $W_a(o)$

Free water holding capacity. The free water holding capacity of snow is the amount of water held within the pack at the time when snow surface melt first appears at the bottom of the pack. This capacity is a function of pack density and several other factors. Since these other factors are very difficult to evaluate, it is common to use a relationship which is a function of average snow pack density alone. Figure 5.4(a) indicates an approximation to a relationship developed by the U. S. Corps of Engineers (49). The following two equations express the relationship shown by this figure.

$$L_c(t) = 0.05\ W_s(t) \quad , \quad (\rho(t) \leq 0.40) \quad . \quad . \quad . \quad . \quad . \quad 5.9$$

$$L_c(t) = [0.1\rho(t) + 0.01]\ W_s(t) \quad , \quad [0.40 < \rho(t) \leq 0.60]$$

. . . . . 5.10

. . . . . 5.10

Snowpack density. The density of a snowpack is influenced in the main by two factors, namely, the density of new snow and the compaction and settling of existing snow. Studies at the Central Sierra Snow Laboratory (49) have shown that the density of new snow varies

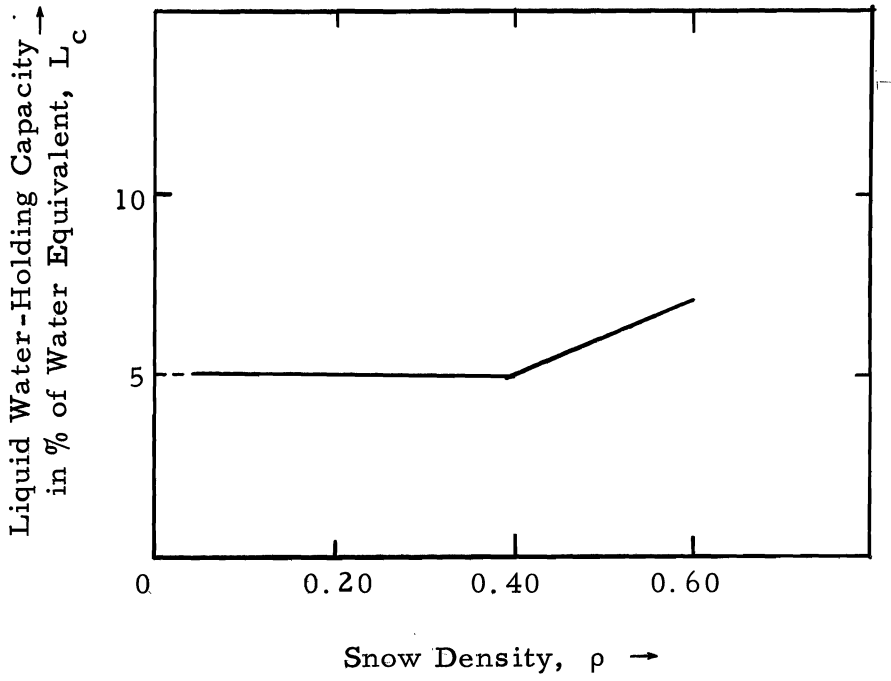

Figure 5.4(a). Liquid water-holding capacity of snow as a function of snow density.

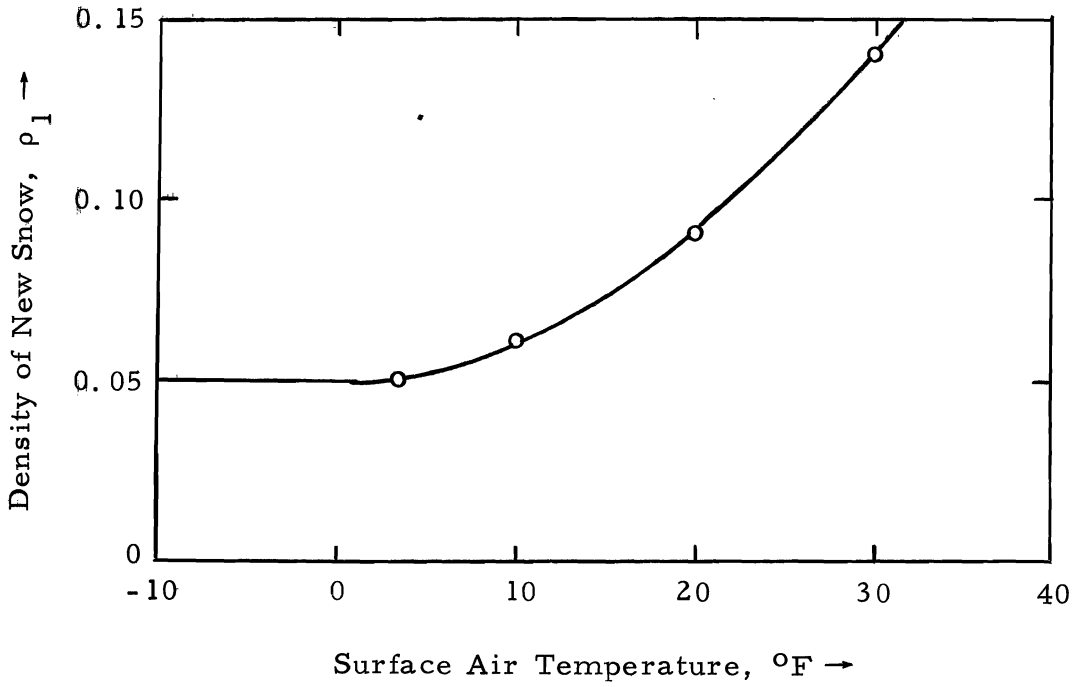

Figure 5.4(b). Density of new snow as a function of surface air temperature.

approximately with the surface air temperature [see figure 5.4(b)] . Thus

$$\frac{d\rho_i}{dT_a} = k_p T_a \quad . \quad . \quad . \quad . \quad . \quad . \quad . \quad . \quad . \quad . \quad . \quad . \quad 5.11$$

in which k_p is a constant equal to about 0.02. Therefore,

$$\rho_i = 0.05 \quad , \quad (T_a \leq 0F) \quad . \quad . \quad . \quad . \quad . \quad . \quad . \quad . \quad 5.12$$

and

$$\rho_i = 0.05 + (\frac{T_a}{10})^2 \quad , \quad (T_a > 0F) \quad . \quad . \quad . \quad . \quad . \quad 5.13$$

The average density of a pack may, of course, be obtained at any time, t, by taking the ratio of the water equivalent to the pack depth at time, t. Changes in snowpack depth are caused by melt, evaporation, snowfall, and settlement. However, it can be assumed with some degree of approximation that evaporation and melt do not cause changes in the average density of the pack. This parameter is then computed by the equation:

$$\rho(t) = \frac{W_a(t)}{D_a(t)} \quad . \quad . \quad . \quad . \quad . \quad . \quad . \quad . \quad . \quad . \quad . \quad . \quad 5.14$$

in which

$W_a(t)$

in which

$$W_a(t) = W_{ao} + \int P_{gr}\, dt \quad . \quad . \quad . \quad . \quad . \quad . \quad . \quad . \quad . \quad 5.15$$

For a given initial snow depth, the value of $D_a(t)$ is increased by

subsequent snowfalls and decreased by settlement of the pack. Observations (49) indicate that the settlement rate of a snowpack can be expressed as a function of the difference between the average pack density at any time and the maximum pack density. For a particular pack water equivalent this function is expressed as follows:

$$C_r(t) = \frac{d[D_a(t)]}{dt} = -k_{sc}[D_a(t) - D_m] \quad . \quad . \quad . \quad . \quad . \quad 5.16$$

in which k_{sc} represents the settlement time constant. An average maximum density for snow in a well-settled pack is approximately 60 percent (49). If this figure is assumed, the minimum settled depth of the pack, D_m, is given by:

$$D_m(t) = \frac{W_a(t)}{0.60} \quad . \quad . \quad . \quad . \quad . \quad . \quad . \quad . \quad . \quad . \quad . \quad 5.17$$

From equation 5.15, equation 5.17 can be written as:

$$D_m(t) = \frac{1}{0.60}\left[W_{ao} + \int_o^t P_{gr}\, dt \right] \quad . \quad . \quad . \quad . \quad . \quad 5.18$$

It is again emphasized that the depth given by equation 5.18 does not take into account evaporation and melt losses from the pack. $D_a(t)$ is given by the following expression:

$$D_a(t) = D_{ao} + \int_o^t \frac{P_{gr}\, dt}{\rho_i} + \int_o^t C_r\, dt \quad . \quad . \quad . \quad . \quad 5.19$$

A combination of equation 5.16 and 5.19 yields:

$$D_a(t) = D_{ao} + \int_o^t \frac{P_{gr}\, dt}{\rho_i} - k_{sc} \int_o^t [\, D_a(t) - D_m(t)]\, dt \quad . \; . \; . \; . \quad 5.20$$

If this equation is written in differential form and combined with equation 5.18, the result is as follows:

$$\frac{d[\, D_a(t)]}{dt} + k_{sc}\, D_a(t) = \frac{P_{gr}}{\rho_i} + \frac{k_{sc}}{0.60} [\, W_{ao} + \int_o^t P_{gr}\, dt] \quad . \; . \; . \; . \quad 5.21$$

The solution of equation 5.21 on the analog computer yields the value of $D_a(t)$ required in equation 5.14. It is noted that if a study is begun before the accumulation of any snow, $D_a(o) = D_{ao} = W_{ao} = 0$.

A test of equation 5.21 is illustrated by figure 5.5, which indicates both predicted and actual depths of a snowpack. The equation was applied on the basis of a daily time increment and k_{sc} was taken as being equal to 0.10. Evaporation and melt losses were assumed to be negligible during this test period.

Snowpack temperatures. A procedure for predicting the temperature profile within a snowpack needs to take into account not only the conduction of heat through the snow crystals, but also heat transferred into the pack from both rain and surface melt. Consider first the development of an expression to describe temperature conditions within the snowpack for given boundary values as a function of both depth and time. If it can be

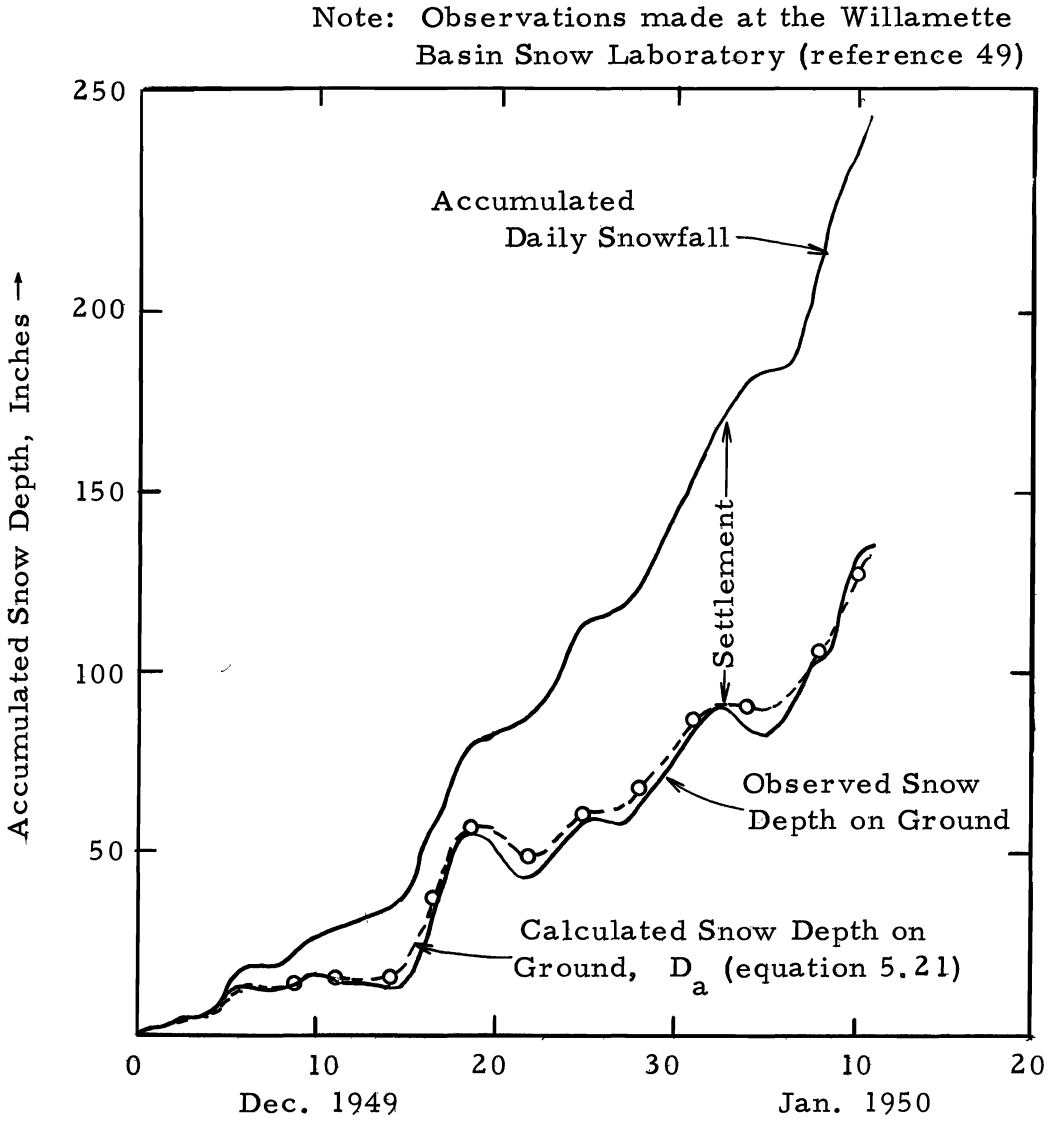

Figure 5.5 Comparison between observed and calculated settled snow depths.

assumed that lateral or horizontal heat transfer within the pack is negligible, then for a column of snow of finite diameter the conditions illustrated by figure 5.6(a) apply. With respect to boundary conditions, the top surface of the snow is assumed equal to the surface air temperature, T_a, for $T_a < 32$ F. For $T_a \geq 32$ F, the snow surface temperature is 32 F. Several studies have indicated that the temperature at the bottom of the pack is usually maintained at approximately 32 F by heat flow from the ground (14, 49). In its simplest form the problem then is characterized by one-dimensional heat flow in an assumed homogeneous column of snow of depth $D(t)$ with insulated sides. The value of $D(t)$ is given by

$$D(t) = \frac{W_s(t)}{\rho(t)} \quad . \quad . \quad . \quad . \quad . \quad . \quad . \quad . \quad . \quad . \quad . \quad . \quad . \quad 5.22$$

in which $\rho(t)$ is given by equation 5.14, and the value of $W(t)$ is given by the expression

$$W_s(t) = \int_0^t (P_{rg} - E_{cr} - M_r)\, dt \quad . \quad . \quad . \quad . \quad . \quad . \quad . \quad 5.23$$

in which P_{rg} is given by equation 5.4 and M_r by equation 5.41 which is presented later in this section. Evaporation losses from snow surfaces (E_{cr} in the above equation) are discussed in Chapter III.

The heat flow equation applicable to this problem is expressed in partial derivative form as follows (16):

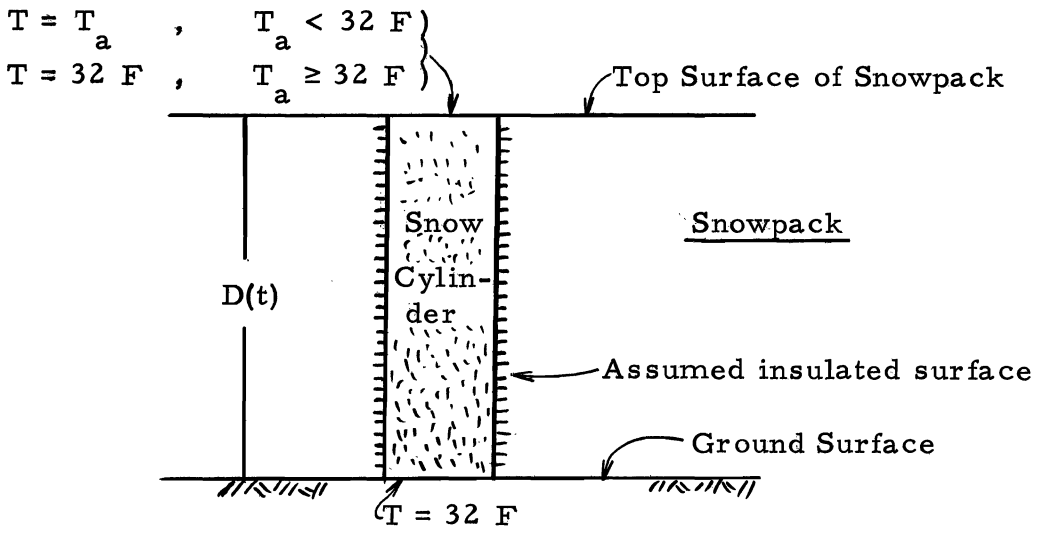

Figure 5.6(a). An assumed snow cylinder showing boundary temperature values.

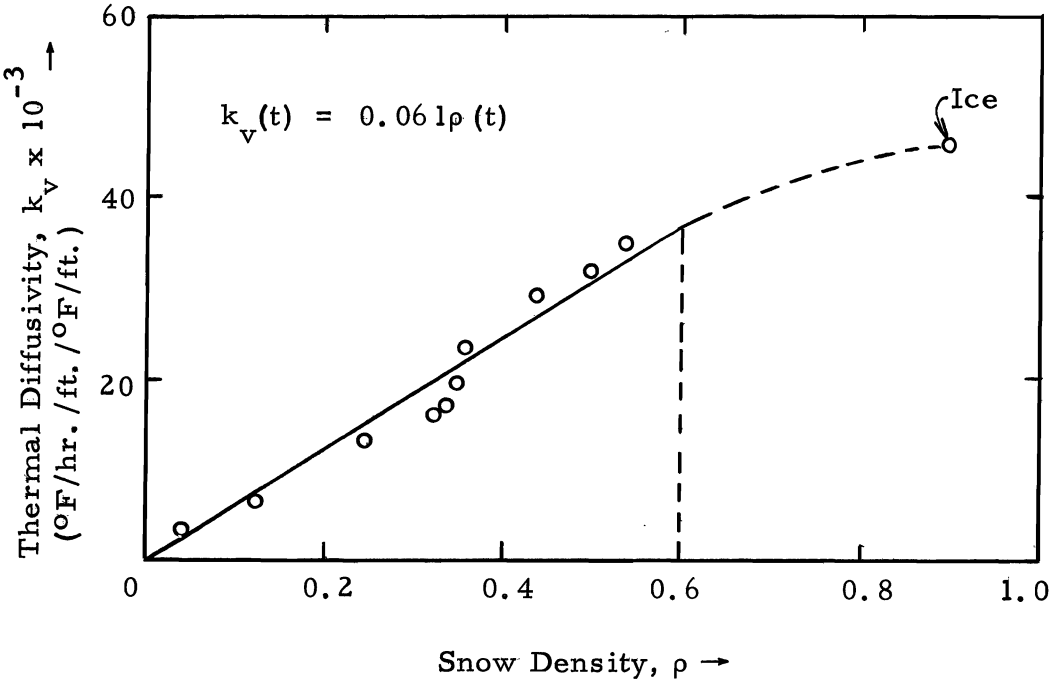

Figure 5.6(b). Thermal diffusivity of snow as a function of density.

$$\frac{\partial^2 T_s}{\partial Z^2} = \frac{1}{K_v} \frac{\partial T_s}{\partial t} \quad \ldots \ldots \ldots \ldots \quad 5.24$$

in which

Z = snow depth in feet

T_s = the snow temperature in degrees Fahrenheit

K_v = the thermal diffusivity of the snow in feet^2/time

The ever-changing thermal and physical properties of the snowpack make the theory of heat flow in snow much more complicated than is the case for a homogeneous solid. Thus, the factors which affect the thermal diffusivity of snow are its structural and crystalline character, the degree of compaction, the extent of ice planes, the degree of wetness, and the temperature of the snow (49). However, experimental work has shown that density is a generally satisfactory index of the thermal properties of the snowpack. Figure 5.6(b) illustrates the following empirical relationship between density and thermal diffusivity of snow (49).

$$K_v(t) = 0.061\,\rho(t) \quad , \quad (0 < \rho \leq 0.60) \quad \ldots \ldots \quad 5.25$$

It is recognized that there is an appreciable variation in snow

It is recognized that there is an appreciable variation in snow
density with depth, and that a more accurate approach to this problem would be to divide the snowpack into finite depth increments and to consider the entire melt process in each zone. This procedure would, however, require more analog computing equipment than is now

available. Further, it is anticipated that the results of the more approximate method will be sufficiently precise to permit an evaluation of the overall approach adopted.

The solution of equation 5.24 will predict both transient and steady-state temperatures with independent variables depth and time for given values of K_v, the thermal diffusivity of the material. However, the analog computer has only one dependent variable, voltage, and one independent variable, time. Therefore, the standard procedure for solving a partial differential equation such as equation 5.24 is to fix one of its independent variables, say distance, and to then solve the resulting ordinary differential equation. The point at which the depth Z is fixed is called a "node." By taking a sufficient number of nodes of the variable in the interval of interest, a set of curves is obtained which represent the solution of the partial differential equation. Thus, in this case, the partial derivatives with respect to Z are approximated by finite differences.

If the snowpack is divided into m equal depth zones, then the thickness of each zone is given by

$$\Delta Z(t) = D(t)/m \quad . \quad . \quad . \quad . \quad . \quad . \quad . \quad . \quad . \quad . \quad . \quad . \quad 5.26$$

$$\Delta Z(t) = D(t)/m \quad . \quad . \quad . \quad . \quad . \quad . \quad . \quad . \quad . \quad . \quad . \quad . \quad 5.26$$

in which the pack depth, $D(t)$, is given by equation 5.22. Now, the second partial derivative with respect to Z at the j-th node is approximated by the following finite difference equation (21):

$$\left.\frac{\partial^2 T}{\partial Z^2}\right|_j = \frac{\left.\frac{\partial T}{\partial Z}\right|_{(j+1)/2} - \left.\frac{\partial T}{\partial Z}\right|_{(j-1)/2}}{[\Delta Z(t)]} = \frac{\frac{T_{j+1} - T_j}{\Delta Z} - \frac{T_j - T_{j-1}}{\Delta Z}}{[\Delta Z(t)]}$$

$$= \frac{T_{j+1} - 2T_j + T_{j-1}}{\Delta Z(t)^2} = \left[\frac{m}{D(t)}\right]^2 (T_{j+1} - 2T_j + T_{j-1}) \quad . \quad 5.27$$

The absence of the fourth and all higher order differences indicates that equation 5.27 is the first approximation of the differential equation 5.24. Equation 5.27 can now be written

$$\frac{1}{K_v(t)} \frac{dT}{dt} + \frac{2T_j}{[\Delta Z(t)]^2} = \frac{T_{j+1} + T_{j-1}}{[\Delta Z(t)]^2} \quad . \quad . \quad . \quad . \quad . \quad 5.28$$

with boundary conditions:

$$T_1 = 32 \text{ F and } T_{m+1} = T_a(t) \quad , \quad T_a < 32 \text{ F}$$

$$T_1 = T_{m+1} = 32 \text{ F} \quad , \quad T_a \geq 32 \text{ F}$$

Initial conditions for the first application of this equation in each year are established at the time of the first snow fall of the season with $T_o = 32$ F and $T_j = T_{m+1}$.

As previously indicated, temperature changes within a snowpack result not only from conduction as expressed by equation 5.28, but also from the freezing within the pack of both rainwater and melt at the snow surface. Thus the temperature increase from this effect within the

j-th depth zone of the pack is given by

$$\frac{dT_j}{dt} = \frac{144}{W(t)/m} \left[M_{rs}(t) + P_{rg}(t) \right] \quad . \quad . \quad . \quad . \quad . \quad . \quad . \quad 5.29$$

In the case of the rain falling on snow the temperature of the rain is assumed to be equal to that of the surface air. For air temperatures in excess of 32 F there might be some question that the heat given up by the rain in cooling to 32 F should be included in the above equation. However, this heat contributes to surface melt, and is therefore included in the melt equation. In the event that the snowpack is not yet isothermal at 32 F, the precipitation and melt (now both at a temperature of 32 F) move downward through the pack until freezing occurs.

To illustrate the application of equations 5.28 and 5.29, assume that the snowpack has been divided into three equal depth zones (m = 3) as shown by figure 5.7. It is noted that temperatures T_1 and T_4 each represent one-sixth of the total pack depth, while T_2 and T_3 each represent temperatures in one-third of the pack. The determination of the total temperature changes at depth, j, during a particular period of time, n, proceeds as follows:

1. Using an initial temperature value of that existing at the end of the previous time period, $T_j(n-1)$, and boundary temperature values

1. Using an initial temperature value of that existing at the end of the

previous time period, $T_3(n-1)$, and boundary temperature values existing during the current period, compute $T_{3c}(n)$ by integrating equation 5.28 over the time period n. Note that the subscript c has been added to indicate a temperature due to the flow of heat by conduction.

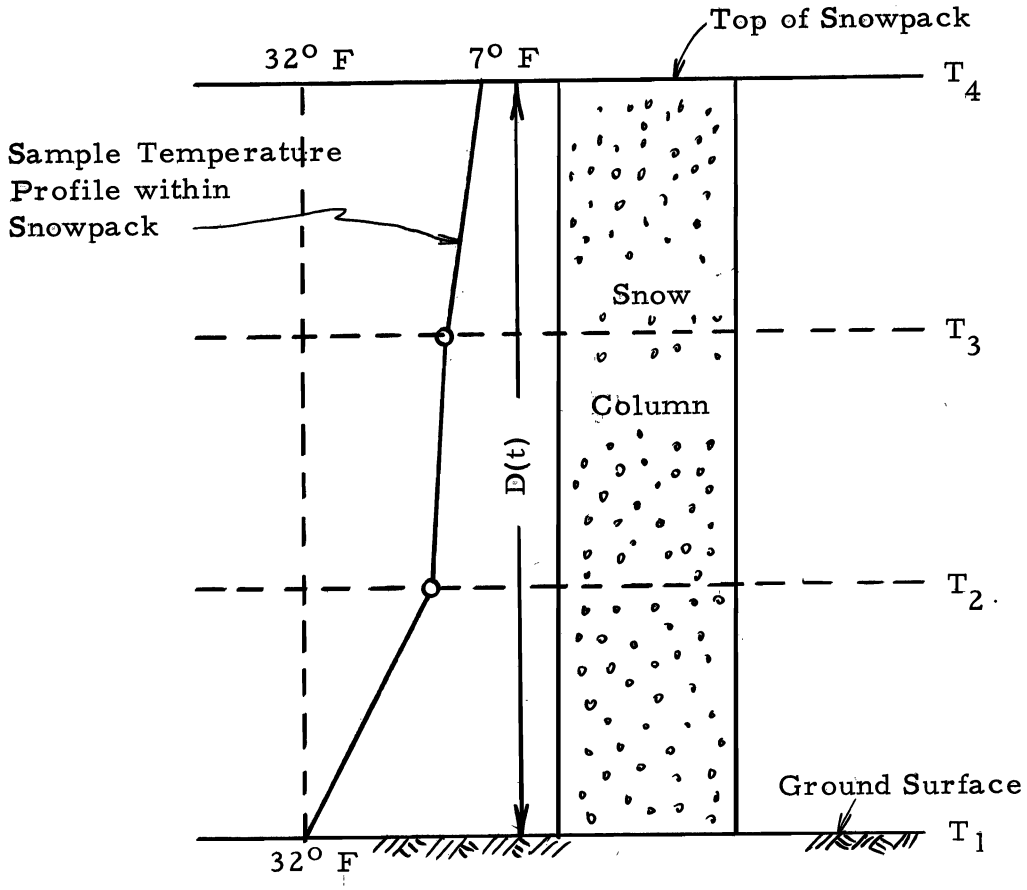

Notes: 1. Number of depth zones, m = 3.

2. Boundary conditions:

$T_4 = T_a$, $T_a < 32$ F

$T_4 = 32$ F, , $T_a \geq 32$ F

$T_1 = 32$ F

$T_1 = 32$ F

Figure 5.7. An example of finite depth increments within the snowpack.

2. Simultaneously apply equation 5.29 over the same time period, n, to determine the temperature change from the freezing of water within the pack, $\Delta T_{3f}(n)$.
3. Add $\Delta T_{3f}(n)$ to $T_{3c}(n)$ to obtain $T_3(n)$. If the result exceeds 32 F, $\Delta T_{2f}(n) = T_3(n) - 32$, and $T_3(n)$ is then set at 32 F. Now, $T_2(n) = \Delta T_{2f}(n) + T_{2c}(n)$.

Obviously, since T_1 is fixed by a boundary condition at 32 F, if $T_2(n)$ as computed above exceeds this value, it is set at 32 F and free water is available in the snowpack. If required, the quantity of this free water, $Q_f(n)$, could be estimated by the relationship

$$Q_f(n) = \frac{\Delta T_{1f}(n) + T_{1c}(n) - 32}{\Delta T_{2f}(n)} [M(n) + P_r(n)] \quad . \quad . \quad . \quad . \quad 5.30$$

For purposes of clarity the preceding illustration of a method of computing snowpack temperature changes has involved comparisons at the termination of a finite time interval. However, as already noted, on the analog computer processes occur continuously throughout the integration period. Thus, for example, if at any time, t, during a finite period of integration, the temperature at one level reaches 32 F, heat being given up by freezing water within the pack immediately begins

heat being given up by freezing water within the pack immediately begins to influence the temperature at the adjacent lower level. Similarly, as soon as the pack is brought to the isothermal state, any further water present in the pack does not freeze but rather enters the free water storage capacity of the snow as estimated by equations 5.9 and

5.10. When this capacity is satisfied, free water (in addition to ground-melt) appears at the bottom of the pack.

If, after a period of melting, the air temperature falls below the freezing point, heat contributions from equation 5.29 cease and pack temperatures at each level are computed only by equation 5.28. Under this situation the quantity of free water held by the pack is again set to zero.

Snowpack melt. Basically the calculation of melt is based on a degree-day factor. The base temperature selected for this computation is 32 F. Thus the rate of melt before any adjustments are made is given by (49, 50):

$$M_{rs} = F(T_a - 32) \quad . \quad . \quad . \quad . \quad . \quad . \quad . \quad . \quad . \quad . \quad . \quad 5.31$$

in which F is a rate factor expressed as inches per unit of time per degree F above 32 F.

As in the case of the evapotranspiration equation, the air temperature parameter is an index of the total insolation received on a regional basis, and the value of F in equation 5.31 will therefore vary with the degree of slope and aspect of the land surface. To provide an adjustment for this variation, the radiation index parameter was again utilized so that

of slope and aspect of the land surface. To provide an adjustment for this variation, the radiation index parameter was again utilized so that

$$F = k_m \left(\frac{RI_s}{RI_h}\right) \quad . \quad . \quad . \quad . \quad . \quad . \quad . \quad . \quad . \quad . \quad . \quad 5.32$$

in which k_m is a constant of proportionality.

As before noted, in the northern hemisphere, the ratio RI_s/RI_h decreases on northerly slopes with decreases in solar declination, while for southerly slopes the ratio increases with decreasing declination. Thus, on northerly slopes equation 5.32 will yield less melt per degree of temperature above 32 F in the winter months than in the spring months. The reverse of this situation will apply for south-facing slopes. These results are in agreement with actual observations (1, 49).

Now, by combining equations 5.31 and 5.32, the melt equation becomes

$$M_{rs} = k_m \frac{RI_s}{RI_h} (T_a - 32) \quad . \quad . \quad . \quad . \quad . \quad . \quad . \quad . \quad . \quad 5.33$$

The effect of vegetative cover on snowmelt can be taken into account by the use of a solar radiation transmission coefficient for vegetation. Studies by the Corps of Engineers (49, 50) indicate the relationship between the effective cover coefficient, C_v (defined by equation 3.6), and the vegetation transmission coefficient, K_v, to be of the form:

$$K_v = \exp(-4C_v) \quad . \quad . \quad . \quad . \quad . \quad . \quad . \quad . \quad . \quad . \quad . \quad . \quad 5.34$$

The melt equation is now written thus:

$$M_{rs} = k_m K_v \left(\frac{RI_s}{RI_h}\right) (T_a - 32) \quad . \quad . \quad . \quad . \quad . \quad . \quad . \quad . \quad . \quad 5.35$$

The albedo, or reflectivity, of the snowpack is important in estimating the amount of solar radiation absorbed by the pack. Albedo

is expressed as the ratio of reflected shortwave radiation to that incident on the snow surface. Values range from about 0.80 for newly fallen snow to as little as 0.40 for melting, late-season snow (37, 49, 51). This decrease in albedo may be expressed as a function of time in the differential form

$$\frac{dA}{dt} = -k_a \left[A(t) - 0.40 \right] \quad , \quad \left[0.40 \leq A(t) \leq 0.80 \right] \quad . \quad 5.36$$

The integrated form of this equation is as follows:

$$A(t) = 0.40 \left(1 + e^{-k_a t}\right) \quad . \quad . \quad . \quad . \quad . \quad . \quad . \quad . \quad . \quad . \quad 5.37$$

The value of the time constant, k_a, is about 0.20. Both equations 5.36 and 5,37 are subject to the two conditions that a fall of new snow returns the value of $A(t)$ to 0.80, and the occurrence of rain causes the value of $A(t)$ to equal 0.40. A comparison of equation 5.37 with an experimentally determined curve (51) is shown by figure 5.8.

The effect of albedo is now included by modifying equation 5.35 as follows:

$$M_{rs} = k_m K_v \left(\frac{RI_s}{RI_h}\right) (T_a - 32) (1 - A) \quad . \quad . \quad . \quad . \quad . \quad . \quad 5.38$$

$$M_{rs} = k_m K_v \left(\frac{\upsilon}{RI_h}\right) (T_a - 32) (1 - A) \quad . \quad . \quad . \quad . \quad . \quad . \quad 5.38$$

Finally, the adjustment of this equation to include the effect of rain falling on a snowpack is accomplished by assuming the temperature of the rain to be equal to that of the air. Thus,

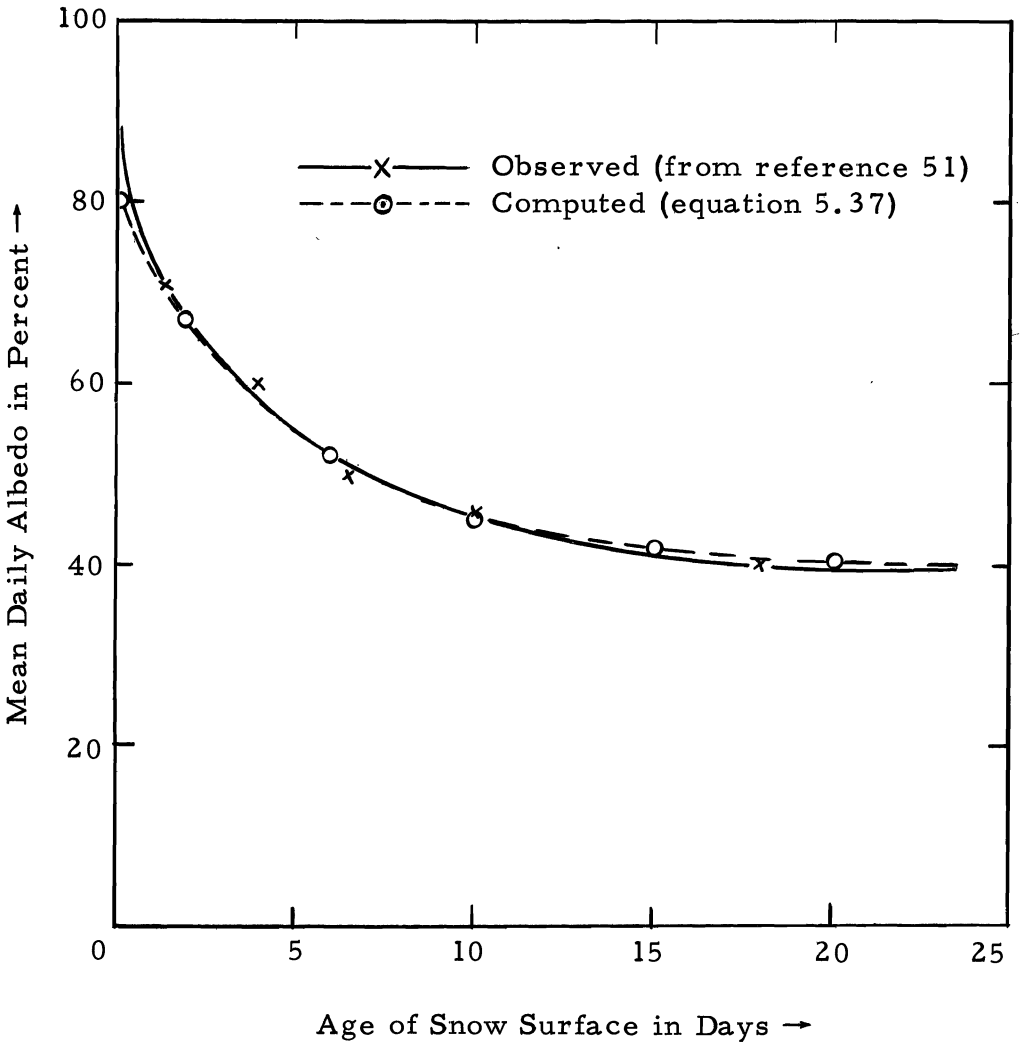

Figure 5.8. A comparison between observed and computed snow surface albedo.

Figure 5.8. A comparison between observed and computed snow surface albedo.

$$M_p = (T_a - 32) \frac{P_{rg}}{144} \quad . \quad . \quad . \quad . \quad . \quad . \quad . \quad . \quad . \quad . \quad 5.39$$

The equation for surface melt then becomes

$$M_{rs} = k_m K_v \left(\frac{RI_s}{RI_h}\right) (T_a - 32)(1 - A) + (T_a - 32) \frac{P_{rg}}{144} \quad . \quad 5.40$$

It should be noted that for each watershed zone a uniform depth of snowpack is assumed to exist throughout the entire winter and snowmelt season. Thus no adjustment is made for partial snow cover over a zone.

A preliminary estimate of the value of the constant k_m in the preceding equations was obtained by applying equation 5.38 to the watershed of the Central Sierra Snow Laboratory (49, 50). This watershed is situated at a latitude of 39^o 22' north, has a mean elevation of approximately 7,500 feet, and an average aspect of about 11 degrees west of due south, and an average slope of approximately 13 percent. An average value of F (equation 5.31) for melt at a point under no forest cover during the snowmelt period has been determined as being 0.106 inch per day per degree day, based on mean daily temperatures. The average declination of the sun during the snowmelt period was 10 degrees. From this information values of RI_s and RI_h were established as being equal to 57 and 55 respectively. The vegetation transmission coefficient, K_v, applicable to the snow courses was estimated to be 0.43 and the value of the albedo during the melt period was assumed at 0.40.

Now substituting in equation 5.38, $0.106 = k_m (0.43 \frac{0.57}{0.55} (1)$ $(1 - 0.40)$ from which $k_m \simeq 0.40$.

The value of k_m computed by the same procedure for the Willamette Basin Snow Laboratory was also approximately equal to this figure.

A uniform groundmelt rate, M_{rg}, of 0.02 inch per day is assumed to occur (1, 37, 49) and this quantity is added to that portion of the surface melt appearing at the bottom of the pack. Thus, total melt, M_r, is given by

$$M_r = M_{rs} + M_{rg} \quad . \quad . \quad . \quad . \quad . \quad . \quad . \quad . \quad . \quad . \quad . \quad . \quad 5.41$$

From this point both snowmelt water and rain falling directly on bare ground enter the soil at an infiltration rate characteristic of the soil, with any surplus water forming surface runoff. The surface runoff component first must satisfy an estimated depression storage requirement for the zone. Additional surface runoff beyond this requirement is then routed off the watershed.

Surface runoff

Surface runoff

Surface runoff from a watershed zone occurs when the rate at which water is available on the soil surface exceeds the sum of the infiltration capacity rate and the rate at which water is able to enter depression storage. Thus:

$$S_r = W_{gr} - F_{cr} - D_{cr} \quad , \quad (S_r \geq 0) \quad . \quad . \quad . \quad . \quad . \quad . \quad 5.42$$

This part of the hydrologic cycle constitutes what is sometimes called the land phase of surface runoff (14). Surface runoff joins with interflow to create the hydrograph of direct runoff from the zone.

Depression storage

Inflow to depression storage occurs when the rate of supply, as represented, for example, by precipitation less interception, exceeds the infiltration capacity of the soil. Losses from this form of storage occur as evaporation and infiltration.

The characteristics of depression storage are very similar to those of interception storage in that the capacity rates of inflow to both forms decrease throughout the period of a storm. As the more shallow ground depressions within the precipitation area become filled, the rate of depression storage increase decreases and consequently, for a particular supply rate, the rate of surface runoff increases. In general terms, the rate of depression storage increase becomes less with time and is a function of the quantity in storage. Thus, the maximum or limiting rate at which precipitation enters depression storage can be

and is a function of the quantity in storage. Thus, the maximum or limiting rate at which precipitation enters depression storage can be

given by an expression of the form:

$$D_{cr} = \frac{dD_s}{dt} = k_d \left[D_{cs} - D_s(t) \right] \quad . \quad . \quad . \quad . \quad . \quad . \quad . \quad . \quad 5.43$$

in which

k_d is a constant depending upon the size distribution of the various depressions within the zone, and

$D_s(t)$ is given by the following expression:

$$D_s(t) = (D_r - E_{cr})\,dt + D(o) \quad . \quad . \quad . \quad . \quad . \quad . \quad . \quad . \quad . \quad 5.44$$

The value of D_r in equation 5.44 is established by the three limiting relationships:

$$D_r = 0 \quad , \quad 0 \geq (W_{gr} - F_{cr}) \quad . \quad . \quad . \quad . \quad 5.45$$

$$D_r = (W_{gr} - F_{cr}) \quad , \quad 0 < (W_{gr} - F_{cr}) < D_{cr} \quad . \quad . \quad 5.46$$

$$D_r = D_{cr} \quad , \quad (W_{gr} - F_{cr}) \geq D_{cr} \quad . \quad . \quad . \quad . \quad 5.47$$

If the value of $(W_{gr} - F_{cr})$ exceeds D_{cr}, surface runoff occurs at rates established by equation 5.42. On the other hand, if the value of this expression lies between zero and D_{cr}, the entire rate of flow as represented by the expression enters depression storage. A net reduction of water in depression storage occurs when the quantity $(D_r - E_{cr})$ in equation 5.44 becomes negative. This reduction continues until either this quantity again becomes positive or depression storage is depleted. Evapotranspiration losses, which are assumed to occur only after the interception storage is depleted, are drawn from the soil moisture within the plant root zone.

Infiltration

There is a maximum rate at which water can enter the soil at a particular point under a given set of conditions, and this rate is usually called the infiltration capacity. Soil infiltration capacity depends on many factors, such as soil type, moisture content, organic matter, vegetative cover, and season (26). Of the soil factors affecting infiltration, noncapillary porosity is perhaps the most important. Porosity determines storage capacity and also affects resistance to flow. Thus infiltration rates tend to increase with porosity. A typical infiltration curve is depicted by figure 5.9. It will be noted that the infiltration capacity, F_{cr}, is at a maximum value, which depends upon the initial soil moisture content at the beginning of a storm, and approaches a low, relatively constant rate, F_c, as the soil profile becomes saturated. The value of F_c is controlled by the subsoil permeability.

The initial curved portion of the infiltration capacity curve might be approximated by the following empirical expression:

$$F_{cr} = \frac{dM_s}{dt} = \frac{k_f}{R} [M_{fs} - M_s(t)] \quad . \quad . \quad . \quad . \quad . \quad . \quad 5.48$$

which is subject to the boundary conditions $0 < M_{cs} > M_{fs}$ and $0 \leq$

which is subject to the boundary conditions $0 < M_{cs} > M_{fs}$ and $0 \leq$

$M_s(t) < M_{cs}$, and in which

k_f = a constant which is dependent upon both soil type and soil surface conditions

R = the average depth of the rooting zone

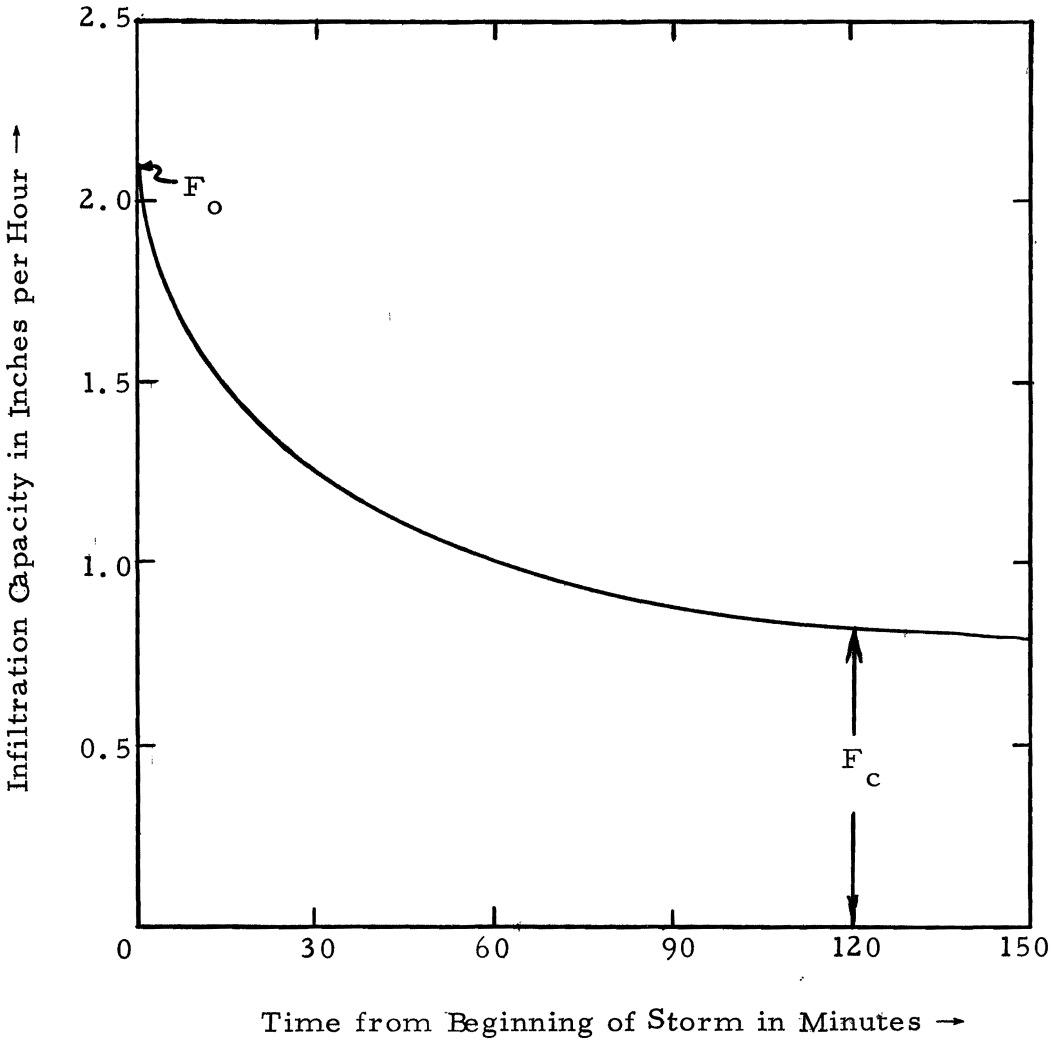

Figure 5.9. A typical infiltration capacity curve expressed as a function of time.

Figure 5.9. A typical infiltration capacity curve expressed as a function of time.

M_{fs} = a limiting soil moisture value which exceeds the soil storage capacity of available water

The value of $M_s(t)$ in equation 5.48 is given by the following expression:

$$M_s(t) = \int_o^t dM_s(t)\, dt = \int_o^t (F_r - ET_r - G_r)\, dt + M_s(0) \quad . \quad . \quad . \quad . \quad . \quad . \quad . \quad . \quad 5.49$$

in which $0 \leq ET_r \leq ET_{cr}$ and $0 \leq F_r \leq F_{cr}$. F_r is given by the two limiting equations:

$$F_r = F_{cr} \quad , \quad [D_s(t) > 0] \quad . \quad . \quad . \quad . \quad . \quad . \quad . \quad . \quad . \quad 5.50$$

$$F_r = W_{gr} \quad , \quad [D_s(t) = 0] \quad . \quad . \quad . \quad . \quad . \quad . \quad . \quad . \quad . \quad 5.51$$

ET_r in equation 5.49 is given by equation 3.20, and G_r by equation 3.24.

The total infiltration quantity, F, during a period of time, t, is given by the equation:

$$F = \int_o^t F_r\, dt \quad . \quad . \quad . \quad . \quad . \quad . \quad . \quad . \quad . \quad . \quad . \quad . \quad . \quad 5.52$$

in which F_r is defined by equations 5.50 and 5.51. As an example of the application of equation 5.52, if equation 5.50 were assumed to apply over a period of time, n, the total infiltration occurring during this period would be given by an integration of equation 5.48 as follows:

$$F(n) = M_{fs} - [M_{fs} - M_s(t_o)] \exp[-k_f (t_n - t_o)] \quad . \quad . \quad . \quad 5.53$$

in which $M_s(t_o)$ represents the available soil moisture level at the beginning of the period. The equation is, of course, subject to the same boundary conditions as equation 5.48.

The horizontal portion of the infiltration curve begins when the level of the soil moisture available to plants reaches its capacity value, M_{cs}, and is represented by the simple expression

$$F_{cr} = F_c \quad , \quad [M_s(t) = M_{cs}] \quad . \quad . \quad . \quad . \quad . \quad . \quad . \quad 5.54$$

When the condition of equation 5.54 is satisfied, equation 5.48 can be written in the form

$$F_{cr} = F_c = \frac{k_f}{R}(M_{fs} - M_{cs}) \quad , \quad [M_s(t) = M_{cs}] \quad . \quad 5.55$$

With an appropriate value for M_{fs}, equation 5.48 therefore defines the infiltration capacity curve through all ranges of soil moisture. For a soil moisture level equal to zero, the equation is of the particular form

$$F_o = \frac{k_f}{R}(M_{fs}) \quad , \quad [M_s(t) = 0] \quad . \quad . \quad . \quad . \quad . \quad . \quad 5.56$$

Now, if, for example, the values F_c, F_o, M_{cs}, and R can be estimated on the basis of soil type, soil surface conditions, and crop Now, if, for example, the values F_c, F_o, M_{cs}, and R can be estimated on the basis of soil type, soil surface conditions, and crop variety, equations 5.55 and 5.56 can be solved simultaneously for values of M_{fs} and k_f.

It should again be emphasized that equation 5.48 establishes the maximum rate at any time at which water is able to enter the soil

through infiltration. If the rate of supply is less than $F_{cr}(t)$, the infiltration rate will, of course, be equal to the supply rate. On the other hand, when the supply rate equals or exceeds $F_{cr}(t)$, infiltration occurs at this limiting rate. Under these conditions all excess water is held on the ground surface in the form of either depression storage or surface runoff.

Evapotranspiration

Evapotranspiration rates, ET_r, are estimated by equation 3.20. In the case of direct evaporation, E_{cr}, equation 3.15 is applied with k_c being taken as equal to 1.0 for water surfaces and 0.25 for snow and bare ground. Values of the various independent parameters and constants in these equations are, of course, those which apply to the particular time and space increments utilized in the model. As previously indicated, transpiration withdrawal from soil moisture is assumed to be negligible during periods when interception exists on plant surfaces.

Deep percolation

Deep percolation is given by equation 3.24, again using units which are applicable to the time scale of the model.

are applicable to the time scale of the model.

Interflow

As with evapotranspiration and deep percolation the expressions presented for the model of Chapter III also apply to models involving short increments of time and space. Thus, equations 3.26 and 3.27 express interflow rate at any time.

Routing or translation

In this section relationships are presented for describing the movement of water in the regimes of surface flow, interflow, and groundwater flow. If verification studies indicate that a time shift in any of the outflow hydrographs from these regimes is required, the shift is accomplished on the analog computer by means of appropriate transport delay networks.

Channel flow. Surface runoff from a watershed occurs first as overland flow, sometimes called the land phase (23), and secondly as channel flow. The time distribution of outflow from surface detention storage (land phase) within a watershed zone might be approximated by the following general expression:

$$q_{rs} = k_s S_s(t) \quad . \quad . \quad . \quad . \quad . \quad . \quad . \quad . \quad . \quad . \quad . \quad . \quad 5.57$$

in which k_s is a constant characteristic of surface conditions and slope within the watershed zone, and surface detention storage is given by

$$S_s(t) = \int (S_r - q_{rs})\, dt \quad . \quad . \quad . \quad . \quad . \quad . \quad . \quad . \quad . \quad . \quad 5.58$$

in which the value of S_r is given by equation 5.42. Using the differ-

in which the value of S_r is given by equation 5.42. Using the differ-

ential form of equation 5.58 and substituting into it equation 5.57 yields the equation

$$q_{rs} + \frac{1}{k_s} \frac{d}{dt} (q_{rs}) = S_r \quad . \quad . \quad . \quad . \quad . \quad . \quad . \quad . \quad 5.59$$

The solution of this differential equation provides an estimate of the required flow rate, q_{rs}.

Several techniques for the routing of surface runoff in the channel phase are described in the literature. Many of these techniques are based upon the familiar continuity of mass principle in which the stream channel is considered as a series of reaches with the length of a given reach being established by the channel distance between the upstream and downstream boundaries of the particular watershed zone in which the reach is situated. Thus, for a particular reach, channel inflow and outflow are related by the following differential equation:

$$i_r \, dt - q_{rc} \, dt = d[\, C_s(t)] \quad . \quad . \quad . \quad . \quad . \quad . \quad . \quad . \quad . \quad 5.60$$

Expressed as an indefinite integral, equation 5.60 appears as

$$C_s(t) = \int (i_r - q_{rc}) \, dt \quad . \quad . \quad . \quad . \quad . \quad . \quad . \quad . \quad . \quad 5.61$$

The form of equation 5.61 is identical to that of equation 5.58 and others which have already appeared in this paper. The channel outflow rate, q_{rc}, is expressed as a function of the channel storage, thus:

$$q_{rc} = k \, C_s \, (t) \quad . \quad . \quad . \quad . \quad . \quad . \quad . \quad . \quad . \quad . \quad . \quad 5.62$$

$$q_{rc} = k \, C_s \, (t) \quad . \quad . \quad . \quad . \quad . \quad . \quad . \quad . \quad . \quad . \quad . \quad 5.62$$

Laurenson (24) expressed equation 5.62 in the form

$$C_s(t) = k' \, q_{rc} \quad . \quad . \quad . \quad . \quad . \quad . \quad . \quad . \quad . \quad . \quad . \quad 5.63$$

in which C_s is expressed in cubic feet, q_{rc} in cubic feet per second, and k' in seconds. In tests conducted on a watershed near Sidney, Australia, he found the value of k' in equation 5.63 to be a function of the channel discharge rate in accordance with the following relationship:

$$k' = k_r q_{rc}^{-0.27} \quad . \quad . \quad . \quad . \quad . \quad . \quad . \quad . \quad . \quad . \quad . \quad . \quad 5.64$$

in which q_{rc} is again expressed in cubic feet per second. Laurenson established the value of k_r be a particular application of equation 5.64 as follows:

$$t_m = k_r q_{rcm}^{-0.27} \quad . \quad . \quad . \quad . \quad . \quad . \quad . \quad . \quad . \quad . \quad . \quad . \quad 5.65$$

in which

t_m = mean lag time in hours for the watershed zone

q_{rcm} = the mean discharge rate in cfs, including base flow, caused by a runoff producing event.

Thus, if values of t_m and q_{rcm} are known, k_r is estimated from equation 5.65. For the particular watershed on which he tested his theories (South Creek), Laurenson found the mean value of k_r to be 64.

From equation 5.64, equation 5.63 can be written as follows:

$$C_s(t) = k_r q_{rc}^{0.73} \quad . \quad . \quad . \quad . \quad . \quad . \quad . \quad . \quad . \quad . \quad . \quad . \quad 5.66$$

in which C_s is expressed in terms of cubic feet. Now, substituting equation 5.66 into equation 5.60 yields the expression

$$q_{rc} + 0.73\, k_r\, q_{rc}^{-0.27} \frac{d(q_{rc})}{dt} = i_r \quad . \quad . \quad . \quad . \quad . \quad . \quad 5.67$$

The solution of this differential equation provides an estimate of the channel discharge rate, q_{rc}. Initial values of q_{rc} are established from streamflow records. In the case of ephemeral streams, $q_{rc}(0)=0$.

The term i_r in equation 5.67 consists not only of surface runoff and interflow from within a particular zone, n, but also of channel flow from a higher zone, m. In addition, i_r is increased by groundwater inflow originating within the zone in the event of an effluent reach, and decreased by seepage losses in the case of an influent channel. Also, channel evaporation losses represent a loss from the zone and should be considered. A general expression for i_r is, therefore, given by

$$i_r(n) = q_{rc}(m) + q_{rs}(n) + q_{rn}(n) + q_{rb}(n) - q_{rg}(n) - E_{cr}(n) \quad . \quad . \quad . \quad . \quad . \quad . \quad . \quad 5.68$$

With reference to the terms on the right side of equation 5.68, $q_{rc}(m)$ is the computed channel runoff rate from zone m which is

With reference to the terms on the right side of equation 5.68, $q_{rc}(m)$ is the computed channel runoff rate from zone m which is situated immediately above zone n. $q_{rs}(n)$ represents the rate of surface runoff from the land phase within zone n as given by equation 5.59. The rate of entry of water to the channel by interflow, q_{rn}, is

given by equations 3.26 and 3.27. The groundwater or base flow inflow rate to a particular effluent reach of channel, $q_{rb}(n)$, is discussed later and is estimated by equation 5.90. It is assumed that within the same reach of channel both q_{rb} and seepage losses, q_{rg}, do not occur simultaneously. An average value of q_{rg} is established for each watershed zone on the basis of the dimensions of the surface channel and the vertical permeability of the bed materials within the zone. From Darcy's equation the rate of channel seepage loss can be written as

$$q_{rg} = k\,i\,a \qquad \ldots\ldots\ldots\ldots\ldots\ldots \quad 5.69$$

in which

k = the permeability of the bed material

i = the gradient

a = the area of surface over which seepage is occurring

If seepage losses are assumed to occur mainly in a vertical direction, equation 5.69 can be written in the form

$$q_{rg}(t) = k_g\, w(t) l \qquad \ldots\ldots\ldots\ldots\ldots\ldots \quad 5.70$$

in which

k_g = the vertical permeability of the bed material

w = the average width of the surface of the water within the channel at any time, t

l = the length of channel within the zone under consideration

For a given volume of water storage per unit length of channel at a particular point, the value of w depends upon the cross-sectional area of flow, A_s, within the channel at this point. Thus,

$$w(t) = f[A_s(t)] \quad . \quad . \quad . \quad . \quad . \quad . \quad . \quad . \quad . \quad . \quad . \quad 5.71$$

in which the function f is dependent upon the shape of the channel cross-section. Now, if the distribution of storage within a zone is assumed to be uniform, the average cross-sectional area of flow at any time, t, is given by

$$A_s(t) = \frac{C_s(t)}{1} \quad . \quad . \quad . \quad . \quad . \quad . \quad . \quad . \quad . \quad . \quad . \quad 5.72$$

Substituting equations 5.71 and 5.72 into equation 5.70 yields the general expression

$$q_{rg}(t) = k_g f\left[\frac{C_s(t)}{1}\right] 1 \quad . \quad . \quad . \quad . \quad . \quad . \quad . \quad . \quad . \quad 5.73$$

The application of equation 5.73 is demonstrated by assuming a trapezoidal channel cross-section with an average side slope equal to m horizontal to one vertical and a base width, b. In this case the average cross-sectional area of flow is given by

$w^2 - b^2$

average cross-sectional area of flow is given by

$$A_s(t) = \frac{w^2 - b^2}{4m} \quad . \quad . \quad . \quad . \quad . \quad . \quad . \quad . \quad . \quad . \quad . \quad 5.74$$

from which

$$w(t) = [b^2 + 4m\, A_s(t)]^{1/2} \quad . \quad . \quad . \quad . \quad . \quad . \quad . \quad . \quad . \quad 5.75$$

From equation 5.72, w now can be expressed in terms of channel storage as follows:

$$w(t) = \left[b^2 + \frac{4m}{l} C_s(t) \right]^{1/2} \quad . \quad . \quad . \quad . \quad . \quad . \quad . \quad . \quad . \quad 5.76$$

Substituting equation 5.76 into equation 5.70 gives

$$q_{rg}(t) = k_g l \left[b^2 + \frac{4m}{l} C_s(t) \right]^{1/2} \quad . \quad . \quad . \quad . \quad . \quad . \quad 5.77$$

Special cases of equation 5.77 occur for rectangular shaped channels (m = 0), and triangular channels (b = 0). It is also noted that this equation establishes a limiting minimum rate for channel seepage losses, namely:

$$q_{rg}(\min) = k_g l b \quad . \quad . \quad . \quad . \quad . \quad . \quad . \quad . \quad . \quad . \quad . \quad . \quad 5.78$$

Thus, in the absence of channel storage, C_s, if the gross inflow rate to a particular reach of channel does not exceed the rate established by equation 5.78, there is no outflow, q_{rc}, from the reach. It therefore follows that the actual total rate of channel loss is given by the sum of the seepage and evaporation terms contained on the right side of equation 5.68 only when the positive or gross inflow terms on the right side of this same equation jointly equal or exceed this sum. When this is not the case, the rate of channel loss is limited by the supply rate.

The remaining term on the right side of equation 5.68, E_{cr}, expresses the rate of evaporation loss from the surface of water stored

within the channels of zone n. This rate is expressed by equation 3.15 ($k_c = 1.0$) applied to the average area, A_w, of the water surface. Thus,

$$A_w(t) = w(t)\, l \quad . \quad . \quad . \quad . \quad . \quad . \quad . \quad . \quad . \quad . \quad . \quad . \quad . \quad 5.79$$

in which w is given by the general expression 5.71, or in particular by equation 5.76, and l is as previously defined in equation 5.70.

In many instances channel evaporation losses are insignificant. However, if the channel includes large areas of exposed water surfaces, such as in the case of a surface storage reservoir, these losses need to be included in the model.

As an example of the application of the preceding channel routing analysis to a particular zone, consider the Walnut Gulch experimental watershed which is situated in southern Arizona. With reference to an estimate of k_r by equation 5.65, the mean lag time of many watersheds is closely approximated by the more easily obtained hydrograph rise time. In the case of the Walnut Gulch watershed the average rise time is given by the expression (39):

$$t_r = 25.3\, A_z^{-0.14} \quad . \quad . \quad . \quad . \quad . \quad . \quad . \quad . \quad . \quad . \quad . \quad . \quad 5.80$$

in which t_r is rise time in minutes, and A_z is the area of the runoff surface or zone in square miles. For this particular watershed rise time is apparently independent of discharge rate so that the value of k' in equation 5.63 is also independent of q_{rc}, and in fact is equal to the

rise time estimated by equation 5.80. Thus, equation 5.63 can be written in the form:

$$C_s(t) = 25.3\, A_z^{-0.14}\, q_{rc} \quad . \quad . \quad . \quad . \quad . \quad . \quad . \quad . \quad . \quad 5.81$$

in which C_s and q_{rc} are expressed in terms of cubic feet and cubic feet per minute, respectively. Substituting equation 5.81 into equation 5.60 yields the result

$$q_{rc} + 25.3\, A_z^{-0.14}\, \frac{d}{dt}\,(q_{rc}) = i_r \quad . \quad . \quad . \quad . \quad . \quad . \quad . \quad 5.82$$

This equation is a particular form of the more general routing equation 5.67.

If for short duration storms channel evaporation losses are neglected and the inflow to channels of interflow, or quick seepage, and base flow is assumed to be negligible, equation 5.68 can be written as

$$i_r(n) = q_{rc}(m) + q_{rs}(n) - q_{rg}(n) \quad . \quad . \quad . \quad . \quad . \quad . \quad . \quad 5.83$$

If a trapezoidal channel cross-section is assumed, q_{rg} is given by equations 5.77 and 5.81 as follows:

$$q_{rg} = k_g\, l\, (b^2 + \frac{4m}{l}\, 25.3\, A_z^{-0.14}\, q_{rc})^{1/2} \quad . \quad . \quad . \quad . \quad 5.84$$

Equations 5.83 and 5.84 are now substituted into equation 5.82 to yield a channel routing expression for Walnut Gulch watershed as follows:

$$q_{rc}(n) + 25.3\, A_z(n)^{-0.14} \frac{d}{dt}\left[q_{rc}(n)\right]$$

$$+ k_g\, l \left[b^2 + \frac{4m}{l}\, 25.3\, A_z^{-0.14}\, q_{rc}\right]^{1/2} = q_{rc}(m) + q_{rs}(n)$$

. . . . . 5.85

Interflow. Interflow, q_{rn}, is routed by equations 3.26 and 3.27 with appropriate adjustment of the constants to provide for the time interval being employed in the study.

Base flow. Water which enters the groundwater basin through deep percolation leaves the watershed either within the stream channels as base flow or as subsurface flow. The total outflow rate, Q_{rg}, from the groundwater basin is estimated by equation 2.24, in which the value of $G_s(t)$ is given by the following differential equation:

$$\left[\sum_{i=1}^{m} G_r(i)\right] dt + \left[\sum_{i=1}^{m} q_{rg}(i)\right] dt - Q_{rg}\, dt = d\left[G_s(t)\right] \quad . \quad 3.86$$

The value of m in this equation is equal to the total number of zones within the watershed. Combining equations 2.24 and 5.86 yields the following expression which is solved for Q_{rg}:

following expression which is solved for Q_{rg}:

$$\frac{1}{k_b} \frac{d}{dt} (Q_{rg}) + Q_{rg} = \sum_{i=1}^{m} \left[G_r(i) + q_{rg}(i)\right] \quad . \quad . \quad . \quad . \quad 5.87$$

Now, the proportion of the total discharge rate from the groundwater basin of the watershed, Q_{rg}, which enters the surface channels and

forms the base flow of the streams is estimated from the geology of each particular zone and a study of available streamflow records. If that proportion of the total outflow rate from the groundwater basin of the watershed which forms the channel base flow component is represented by h_w, then the total base flow discharge rate, Q_{rb}, is given by:

$$Q_{rb} = h_w Q_{rg} \quad , \quad (0 \leq h_w \leq 1) \quad . \quad . \quad . \quad . \quad . \quad . \quad . \quad 5.88$$

in which

$$h_w = \sum_{i=1}^{m} h_i \quad . \quad . \quad . \quad . \quad . \quad . \quad . \quad . \quad . \quad . \quad . \quad . \quad . \quad 5.89$$

As before, m represents the total number of zones within the watershed.

Within a particular watershed zone, n, the rate of flow from the groundwater basin into an effluent reach of channel, $q_{rb}(n)$, is estimated by:

$$q_{rb}(n) = h_n Q_{rg} \quad . \quad . \quad . \quad . \quad . \quad . \quad . \quad . \quad . \quad . \quad . \quad . \quad 5.90$$

The quantity $q_{rb}(n)$ has already been referred to by equation 5.68.

Subsurface outflow. The total rate of subsurface or groundwater outflow from a watershed, Q_{ru}, is that portion of the discharge rate from the groundwater basin which does not form the channel base flow. Thus, from equation 5.88

$$Q_{ru} = Q_{rg} - Q_{rb} = (1 - h_w) Q_{rg} \quad . \quad . \quad . \quad . \quad . \quad . \quad . \quad 5.91$$

Total outflow

The total outflow rate from a watershed is given by the sum of the surface and subsurface outflow rates. This sum is expressed in mathematical terms as follows:

$$Q_{rt} = Q_{rs} + Q_{ru} \quad . \quad . \quad . \quad . \quad . \quad . \quad . \quad . \quad . \quad . \quad . \quad . \quad 5.92$$

in which Q_{ru} is given by equation 5.91, and Q_{rs} consists of surface flows, interflows, and base flows routed to the point or points of discharge from the watershed. This quantity is, therefore, equal to the computed channel discharge rate, q_{rc}, as given by equation 5.60, for the lowest zone on the watershed.

CHAPTER VI

TESTING AND VERIFICATION OF THE THIRD MODEL

Preliminary tests of the hydrologic model developed in Chapter V were made by simulating a subbasin of the Walnut Gulch experimental watershed. This watershed contains approximately 37,200 acres and is situated at Tombstone in southeastern Arizona. It is an ephemeral tributary of the San Pedro River. Runoff characteristics of the area are being intensively studied by the Agricultural Research Service of the U. S. Department of Agriculture and hydrologic instrumentation is therefore very complete (20, 30, 39). Figure 6.1 shows the general outline of the basin and the approximate locations of the precipitation and runoff measuring stations. Annual precipitation on the watershed is approximately 14 inches, with between 50 percent and 70 percent, and essentially all of the runoff, occurring during the June to September period as the result of intense, small-diameter, convective storms. Precipitation is measured with a network of 91 recording rain gages. Runoff is measured at the watershed outlet and from seven subwatersheds.

Elevations vary from 4,200 feet above mean sea level at the watershed outlet to over 6,000 feet at the upper portions of the drainage area. Stream channels in the watershed are typical of the semiarid Southwest. Gradients are steep (approximately one percent), and

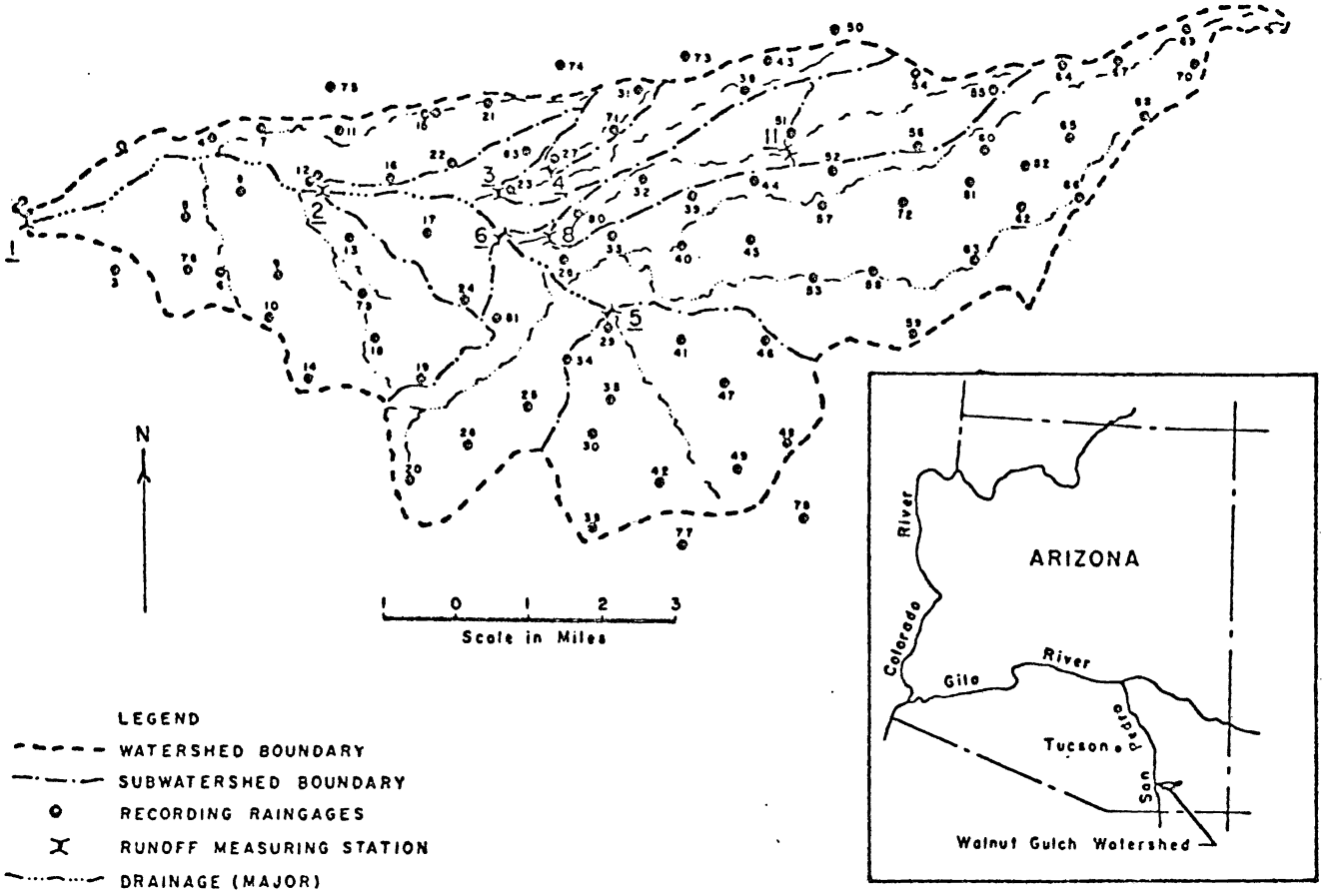

Fig. 6.1. Walnut Gulch experimental watershed.

consequently flow velocities are high. Throughout most of the channel system several feet of sand and gravel overlie a more consolidated material of fine-textured sediment or rock. The vegetative cover is the grama grass and creosote brush mixture typical of many of the rangelands of the Southwest. The regional groundwater table is situated at a depth of approximately 400 feet beneath the land surface.

The subunit of the Walnut Gulch watershed which was selected for initial simulation was subwatershed 11. Good precipitation and runoff data are available for four storms which occurred within this particular catchment area during July of 1966. This report will present simulation results corresponding to the single event of July 20, 1966. An enlarged plan of subwatershed 11, which contains a total area of 2,035 acres, is shown by figure 6.2.

The hydrologic flow chart which was followed in the development of a model for subwatershed 11 is shown by figure 6.3. It will be noted that this chart is much simpler than that of the general hydrologic system depicted by figure 5.1. This simplification resulted, in part, from the fact that precipitation does not occur in the form of snow on the watershed. In addition, evaporation was assumed to be negligible during the period of a typical runoff-producing event. For the initial model discussed here only the surface hydrologic system was simulated, so that as water entered the soil surface it was removed from any further consideration in the model. Equation 5.48 was, therefore, not

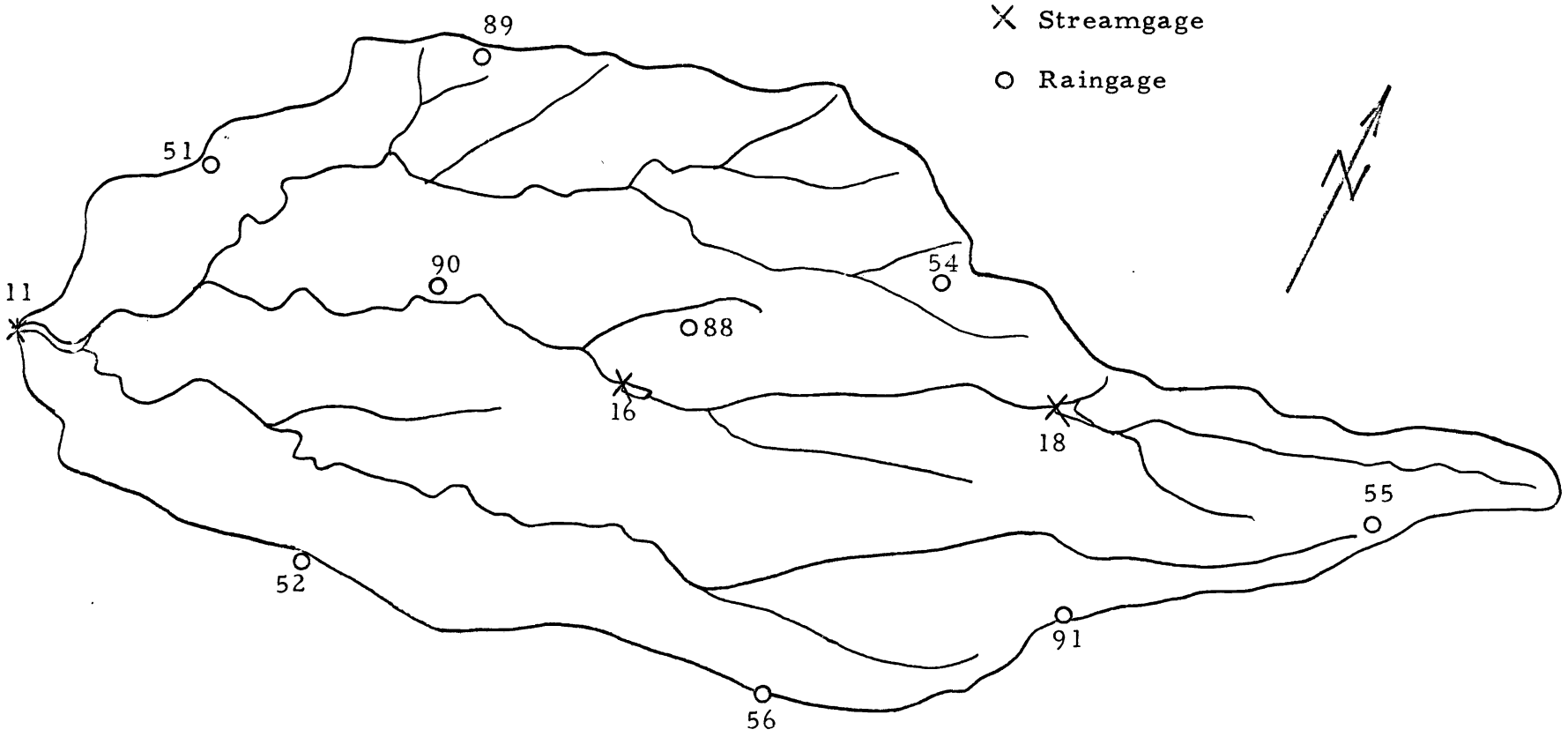

Fig. 6.2. Outline of subwatershed 11, Walnut Gulch, Arizona

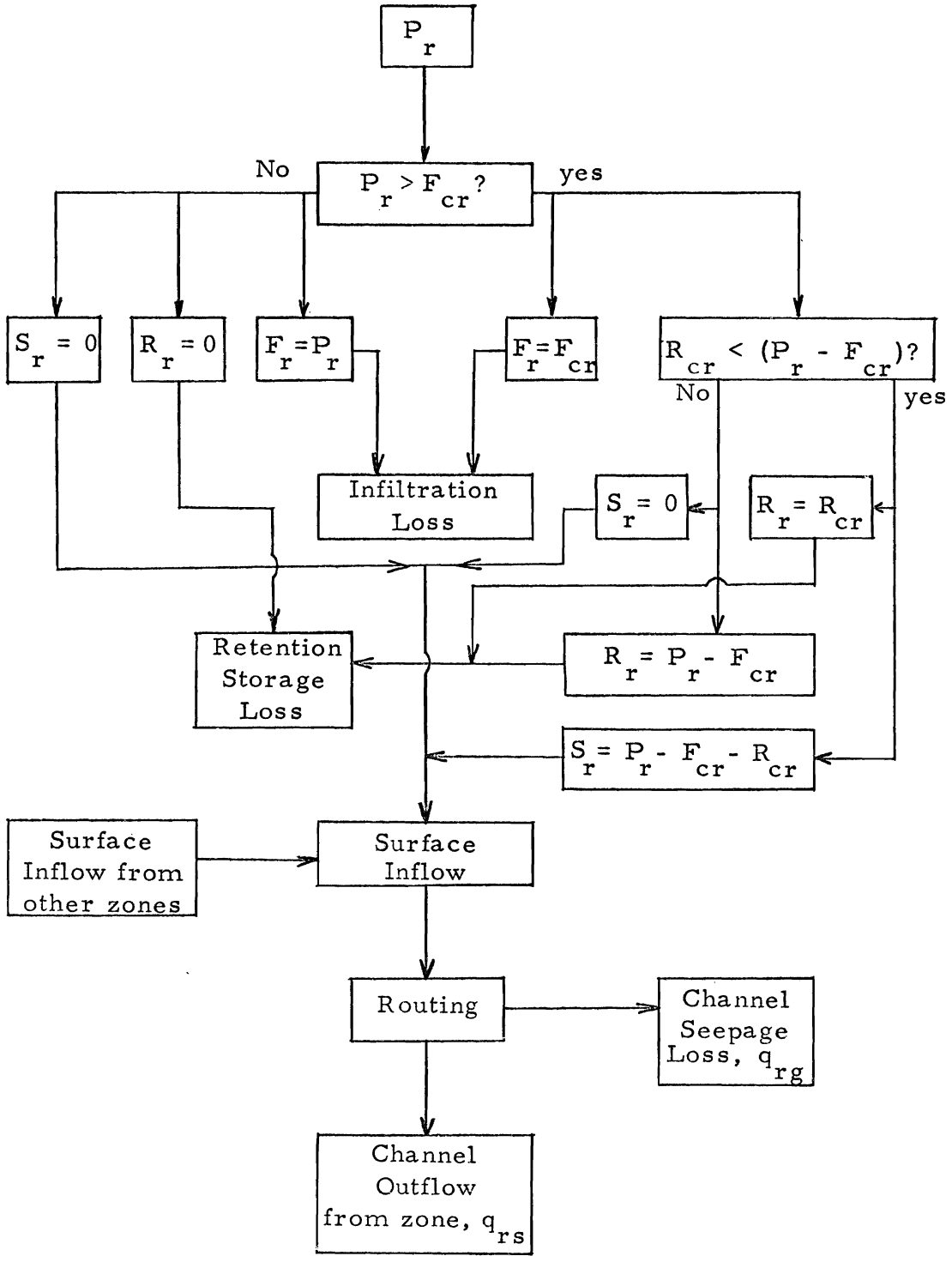

Figure 6.3. Hydrologic chart for the surface flow system of sub-watershed 11, Walnut Gulch, Arizona.

employed for the calculation of infiltration capacity rate. Instead, the equation proposed by Horton (17) was used. This equation is entirely time dependent, and is of the form:

$$F_{cr} = F_c + (F_o - F_c) \exp(-kt) \quad . \quad . \quad . \quad . \quad . \quad . \quad . \quad . \quad 6.1$$

in which

k is an empirical constant depending upon the soil type,

t is the time from the beginning of rainfall, and

F_c and F_o are defined by figure 5.9

A further simplification of the general model was adopted. Precipitation which enters interception storage is lost through evaporation. The component of precipitation which enters depression storage eventually infiltrates into the soil profile, and in this model is also lost because only the surface system was simulated. In addition, the rate functions for the interception and depression storages are identical in form. Thus, it was possible to combine both forms of storage and to treat them as a single entity termed retention storage.

Spatial integration of precipitation was performed on the computer by means of the Thiessen weighting technique. Studies conducted by personnel of the Agricultural Research Service for the Walnut Gulch by means of the Thiessen weighting technique. Studies conducted by personnel of the Agricultural Research Service for the Walnut Gulch watershed indicated no significant difference between the results of the Thiessen and isohyetal methods for computing average precipitation over an area during a particular period of time. The time increment adopted for the model was five minutes. Thus, the precipitation inputs

to the computer were those quantities which occurred at each rain gage during succeeding five-minute intervals throughout the storm.

The relationship for establishing the limiting or capacity surface retention rate, R_{rc}, is identical in form to equations 5.2 and 5.48. Thus,

$$R_{cr} = k_r [R_{cs} - R_s(t)] \quad . \quad . \quad . \quad . \quad . \quad . \quad . \quad . \quad . \quad . \quad 6.2$$

in which

k_r = a constant depending upon vegetation and soil surface characteristics

R_{cs} = retention storage capacity of the vegetation and land surface within a particular area.

The value of $R_s(t)$ in equation 6.2 is given by the following expression:

$$R_s(t) = \int_o^t (R_r)\, dt \quad . \quad . \quad . \quad . \quad . \quad . \quad . \quad . \quad . \quad . \quad . \quad 6.3$$

in which the actual retention rate, R_r, is given by the three limiting equations:

$$R_r = 0 \quad , \quad 0 \geq (P_r - F_{cr}) \quad . \quad . \quad . \quad . \quad . \quad . \quad . \quad . \quad 6.4$$

$$R_r = 0 \quad , \quad 0 \geq (P_r - F_{cr}) \quad . \quad . \quad . \quad . \quad . \quad . \quad . \quad . \quad 6.4$$

$$R_r = (P_r - F_{cr}) \quad , \quad 0 < (P_r - F_{cr}) < R_{cr} \quad . \quad . \quad . \quad 6.5$$

$$R_r = R_{cr} \quad , \quad (P_r - F_{cr}) \geq R_{cr} \quad . \quad . \quad . \quad . \quad . \quad . \quad 6.6$$

As shown by figure 6.3, surface runoff occurs when the rate of precipitation exceeds the sum of the capacity retention and infiltration rates at any particular time. Thus,

$$S_r = P_r - F_{cr} - R_{cr} \quad , \quad S_r \geq 0 \quad . \quad . \quad . \quad . \quad . \quad . \quad 6.7$$

The quantity S_r in the above equation represents the rate of inflow to surface detention storage. In the model the time distribution of outflow from this form of storage to the stream channels was given by equation 5.57, while equation 5.83 was applied as the channel routing function.

Precipitation input data are shown by table C1. Although these data were received in digital form, the time increment varied considerably. A digital computer program was therefore developed to convert these data into the desired format of table C1. This program together with sample input and output information are included within appendix C of this report. It will be noted that the data have been output for three particular time intervals. Any desired interval within the range of the data may be specified in the digital program Input values characteristic of the prototype area are included within table C2. Most of the information in this table was obtained from the results of field studies

of the prototype area are included within table C2. Most of the information in this table was obtained from the results of field studies
carried out by personnel of the Agricultural Research Service.

Analog computer output functions plotted directly on the x-y variplotter are shown by figure 6.4. It will be noted that the vertical scale

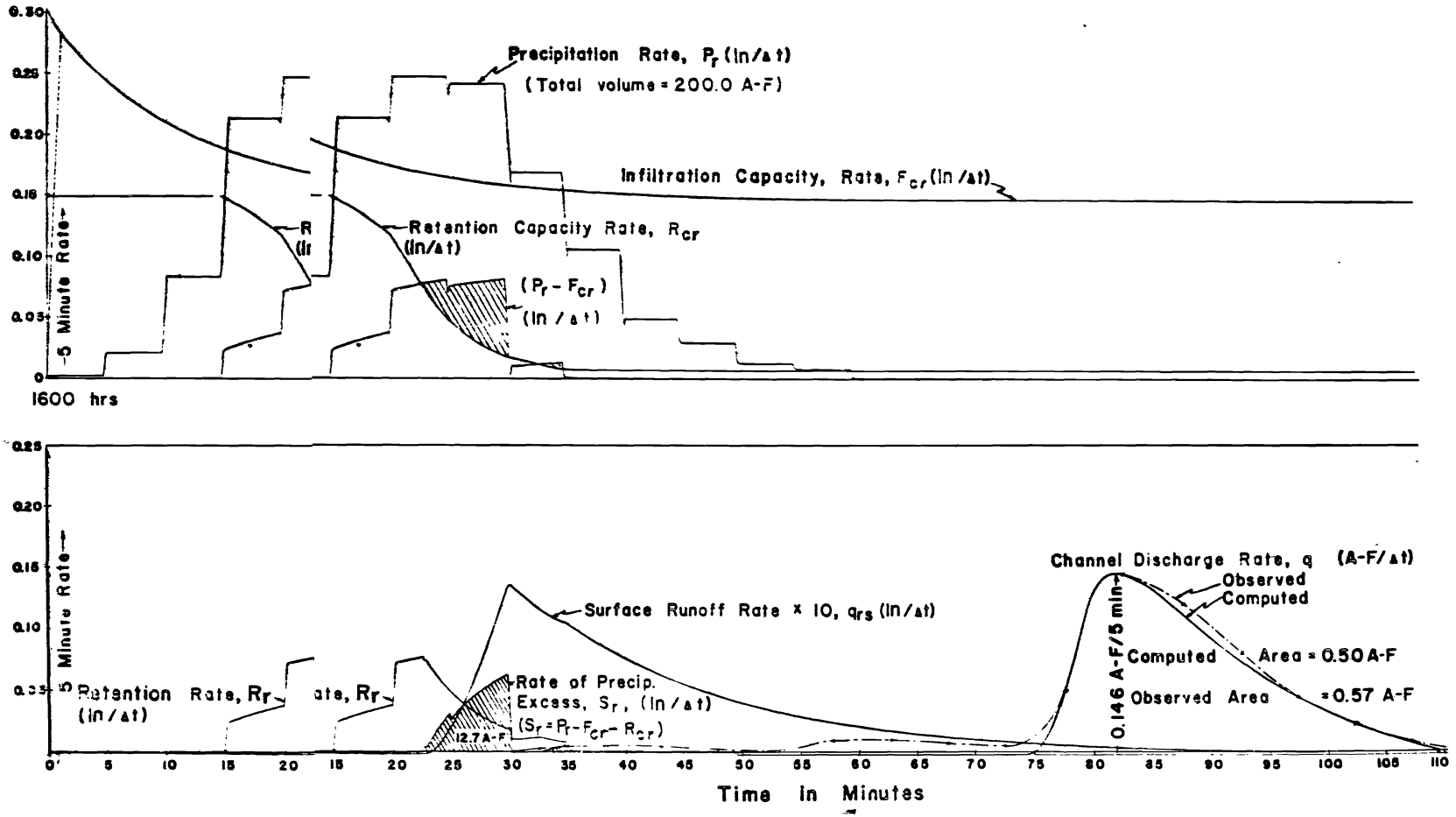

Figure 6.4. Analog cornalog computer plots for event of July 20, 1966, on subwatershed 11, Walnut Gulch, Arizona.

of the curve representing the rate of inflow to surface channels, q_{rs}, is ten times larger than that of the other accompanying curves. The area beneath this curve is, therefore, ten times greater than the cross-hatched area beneath the plot which represents the rate of input to surface detention storage. Except for the discharge hydrograph, all values are expressed in terms of inches over the area of the subwatershed per time interval. The outflow hydrographs are expressed in terms of acre-feet per time interval. Reasonable agreement was achieved between the computed and observed hydrographs. The peak discharge rates of 0.146 acre-feet per five minutes (approximately 20 cfs) coincided exactly.

The time delay, in this case about 50 minutes, between the outflow from detention storage and the appearance of an appreciable flow at the stream gaging station is dependent largely upon the location of the storm on the subwatershed. This variable delay problem can be approached by subdividing the area into a number of small zones and routing down the channels from one zone to the next. In subsequent simulation studies of subwatershed 11 it is proposed to model this area as eight individual zones.

Unfortunately, the only point at which quantitative verification of the model was possible was at the stream gaging station. However.

Unfortunately, the only point at which quantitative verification of the model was possible was at the stream gaging station. However, channel transmission losses for portions of the Walnut Gulch watershed have been estimated as a function of average peak discharge (39). On the basis of this relationship the computed transmission loss of about

12 acre-feet for the storm of July 20, 1966, on subwatershed 11 is a reasonable value.

CHAPTER VII

SUMMARY AND CONCLUSIONS

In this report three models of complicated hydrologic systems have been proposed. The basis of each model is a fundamental and logical mathematical representation of the various hydrologic processes. Each succeeding model contains improved relationships and better definition in terms of time and space, and therefore is capable of more faithfully representing the prototype system. The resulting trend toward increasing model complexity is illustrated by comparing the flow diagrams of figures 2.1, 3.1, and 5.1, respectively.

Electronic analog simulation of hydrologic systems has many practical applications in the areas of both research and project planning and management. As a research tool the computer is valuable in the process of investigating and improving mathematical relationships. In this respect, the computer is applied not only for its calculating potential, but also for its ability to yield optimum solutions. Simulation is also ideal for investigations of hydrologic sensitivity. Problems range from the influence of a single factor upon a particular process to

tion is also ideal for investigations of hydrologic sensitivity. Problems range from the influence of a single factor upon a particular process to the effects of an entire process, such as evapotranspiration, upon the system as a whole.

In many ways analog simulation can assist in planning and development work. Models can provide the designer with runoff estimates

from the input of recorded precipitation data. In addition, simulated streamflow records from statistically generated input information enable the establishment of synthetic flow frequency distribution patterns.

In the area of water resource management, analog computer simulation will permit the rapid evaluation of the effects of various management alternatives upon the entire system. These alternatives might involve such variables as watershed treatment, including urbanization, the construction of a storage reservoir, or changes in irrigation practices within a basin.

The mathematical relationships presented for each of the three models were developed for application to areas where data are relatively sparse. For example, the basic input functions are temperature and precipitation. Parameters are included in the equations to provide for other variables such as those which are attributable to the sloping land surfaces, elevation differences, and often low available soil moisture values of a typical mountain watershed.

To test individual equations and to verify the models, particular hydrologic units are simulated. Flow records at the outlet of the subbasins provide data for quantitative verification of the models. For model two close agreement between computed and observed outflows

basins provide data for quantitative verification of the models. For model two close agreement between computed and observed outflows

was achieved on both a monthly and a total annual basis. For 1962 the computed accumulative outflow exceeded the observed by about 5 percent. Terminal conditions for 1962 were input as initial conditions for

1963 and outflow values computed. The accumulated outflow for this year exceeded the observed by less than 5 percent. The evaluation of model three is still in the early stages. However, results of a preliminary test have been very encouraging. Since the first model has already undergone extensive testing in operational studies, verification results for this model are not presented in this report. Continued testing of both models will be undertaken through watershed simulation studies associated with several planned investigations.

In a research program of this nature certain constraints or boundary conditions limit the degree of achievement during any particular phase of the overall program. The most important of these limiting features are the extent to which research information and basic input data are available, the degree of accuracy established by the time and spatial increments adopted for the model, equipment limitations, and the necessary time limit imposed upon the investigation period.

Electronic analog simulation of hydrologic phenomena has been under active development at Utah State University for about three years. The development of this research program has followed the logical pattern of proceeding in stages to increasingly detailed modeling. The important underlying feature throughout the entire program has been

pattern of proceeding in stages to increasingly detailed modeling. The important underlying feature throughout the entire program has been that all of the separately described hydrologic processes and phenomena are interlinked into a total hydrologic system. Thus, for each model it was possible to evaluate the relative importance of the various

hydrologic items, expose critical areas where data and perhaps theory were lacking, and establish guidelines for more fruitful and meaningful study in subsequent phases of the work. The first hydrologic model (Chapter II), using monthly time increments, gave good results for interbasin effects. The second model, described in Chapter III, was designed for an investigation of in-basin problems, but still utilizing a large time increment. Under the third phase of this program a model is now being developed (Chapter V) which will simulate the hydrologic processes over small geographic units and short periods of time. The development of this model is presenting many challenges not only in the mathematical representations of the hydrologic processes, but also in equipment requirements and modeling techniques. For example, improved channel routing techniques which employ the continuity concepts of both mass and momentum are being investigated for incorporation into the model.

In a subsequent phase the joint simulation of a single hydrologic entity by means of both models two and three will be considered. For the continuous operation of a hydrologic model over an extended period of time, geometric and time scales need to be altered to accomplish accurate description of the system during periods of rapid change. Joint simulation would permit this change as required to accurately describe the phenomena of interest within any particular time period.

Analog simulation of hydrologic systems has vast potential. For example, consideration is now being given at this institution to expanding

the model of the physical system by superimposing the related dimensions of water quality and economics. Many other possibilities remain to be explored. However, present achievements at Utah State University have demonstrated the soundness and validity of this approach to hydrologic problems, and have provided a basis for future applications of analog models to the comprehensive flow systems encountered in the development and management of water resources.

LITERATURE CITED

1. Anderson, Eric A., and Norman H. Crawford. The synthesis of continuous snowmelt runoff hydrographs on a digital computer. Technical Report No. 36, Department of Civil Engineering, Stanford University, Stanford, California. 1964. 103 p.

2. Bagley, Jay M., D G. Chadwick, J. P Riley, and R. Sampson. The development of an electronic analog device for hydrologic investigations and conservation planning in the Sevier River basin. Utah Water Research Laboratory, Utah State University, Logan, Utah. Manuscript in preparation.

3. Bagley, Jay M., Robert B Hickok, D. G. Chadwick, Marvin J. Rosa, and D. L Brakensiek. Report on feasibility of an electronic analog approach to Sevier River basin investigations for water resources development and conservation planning. Report No. EC-51-g-1, Engineering Experiment Station, Utah State University, Logan, Utah. 1963. 47 p.

4. Blaney, Harry F., and Wayne D. Criddle. Determining water requirement in irrigated areas from climatological and irrigation data. Technical Paper 96, Soil Conservation Service, U. S. Department of Agriculture. February 1950. 48 p.

5. Carpenter, Carl H., Gerald B. Robinson, Jr., and Louis J. Bjorklund. Selected hydrologic data, upper Sevier River basin, Utah. Basic-Data Report No. 8, U. S. Geological Survey and Utah State Engineer. 1964. 29 p.

6. Carreker, John R. The relation of solar radiation to evapotranspiration from cotton. Journal of Geophysical Research 68(16):4731-4741. 1963.

7. Crawford, N. H., and R. K Linsley. The synthesis of continuous streamflow hydrographs on a digital computer. Technical Report

7. Crawford, N. H., and R. K Linsley. The synthesis of continuous streamflow hydrographs on a digital computer. Technical Report

No. 12, Department of Civil Engineering, Stanford University, Stanford, California. 1962. 121 p.

8. Crawford, N. H., and R. K. Linsley. Digital simulation in hydrology: Stanford watershed model IV. Technical Report No. 39, Department of Civil Engineering, Stanford University, Stanford, California. 1962. 209 p.

9. Criddle, Wayne D. Methods of computing consumptive use of water. Journal of Irrigation and Drainage Division, Proceedings, American Society of Civil Engineers 84(IR 1):1-27. 1958.

10. Criddle, Wayne D., Karl Harris, and Lyman S. Willardson. Consumptive use and water requirements for Utah. Technical Publication No. 8 (Revised), Office of the Utah State Engineer. 1962. 47 p.

11. Dalton, J. Experimental essays on the constitution of mixed gases; on the force of steam or vapor from waters and other liquids in different temperatures, both in a torricelliam of gases by heat. Memoirs, Manchester Literary and Philosophical Society 5:535-602. 1798.

12. Frank, Ernest C., and Richard Lee. Potential solar beam irradiation on slopes: Tables for 30° to 50° latitude. Research Paper RM-18, Rocky Mountain Forest and Range Experiment Station, Fort Collins, Colorado. March 1966. 116 p.

13. Gardner, W. R., and C. F. Ehlig. The influence of soil water on transpiration by plants. Journal of Geophysical Research 68(20): 5719-5724. 1963.

14. Garstka, W. U., L. D. Love, B. C. Goodell, and F. A. Bertle. Factors affecting snowmelt and streamflow. U. S. Bureau of Reclamation and U. S. Forest Service. 1958. 189 p. U. S. Government Printing Office, Washington, D. C.

15. Harder, J. A., Lyle Mockros, and Ray Nishizaki. Flood control analogs. Water Resources Center Contribution No. 24, Hydraulic Laboratory, University of California, Berkeley, California. 1960. 40 p.

16. Hildebrand, F. B. Advanced calculus for applications. Prentice-Hall, Inc., Englewood Cliffs, New Jersey. 1962. 646 p.

17. Horton, R. E. The role of infiltration in the hydrologic cycle. Transactions, American Geophysical Union 14:446-460. 1933.

Hall, Inc., Englewood Cliffs, New Jersey. 1962. 646 p.

17. Horton, R. E. The role of infiltration in the hydrologic cycle. Transactions, American Geophysical Union 14:446-460. 1933.

18. Jensen, Marvin E., and Howard R. Haise. Estimating evapotranspiration from solar radiation. Journal of the Irrigation and Drainage Division, Proceedings, American Society of Civil Engineers 89(IR4): 15-41. 1963.

19. Johnson, W. M. The interception of rain and snow by a forest of young ponderosa pine. Transactions, American Geophysical Union, 23:566-569. 1942.

20. Kincaid, D. R., J. L. Gardner, and H. A. Schreiber. Soil and vegetation parameters affecting infiltration under semiarid conditions. Extract of publication No. 65, Land erosion, precipitations, hydrometry, soil moisture, of the International Association of Scientific Hydrology, p. 440-453. 1966.

21. Kunz, Kaiser S. Numerical analysis. McGraw-Hill Book Company, Inc., New York. 1957. 381 p.

22. Lane, Robert K. Estimating evaporation from insolation. Journal of the Hydraulics Division, Proceedings, American Society of Civil Engineers 90(HY5):33-41. 1964.

23. Larson, Curtis Luverne. A two-phase approach to the prediction of peak rates and frequencies of runoff for small, ungaged watersheds. Ph. D. dissertation, Stanford University, Stanford, California. 1965. 109 p.

24. Laurenson, E. M. A catchment storage model for runoff routing. Journal of Hydrology 2:141-163. 1964.

25. Lee, Richard. Evaluation of solar beam irradiation as a climatic parameter of mountain watersheds. Hydrology Papers No. 2, Colorado State University, Fort Collins, Colorado. 1963. 50 p.

26. Linsley, Ray K., Jr., Max A. Kohler, and Joseph L. H. Paulhus. Hydrology for engineers. McGraw-Hill Book Company, Inc., New York. 1958. 340 p.

27. List, Robert J. Smithsonian meteorological tables. Smithsonian Institution, Washington, D. C. 1951. 527 p.

28. Lowry, R. L., and A. F. Johnson. Consumptive use of water for agriculture. Transactions, American Society of Civil Engineers 107:1243-1302. 1942.

29. Morton, Fred I. Potential evaporation and river basin evaporation. Journal of the Hydraulics Division, Proceedings, American Society of Civil Engineers 91(HY6):67-97. 1965.

30. Osborn, Herbert B., and Robert V. Keppel. Dense rain gage networks as a supplement to regional networks in semiarid regions. Extract of publication No. 68, Symposium on design of hydrological networks, of the International Association of Scientific Hydrology, p. 675-687. 1966.

31. Otoba, Kotaro, Kozi Shibatani, and Hiroshi Kuwata. Flood simulator for the River Kitakami. Simulation 4(2):86-98. 1965.

32. Papadakis, J. Climatic tables for the world. Buenos Aires (Av. Cordoba 4564), Argentina. 1961.

33. Patil, Uttamrao. A study of the relationship between consumptive use of water and evaporation. M.S. thesis, Utah State University, Logan, Utah. 1954. 49 p.

34. Penman, H. L. Natural evaporation from open water, bare soil, and grass. Proceedings, Royal Society of London, Series A. 193: 120-146. 1950.

35. Phelan, John T. Estimating monthly "k" values for the Blaney-Criddle formula. Presented at the Agricultural Research Service-Soil Conservation Service Workshop on Consumptive Use, Phoenix, Arizona, March 6-8, 1962. 11 p.

36. Quackenbush, Tyler H., and John T. Phelan. Irrigation water requirements of lawns. Journal of the Irrigation and Drainage Division, Proceedings, American Society of Civil Engineers 91(IR2):11-19. 1965.

37. Rantz, S. E. Snowmelt hydrology of a Sierra Nevada stream. Water-supply Paper 1779-R, U. S. Geological Survey. U. S. Government Printing Office, Washington, D. C. 1964. 36 p.

38. Reisenauer, A. E. Methods for solving problems of multi-dimensional, partially saturated steady flow in soils. Journal of Geophysical Research 68(20):5724-5733. 1963.

39. Renard, Kenneth G. and Robert V. Keppel. Hydrographs of ephemeral streams in the southwest. Journal of the Hydraulics Division, Proceedings, American Society of Civil Engineers 92(HY2):33-52. 1966.

40. Shaw, Sir Napier. Manual of meteorology. Volume 2. Cambridge University Press, Cambridge, England. 1936. 470 p.

41. Shen, John. Use of analog models in the analysis of flood runoff. Professional Paper 506-A, U. S. Geological Survey. 1965. 24 p.

42. Silina, A. A. Transpiration of woody species of the Tellerman Forest Range. (Translated from Russian.) Israel Program for Scientific Translations Catalog No. 300. Office of Technical Services, U. S. Department of Commerce, Washington 25, D. C. 1955. 13 p.

43. Smirnov, K. I. Evaporation from the soil in the Kustanayskaya Province. (Translated from Russian.) Soviet Hydrology: Selected Paper No. 2, American Geophysical Union. 1963. p. 156-174.

44. Swift, Lloyd W., Jr. A method for computing the effect of mountain topography upon available solar energy. Southeastern Forest Experiment Station Inservice (FS-1-w1-7-SE), North Carolina State College, Raleigh, North Carolina. 1960. 25 p.

45. Swift, Lloyd W., Jr., and C. H. M. van Bavel. Mountain topography and solar energy available for evapotranspiration. Presented before the Section of Hydrology, American Geophysical Union, North Carolina State College, Raleigh, North Carolina, April 1961. 7 p.

46. Thomas, H. A., Jr., and R. P. Burden. Indus River basin studies. Harvard Water Resources Group, Harvard University, Cambridge, Massachusetts. 1965. p. 5-1 to 5-64.

47. Thornthwaite, C. W., and J. R. Mather. The water balance. Drexel Institute Technical Publication in Climatology VIII(1):1-104. 1955.

48. Turner, J. A. The uses of evaporation data and theory in forest management. Proceedings of Hydrology Symposium No. 2: Evaporation. National Research Council, Toronto, March 1 and 2, 1961. p. 200-208. Queens Printer, Ottawa, Canada.

49. U. S. Army. Corps of Engineers. Snow hydrology: summary report Evaporation. National Research Council, Toronto, March 1 and 2, 1961. p. 200-208. Queens Printer, Ottawa, Canada.

49. U. S. Army. Corps of Engineers. Snow hydrology; summary report of the snow investigations. North Pacific Division, Portland, Oregon. 1956. 437 p.

50. U. S. Army. Corps of Engineers. Runoff from snowmelt. Engineering and Design Manual 1110-2-1406. 1960. 75 p.

51. U. S. Civil Works Investigations. Technical Bulletin No. 6, Project CE-171. April 1950. 7 p.

52. U. S. Congress. Evapotranspiration reduction. In: Water Resources Activities in the U. S., Committee Print No. 21, 86th Congress, p. 18. February 1960.

53. U. S. Weather Bureau. U. S. climatological data, national summary. Volumes 1 to 14. 1950 to 1963.

54. U. S. Weather Bureau. Three charts showing normal precipitation for the State of Utah for the three periods, October to April, May to September, and the full year, based upon the period of record 1931 to 1960. Office of the Utah State Engineer, Utah Water and Power Board, and Soil Conservation Service. 1963.

55. U. S. Weather Bureau. Mean precipitable water in the United States. Technical Paper No. 10. 1949. 48 p.

56. Veihmeyer, F. J. Some factors affecting the irrigation requirements of deciduous orchards. Hilgardia 2:125-291. 1927.

57. Veihmeyer, F. J., W. O. Pruitt, and W. D. McMillan. Soil moisture as a factor in evapotranspiration equations. Paper 60-202, presented at the annual meeting, American Society of Agricultural Engineers, University of California, Davis, California. 1960.

58. West, A. J. Snow evaporation and condensation. Proceedings, Western Snow Conference, 1959. p. 66-74.

59. Willardson, Lyman S., and Wendell L. Pope. Separation of evapotranspiration and deep percolation. Journal of the Irrigation and Drainage Division, Proceedings, American Society of Civil Engineers 89(IR3):77-88. 1963.

60. Williams, G. P. Evaporation from snow covers in eastern Canada. Research Paper 73, National Research Council, Division of Building Research. 1959. 14 p.

60. Williams, G. P. Evaporation from snow covers in eastern Canada. Research Paper 73, National Research Council, Division of Building Research. 1959. 14 p.

61. Williams, G. P. Evaporation from water, snow, and ice. Proceedings of Hydrology Symposium No. 2: Evaporation. National Research Council, Toronto, March 1 and 2, 1961. p. 31-54. Queens Printer, Ottawa, Canada.

62. Woods, Philip C., and Gerald T. Orlob. The Lost River system, a water quality management investigation. Sanitary Engineering Research Laboratory, University of California, Berkeley, California. 1963. 54 p.

63. Young, Arthur A., and Harry F. Blaney. Use of water by native vegetation. Bulletin 50, California Department of Public Works, Division of Water Resources. 1942. 160 p.

APPENDIXES

Appendix A

Computation of Radiation Index Values

In the concept of potential insolation the earth's atmosphere is ignored. Thus, irradiation of a surface by direct sunshine is considered to be only a function of the angle between the surface and the sun's rays. This angle, in turn, is a function only of the geometric relationships between the surface and the sun as expressed by latitude, degree of slope and aspect of the surface, and the declination and hour angle of the sun. For a given site the only variation in instantaneous potential insolation will be perfectly cyclical with time, depending upon the changes in hour angle and declination. In the development of a procedure for computing potential insolation, consider first the following symbols:

D = declination of the sun in degrees, north (+) and south (-). This angle is a function of time.

e = ratio of the earth to sun distance at any time and the mean of this distance

h = azimuth (degrees), measured clockwise from north

this distance

h = azimuth (degrees), measured clockwise from north

I_o = the solar constant, 2.00 gm cal/cm^2/min (langleys/min)

I_q = quantity of insolation (langleys)

I_p = maximum potential insolation, or I_o/e^2

RI = radiation index, percent I_q of I_p

θ = slope inclination in degrees or percent

L = latitude of observation in degrees, north (+) and south (-)

T = longitude of observation in degrees

τ = number of days from January 1 of each year

t_1 = minutes from true solar noon to sunrise

t_2 = minutes from true solar noon to sunset

ω = angular velocity of the earth's rotation in radians per minute

N = the number of days from the nearest equinox (September 23 or March 21) in degrees

ψ = angle between the sun's rays and the normal to the irradiated surface, degrees. This angle is a function of time.

In the discussion which follows, true solar noon is taken as being the zero or reference point. Thus, time intervals before solar noon are assigned negative values, while those after solar noon are assumed to be positive. In general terms, the values of t_1 are negative, while those of t_2 are positive.

The quantity of insolation received at a surface for any particular day is given by:

$$I_q = \frac{I_o}{e^2} \int_{t_1}^{t_2} \cos \psi \, dt \quad . \quad . \quad . \quad . \quad . \quad . \quad . \quad . \quad . \quad A1$$

$$I_q = \frac{I_o}{e^2} \int_{t_1}^{t_2} \cos \psi \, dt \quad . \quad . \quad . \quad . \quad . \quad . \quad . \quad . \quad . \quad A1$$

Cos ψ is obtained by taking the dot product of the vector representing the sun's rays and the normal vector to the irradiated surface. Thus, for a horizontal surface:

$$\cos \psi = \cos D \cos L \cos \omega\ t + \sin D \sin L \quad . \quad . \quad . \quad . \quad A2$$

from which

$$I_q = \frac{I_o}{e^2} \int_{t_1}^{t_2} (\cos D \cos L \cos \omega\ t + \sin D \sin L)\, dt$$

$$= \frac{I_o}{e^2} \left[\frac{1}{\omega} \cos D \cos L (\sin \omega\ t_2 - \sin \omega\ t_1) \right.$$

$$\left. + (t_2 - t_1) \sin D \sin L \right] \quad . \quad . \quad . \quad . \quad . \quad . \quad A3$$

The change in declination with time is approximated by the following equation:

$$D = 23.5 \sin N \quad . \quad . \quad . \quad . \quad . \quad . \quad . \quad . \quad . \quad . \quad . \quad . \quad A4$$

and values of I_o/e^2 are estimated by the expression:

$$\frac{I_o}{e^2} = 0.07 \cos \tau + 2.00 \quad . \quad . \quad . \quad . \quad . \quad . \quad . \quad . \quad . \quad A5$$

The insolation equations for sloping or inclined surfaces are much more complex than those for horizontal surfaces. However, the theory of "equivalent slope" offers a simple approach to this problem. This concept is derived from the fact that every inclined surface on the face of a sphere is parallel to some horizontal surface whose location is mathematically defined. The determination of the location of this equivalent slope in terms of increments of latitude and longitude requires the solution of a terrestrial spherical triangle. The difference

in longitude between the location of a given slope and that of an equivalent horizontal area is given by:

$$\Delta T = \tan^{-1} \left(\frac{\sin h \cdot \sin \theta}{\cos \theta \cdot \cos L - \cos h \cdot \sin \theta \cdot \sin L} \right) . \quad A6$$

The latitude of the equivalent slope is given by:

$$L' = \sin^{-1} (\sin \theta \cdot \cos h \cdot \cos L + \cos \theta \cdot \sin L) \quad . \quad . \quad A7$$

It will be noted that in the above equations h defines the direction or aspect of the given slope.

The potential insolation of the given slope can now be computed from equation A3 in terms of its equivalent horizontal slope providing the appropriate length of day can be established. On the basis that the earth rotates at the rate of 15 degrees per hour, the time shirt in minutes between the given and equivalent slopes is equal to $4(\Delta T)$. For a horizontal surface both t_1 and t_2 are given by:

$$t = 4 \cos^{-1} (-\tan L \tan D) \quad . \quad . \quad . \quad . \quad . \quad . \quad . \quad . \quad . \quad A8$$

Now, in the case of an east-facing slope, the sunrise will obviously occur at the same time as for a horizontal surface at the same location. Thus, t_1 is given by equation A8. In this case the time from solar noon to sunrise at the equivalent slope, represented by t'_1, is established from the local time at the actual slope and is given by:

$$t'_1 = t_1 + 4(\Delta T) \quad . \quad . \quad . \quad . \quad . \quad . \quad . \quad . \quad . \quad . \quad . \quad A9$$

Combining equations A8 and A9 yields

$$t'_1 = 4 \left[\cos^{-1} (-\tan L \tan D) + \Delta T \right] \quad . \quad . \quad . \quad . \quad . \quad . \quad A10$$

The time between solar noon and sunset, t'_2, at an equivalent site for an east-facing slope is given by equation A8 as follows:

$$t'_2 = 4 \cos^{-1} (-\tan L' \tan D) \quad . \quad . \quad . \quad . \quad . \quad . \quad . \quad . \quad . \quad A11$$

The afternoon sun will leave the surfaces of the horizontal equivalent slope and the east-facing actual slope at the same time. The period between solar noon and sunset at the actual slope is given by:

$$t_2 = t'_2 - 4(\Delta T) \quad . \quad . \quad . \quad . \quad . \quad . \quad . \quad . \quad . \quad . \quad . \quad . \quad A12$$

For a west-facing slope t_2 is determined by equation A8, and t'_2 by either equation A9 or A10. In this case equations A11 and A12 establish the time periods t'_1 and t_1, respectively. It is again emphasized that in most cases t'_1 represents a period before solar noon and is usually negative, while t'_2 most frequently occurs after solar noon and is usually positive in value. From the appropriate values of t'_1, t'_2, and L', the potential insolation received on the given sloping surface over the period of time $(t_2 - t_1)$ is now computed by substitution into equation A3 as follows:

$$I_q = \frac{I_o}{e^2} \left[\frac{1}{\omega} \cos D \cos L' (\sin \omega \, t'_2 - \sin \, t'_1) + (t'_2 - t'_1) \right.$$

$$\left. \sin D \sin L \right] \quad . \quad . \quad . \quad . \quad . \quad . \quad . \quad A13$$

It will be noted that for a particular surface, ΔT and L remain constant so that the daily values of I_q are computed from equations A4, A5, A8, A9, A11, and A13, respectively.

Because mapped areas represent the horizontal projection of sloping surfaces, the computed potential insolation per unit area on a sloping surface is adjusted to account for this factor. Thus:

$$I_q(H) = I_q \sec \theta \quad . \; . \; . \; . \; . \; . \; . \; . \; . \; . \; . \; . \; . \; . \; . \qquad A14$$

where $I_q(H)$ represents the potential insolation in langleys on the horizontal projection of the sloping surface.

The radiation index for a surface for any particular day is given by the following ratio:

$$RI = \frac{100\, I_q(H)}{I_p\,(2t)} = \frac{100\, I_q(H)}{I_o/e^2\,(2t} \quad . \; . \; . \; . \; . \; . \; . \; . \; . \; . \qquad A15$$

where t is the time in minutes from noon to either sunrise or sunset for a horizontal surface at the particular location. Substituting for $I_q(H)$ its equivalent from equations A13 and A14

$$RI = \frac{50}{t} \sec \theta \;\; [\frac{1}{\omega} \cos D \cos L' (\sin \omega \; t'_2 - \sin \quad t'_1)$$

$$+ (t'_2 - t'_1) \sin D \sin L'] \quad . \; . \; . \; . \; . \; . \; . \qquad A16$$

The following digital computer program has been written incorpo-
$$+ (t'_2 - t'_1) \sin D \sin L'] \quad . \; . \; . \; . \; . \; . \; . \qquad A16$$

The following digital computer program has been written incorporating the equations presented in this section. From this program it is possible to compute the variation of potential insolation with solar declination for any surface established by latitude, aspect, and degree of

slope. Some sample output from the program is also included. Figures 3.3 and A1 illustrate computer plots of radiation index values calculated from equation A16.

Radiation Indexes

```
      DIMENSION DMON(50), DAY(50), DECL(50), AIP(50), SRISE(50), RI(50),
     1DD(50), TM(50)
       READ 1, AL, H, XS, XB, N
    1  FORMAT (4F8.0, I3)
      READ 2, (DMON(I), DAY(I), I= 1,N)
    2 FORMAT (2F5.0)
      XL = (XB - XS)/10.0
       CALL PLOT (101, XS, XB, XL, 10.0, 0.0, 180.0, 6.0, 30.0)
      PUNCH 3, AL, H
    3 FORMAT (10H LATITUDE-, 3X, F5.0, 2H N, 8X, 9H AZIMUTH-, 3X,
     1F5.0, 5H DEG.//)
      PUNCH 4
    4 FORMAT (19X, 5H MON.,1X, 4H DAY, 5X, 6H SRISE, 6X, 5H SSET,
     18X, 3H IO, 8X, 3H RI)
      V = 1.5708/90.0
      AL = AL*V
      H = H*V
      W = V/4.0
      DO 8 L = 1,N
      IF (DMON(L) - 7.0) 10,10,13
   10 K = DMON(L)/2.0
      C = K
      IF (DMON(L) - 2.0) 11,11,12
   11 TDAY = (DMON(L) - 1.0)*30.0 + C + DAY(L)
      AN = (80.0 - TDAY)*V
      S = -1.0
      TM(L) = TDAY + 10.0
      GO TO 22
   12 TDAY = (DMON(L) - 1.0)*30.0 + C - 2.0 + DAY(L)
      GO TO 14
   13 K = (DMON(L) + 1.0)/2.0
      C = K
      TDAY = (DMON(L) - 1.0)*30.0 + C - 2.0 + DAY(L)
   14 B = TDAY - 80.0
      IF (ABSF(B) - 90.0) 15,15,16
   15 AN = ABSF(B)*V
      TM(L) = TDAY + 10.0
      GO TO
   16 B = 2[illegible].0 - TDAY
      IF (ABSF(B) - 90.0) 17,17,18
   17 AN = ABSF(B)*V
      TM(L) = 356.0 - TDAY
      GO TO 21
   18 B = 365.0 - TDAY
      IF (B - 10.0) 19,19,20
   19 AN = (B + 80.0)*V
      TM(L) = TDAY - 356.0
      S = -1.0
      GO TO 22
   20 AN = 90.0*V
      TM(L) = 180.0
   21 IF(B) 27, 25, 27
   25 DECL(L) = 0.0
```

Radiation Indexes (Continued)

```
      GO TO 26
   27 S = B/ABSF(B)
   22 DECL(L) = S*23.5*SINF(AN)*V
   26 IF (TDAY - 360.0) 24,24,23
   23 TDAY = 360.0
   24 AIP(L) = 2.0 + 0.07*COSF(TDAY*V)
      DE = DECL(L)
      DD(L) = TM(L)
      C = -SINF(AL)*SINF(DE)/ (COSF(AL)*COSF(DE))
      IF (C) 31,34,32
   34 SRISE(L) =-360.0
      GO TO 8
   31 SRISE(L) = -4.0*(3.1416 - ATANF(ABSF(SQRTF(1.0-C**2)/C)))/V
      GO TO 8
   32 SRISE(L) = -4.0*ATANF(SQRTF(1.0 - C**2)/C)/V
    8 CONTINUE
      NA = N-1
      DO 80 J = 1,NA
      K = J+1
      DO 80 JA = K, N
      IF (DD(J) - DD(JA)) 80,80,81
   81 TEMP = DD(JA)
      DD(JA) = DD(J)
      DD(J) = TEMP
   80 CONTINUE
      DO 140 J = 1,N
      DO 120 JA = 1,N
      IF (DD(J) - TM(JA)) 120,130,120
  120 CONTINUE
  130 DD(J) = JA
  140 CONTINUE
      TU = XS - 6.0
      CALL PLOT (90, TU, 0.0)
      CALL PLOT (90, TU, 180.0)
      DO 100 IA = 1,12,2
      Y = TM(IA)
  100 CALL PLOT (9, TU, Y)
      TL = XS - 10.0
      CALL PLOT (90, TL, 0.0)
      CALL PLOT (90, TL, 180.0)
      DO 110 IA = 13,24,2
      Y = TM(IA)
  110 CALL PLOT (9, TL, Y)
      DO 5 I = 10,110,10
      DO 110 IA = 13,24,2
      Y = TM(IA)
  110 CALL PLOT (9, TL, Y)
      DO 5 I = 10,110,10
      DI = I - 10
      PUNCH 33, DI
   33 FORMAT (7H SLOPE-, 1X, F5.0, 4H PCT)
      P = ATANF(DI/100.0)
      AR = SINF(H)*SINF(P)/(COSF(P)*COSF(AL) - COSF(H)*SINF(P)*
     1SINF(AL))
      IF (AR) 6,7,7
    6 DT = 3.1416 - ATANF(ABSF(AR))
      GO TO 9
    7 DT = ATANF(AR)
```

Radiation indexes (Continued)

```
 9 C = SINF(P)*COSF(H)*COSF(AL) + COSF(P)*SINF(AL)
   ALP = ATANF(C/SQRTF(1.0-C**2))
   DO 60 L = 1,N
   DE = DECL(L)
   C = -SINF(ALP)*SINF(DE)/(COSF(ALP)*COSF(DE))
   IF (C) 36,35,37
35 SSET = (4.0*1.5708 - 4.0*DT)/V
   GO TO 40
36 SSET = (4.0*(3.1416 - ATANF(ABSF(SQRTF(1.0-C**2)/C)))-4.0*DT)/V
   GO TO 40
37 SSET = (4.0*ATANF(SQRTF(1.0 - C**2)/C) - 4.0*DT)/V
40 AIQ = AIP(L)*(COSF(DE)*COSF(ALP)*(SINF(W*(-SRISE(L)-4.0*DT/V)) +
  1SINF(W*(SSET+4.0*DT/V)))/W + (-SRISE(L)+SSET)*SINF(DE)*SINF(ALP))
   RI(L) = 50.0*AIQ/(-SRISE(L)*AIP(L)*COSF(P))
   PUNCH 50, DMON(L), DAY(L), SRISE(L), SSET   , AIQ, RI(L)
50 FORMAT (20X, F4.0, F5.0, 2X, 4F11.3)
60 CONTINUE
   DO 90 JB = 1,N
   KB = DD(JB)
90 CALL PLOT (90, RI(KB), TM(KB))
   CALL PLOT (99)
 5 CONTINUE
   END
```

Sample of Output from Radiation Index Program

C C
LATITUDE- 40. N AZIMUTH- 45. DEG.

	MON.	DAY	SRISE	SSET	IO	RI
SLOPE- 0. PCT						
	1.	1.	-276.246	276.246	336.510	29.424
	1.	15.	-283.622	283.622	365.366	31.152
	2.	1.	-298.771	298.771	427.918	34.774
	2.	15.	-314.810	314.810	498.422	38.641
	3.	1.	-332.779	332.779	580.812	42.882
	3.	21.	-360.000	360.000	706.523	48.767
	4.	1.	-375.092	375.092	773.514	51.586
	4.	15.	-393.795	393.795	851.073	54.524
	5.	1.	-413.519	413.519	924.298	56.905
	5.	15.	-428.158	428.158	972.162	58.204
	6.	1.	-440.726	440.726	1008.371	59.023
	6.	22.	-445.594	445.594	1019.758	59.272
	7.	1.	-445.043	445.043	1017.791	59.246
	7.	15.	-439.613	439.613	1001.923	58.961
	8.	1.	-426.267	426.267	960.878	58.058
	8.	15.	-411.196	411.196	909.748	56.663
	9.	1.	-389.867	389.867	828.597	53.961
	9.	23.	-360.000	360.000	700.540	48.767
	10.	1.	-349.005	349.005	650.695	46.497
	10.	15.	-330.132	330.132	564.229	42.270
	11.	1.	-308.803	308.803	468.670	37.195
	11.	15.	-293.732	293.732	404.744	33.561
	12.	1.	-280.982	280.982	354.025	30.530
	12.	22.	-274.405	274.405	329.394	28.997
SLOPE- 10. PCT						
	1.	1.	-276.246	240.776	277.322	24.369
	1.	15.	-283.622	249.420	306.197	26.237

Sample of Output from Radiation Index Program (Continued)

2.	1.	-298.771	267.070	369.607	30.185
2.	15.	-314.810	285.634	442.211	34.454
3.	1.	-332.779	306.333	528.449	39.211
3.	21.	-360.000	337.582	662.892	45.984
4.	1.	-375.092	354.899	736.045	49.332
4.	15.	-393.795	376.395	822.241	52.939
5.	1.	-413.519	399.158	905.390	56.019
5.	15.	-428.158	416.152	960.910	57.817
6.	1.	-440.726	430.836	1003.754	59.046
6.	22.	-445.594	436.553	1017.708	59.448
7.	1.	-445.043	435.905	1015.453	59.404
7.	15.	-439.613	429.531	996.737	58.948
8.	1.	-426.267	413.951	948.699	57.608
8.	15.	-411.196	396.470	889.783	55.696
9.	1.	-389.867	371.875	798.125	52.235
9.	23.	-360.000	337.582	657.279	45.984
10.	1.	-349.005	324.968	603.533	43.342
10.	15.	-330.132	303.289	511.602	38.518
11.	1.	-308.803	278.694	411.879	32.851
11.	15.	-293.732	261.213	346.300	28.858
12.	1.	-280.982	246.331	294.968	25.564
12.	22.	-274.405	238.611	270.257	23.910

SLOPE- 20. PCT

1.	1.	-276.246	202.159	224.012	19.975
1.	15.	-283.622	212.197	252.299	21.937
2.	1.	-298.771	232.540	315.244	26.125
2.	15.	-314.810	253.766	388.453	30.712
3.	1.	-332.779	277.296	476.780	35.899
3.	21.	-360.000	312.677	617.216	43.447
4.	1.	-375.092	332.272	695.035	47.270

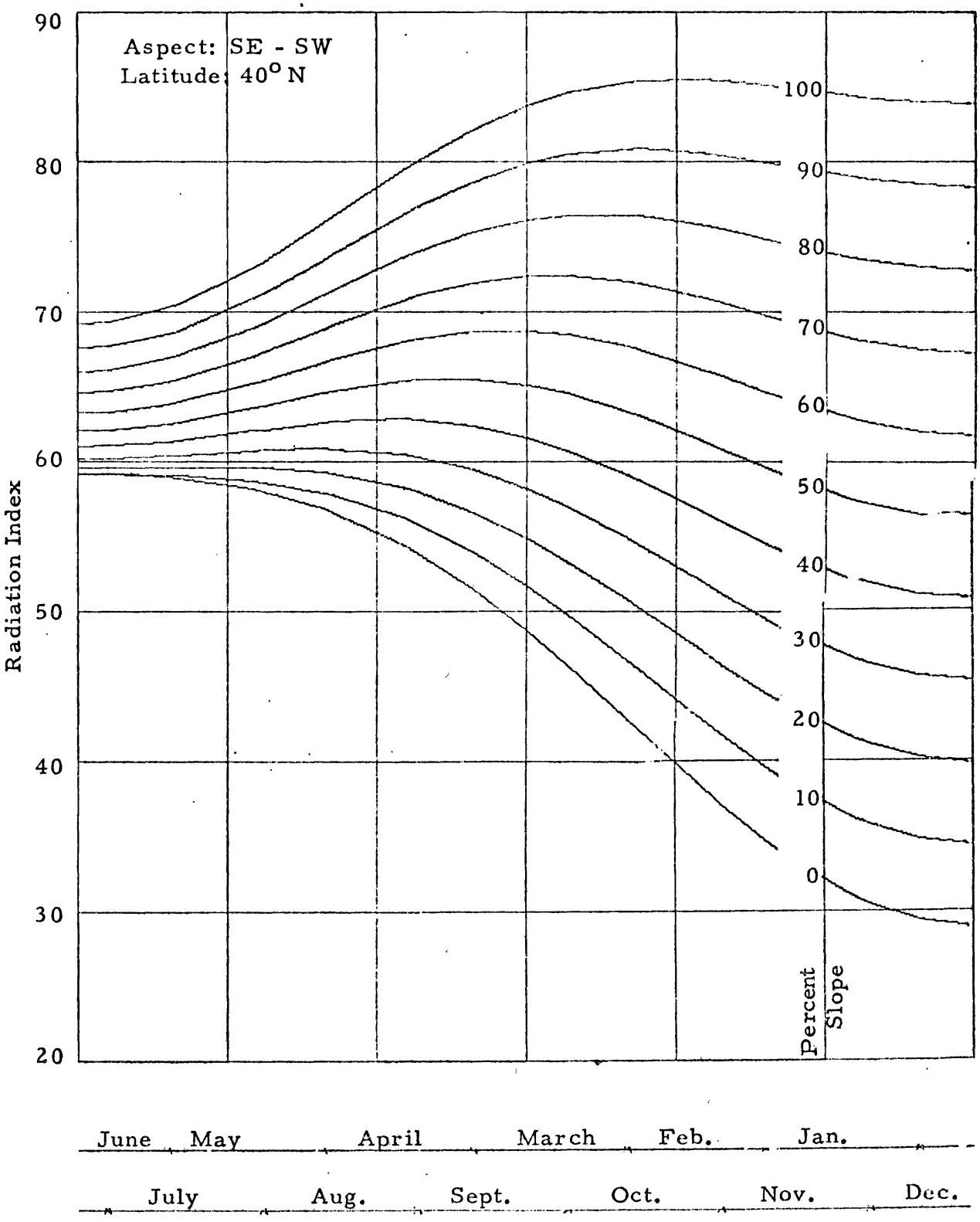

Figure A1. Radiation index values as a function of slope inclination and time of year.

Appendix B

Hydrologic Data for Circle Valley Model

Table B1. Average radiation index values for the Circle Valley watershed.

No.	Month	Radiation Indexes				Ratio RI_s / RI_h col. 5 by col. 6
		S. E. Slope 60%	N. W. Slope 60%	Avg. for the S.E. &N.W.Slopes	Horiz. Surface	
1	January	63.0	11.0	37.0	31.0	1.16
2	February	66.0	22.0	44.0	38.0	1.16
3	March	68.5	35.0	51.8	47.5	1.09
4	April	68.0	48.0	58.0	55.0	1.06
5	May	66.0	57.0	61.5	58.0	1.06
6	June	63.0	61.0	62.0	59.0	1.05
7	July	64.0	58.0	61.0	58.5	1.04
8	August	67.0	52.0	59.5	56.0	1.06
9	September	69.0	39.0	54.0	50.0	1.08
10	October	68.0	24.0	46.0	41.5	1.11
11	November	63.0	14.0	38.5	33.0	1.17
12	December	62.0	9.0	35.5	29.0	1.22

Table B2. Constant input values for the Circle Valley subbasin.

Symbol	Description	Value
E_c	elevation correction factor applied in the computation of evapotranspiration	0.081"/mo./1000'
j	proportion of irrigation surface runoff returning directly to the river	0.50
k_b	a constant applied in the computation of the rate of baseflow from a watershed	0.10
k_g	a constant applied in the computation of deep percolation rate	0.10
k_n	a constant applied in the computation of interflow rate	0.40
k_s	a constant applied in the computation of snowmelt rate	0.10
k_c	a surface irrigation efficiency factor for canal diversions	0.40
k_p	a surface irrigation efficiency factor for pump diversions	0.40
M_{cs}	available soil moisture storage capacity--watershed cultivated area	6" 10"
M_{es}	a limiting value of available soil moisture applied in the computation of evapotranspiration--watershed cultivated area	3" 4"

Table B3. Constant monthly input values for the Circle Valley subbasin.

Month	Temp. Lapse °F		Percent Daylight Hours		Radiation for ET (RI_s/RI_h M_{es})		Radiation for Snowmelt (100/15) k_s RI_s/RI_h		Watershed Coef.	
	Actual Value	Volts[1] (0.5ΔT)	Actual Value	Volts (6.25PDH)	Actual Value	Volts	Actual	Volts	Actual	Volts (0.5 k_c)
1	3.64	1.82	6.86	21.4	0.386	19.30	0.773	38.6	0.48	12.00
2	4.76	2.38	6.79	21.2	0.386	19.30	0.773	38.6	0.56	14.25
3	5.60	2.80	8.34	26.1	0.363	18.15	0.726	36.3	0.72	18.25
4	5.88	2.94	8.90	27.8	0.353	17.65	0.707	35.4	0.84	21.25
5	6.16	3.08	9.92	30.9	0.353	17.65	0.707	35.4	0.90	22.50
6	6.16	3.08	9.66	31.1	0.350	17.50	0.700	35.0	0.92	23.00
7	6.16	3.08	10.11	31.6	0.346	17.30	0.694	34.7	0.92	23.00
8	6.16	3.08	9.48	29.6	0.353	17.65	0.707	35.4	0.92	22.75
9	5.88	2.94	8.38	26.2	0.360	18.00	0.720	36.0	0.88	21.75
10	5.60	2.80	7.80	24.3	0.370	18.50	0.740	37.0	0.80	20.00
11	4.20	2.10	6.81	21.2	0.390	19.50	0.780	39.0	0.68	16.75
12	3.08	1.54	6.65	23.5	0.406	20.30	0.813	40.6	0.56	13.75

Month	Grain Coeff.		Potato Coeff.		Corn Coeff.		Alfalfa Coeff.		Wet Area Coeff.	
	Actual	Volts (0.5 k_c)	Actual	Volts (0.5 k_c)	Actual	Volts (0.5 k_c)	Actual	Volts (0.5 k_c)	Actual	Volts (0.5 k_c)
1	0.25	6.25	0.25	6.25	0.25	6.25	0.68	17.00	0.70	17.5
2	0.25	6.25	0.25	6.25	0.25	6.25	0.80	19.75	0.70	17.5
3	0.25	6.25	0.25	6.25	0.25	6.25	0.88	22.25	0.75	18.6
4	0.26	6.50	0.25	6.25	0.25	6.25	1.00	24.75	0.81	20.3
5	0.50	12.50	0.25	6.25	0.26	6.50	1.08	27.00	0.89	22.3
6	1.54	38.50	0.38	9.50	0.60	15.00	1.12	27.75	1.02	25.5
7	1.12	28.25	0.90	22.50	1.28	32.25	1.10	27.50	1.18	29.5
8	0.25	6.25	1.32	32.75	1.08	27.00	1.08	27.00	1.28	32.0
9	0.25	6.25	1.32	33.00	0.42	10.50	1.00	25.25	1.29	32.2
10	0.25	6.25	0.25	6.25	0.25	6.25	0.92	23.00	1.19	29.7
11	0.25	6.25	0.25	6.25	0.25	6.25	0.80	20.25	1.04	26.0
12	0.25	6.25	0.25	6.25	0.25	6.25	0.68	17.25	0.86	21.5

[1] The computer reference voltage is 50 volts.

Table B4. Variable monthly input values for the Circle Valley subbasin for 1962 and 1963.

1962 Month	Precipitation (Inches/Month)		Valley Temp. (°F)		Canal Div. (A-F/Month)		Pumped Div. (A-F/Month)		River Inflow (A-F/Month)	
	Actual Value	Volts[1] 10 P	Actual Value	Volts 0.5 T	Actual Value	Volts $0.005Q_c$	Actual Value	Volts $0.005Q_p$	Actual Value	Volts 0.002IR
1	0.75	7.5	22.2	11.1	320	1.60	---		5060	10.12
2	0.86	8.6	31.7	15.8	480	2.40	---		8690	17.38
3	0.70	7.0	34.6	17.3	590	2.95	---		11030	22.06
4	1.25	12.5	50.7	25.4	5240	26.20	---		18370	36.74
5	0.72	7.2	53.3	26.6	7410	37.05	---		18290	36.58
6	0.54	5.4	62.5	31.2	5360	26.80	---		7270	14.54
7	0.30	3.0	69.2	34.6	2890	14.45	---		3230	6.46
8	0.12	1.2	68.1	34.0	2500	12.50	-31	0.155	2640	5.28
9	0.85	8.5	61.3	30.6	3390	16.95	188	0.940	3780	7.56
10	0.37	3.7	51.7	25.8	4510	22.55	166	0.830	5270	10.54
11	0.12	1.2	40.3	20.2	3390	16.95	---		6330	12.66
12	0.23	2.3	29.8	14.9	750	3.75	---		6210	12.42
1963										
1	0.34	3.4	24.0	12.0	0	0	---		4650	9.30
2	0.82	8.2	37.1	18.6	440	2.20	---		7100	14.20
3	0.32	3.2	36.3	18.2	2431	12.16	---		6120	12.24
4	0.74	7.4	41.2	20.6	3037	15.18	---		3580	7.16
5	0.11	1.1	58.2	29.1	4504	22.52	189	0.95	5350	10.70
6	0.74	7.4	60.0	30.0	1677	8.38	188	0.94	1820	3.64
7	0.46	4.6	70.8	35.4	1423	7.12	204	1.02	1600	3.20
8	3.43	34.3	67.6	33.8	2404	12.02	163	0.82	2710	5.42
9	1.31	13.1	61.8	30.9	3234	16.17	101	0.50	3780	7.56
10	0.49	4.9	54.2	27.1	2446	12.23	---		2650	5.30
11	0.62	6.2	38.5	19.2	2280	11.40	---		4430	8.86
12	0.15	1.5	25.9	13.0	450	2.25	---		6210	12.42

[1] The computer reference voltage is 50 volts.

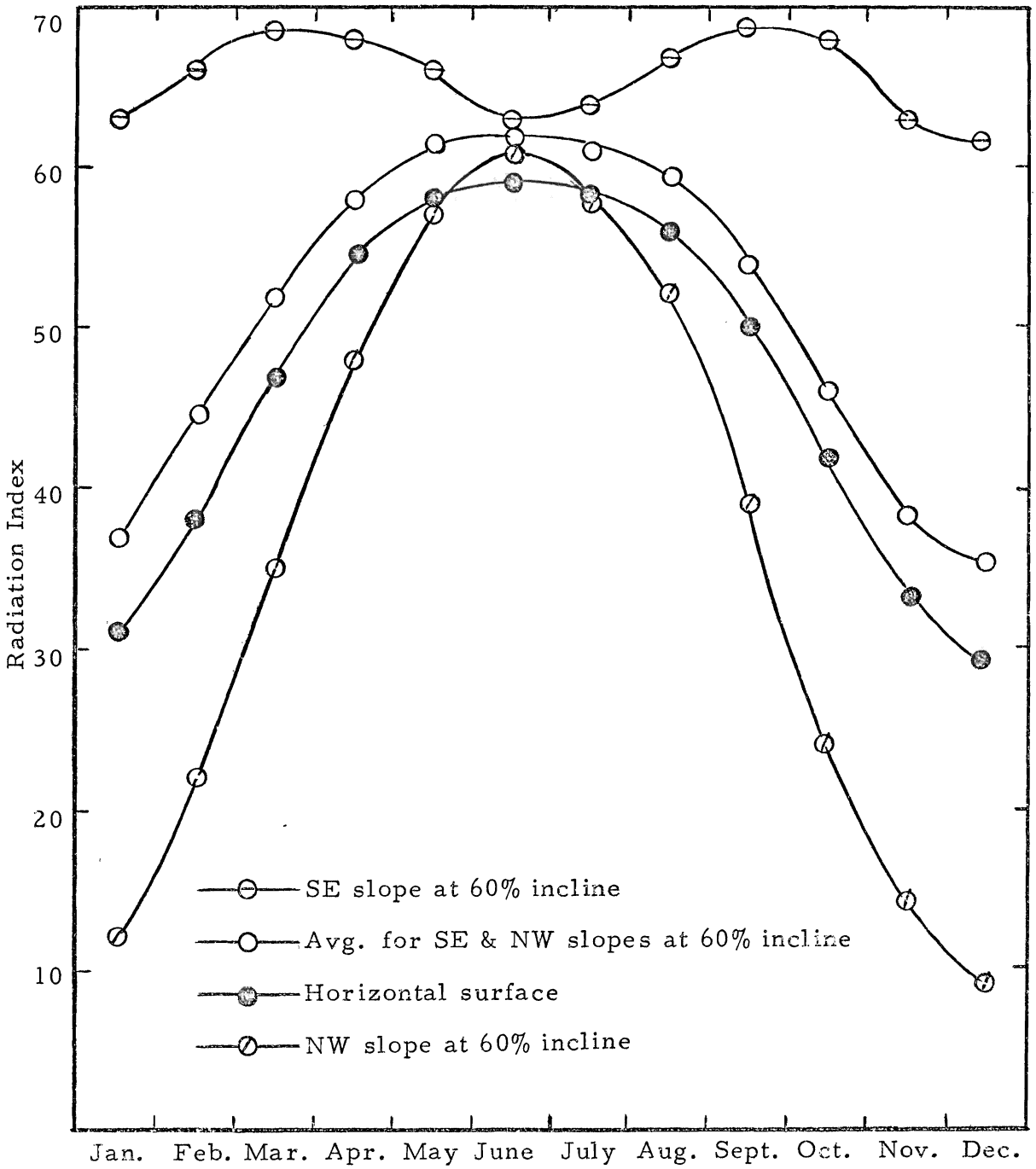

Figure B1. An average radiation index curve for the Circle Valley watershed.

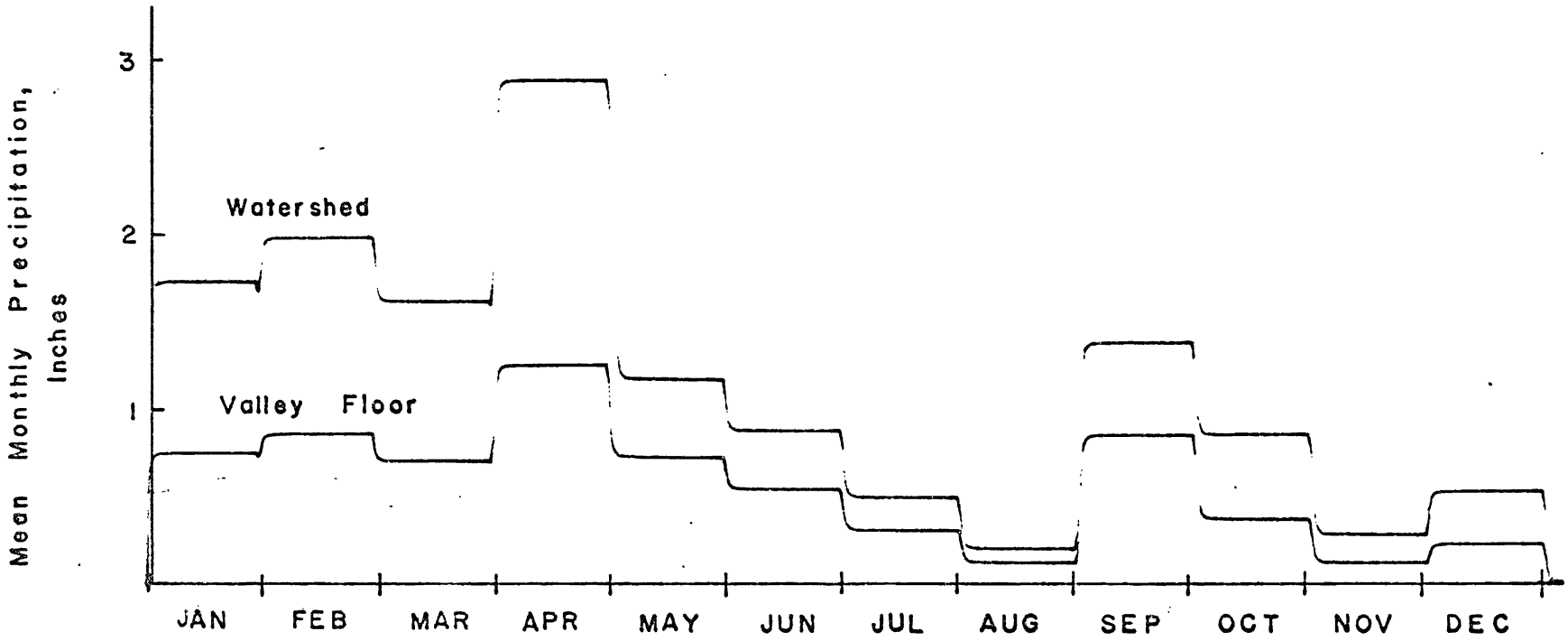

Figure B2. Mean monthly precipitation rates for the valley floor (observed) and the watershed area (computed), Circle Valley, 1962.

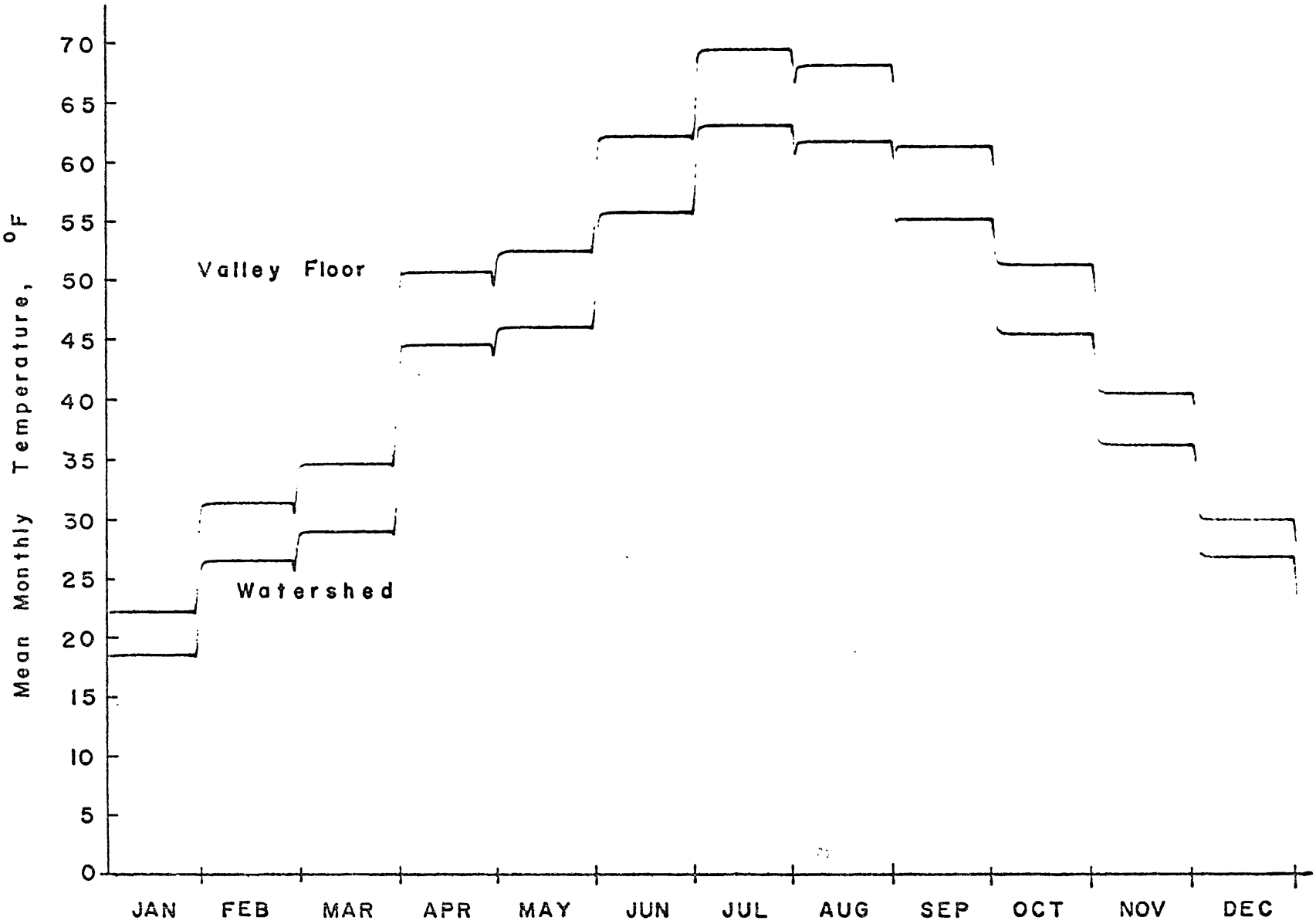

Figure B3. Mean monthly temperature for the valley floor (observed) and the watershed area (computed), Circle Valley, 1962.

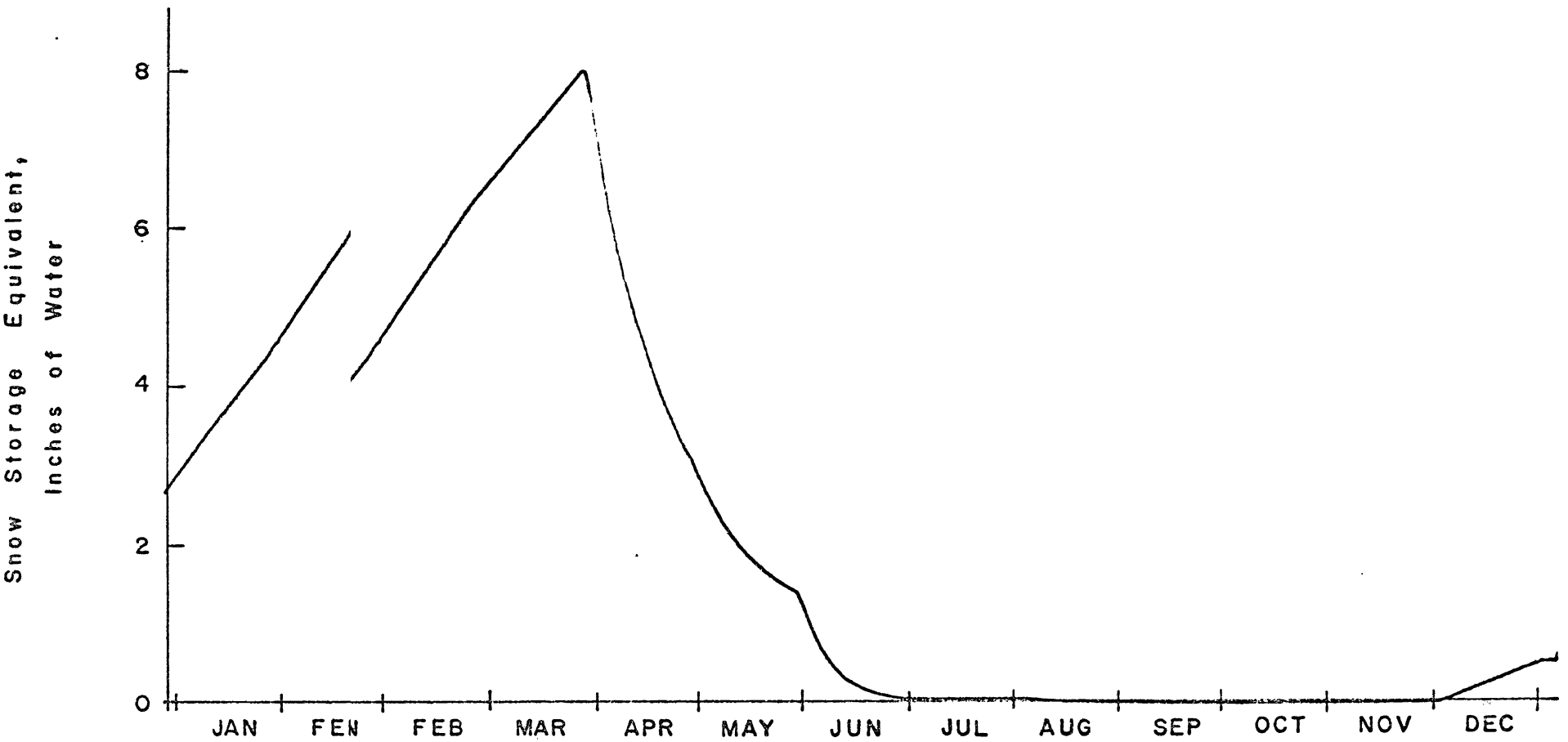

Figure B4. Con4. Computed accumulated snow storage equivalent on the watershed area of Circle Vall Valley during 1962.

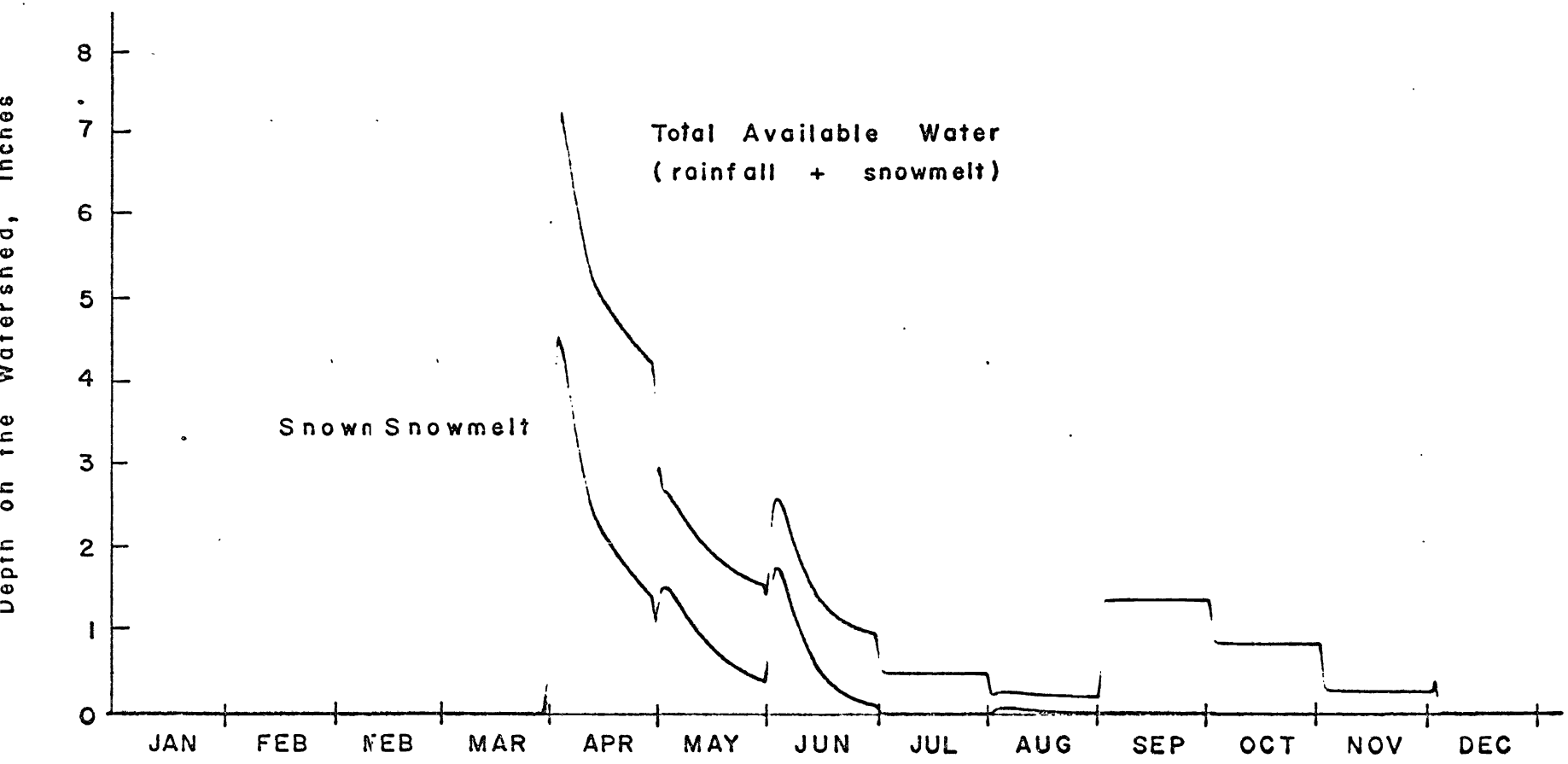

Figure B5. Computeomputed values of available water within the watershed area of Circle Valley during lluring 1962.

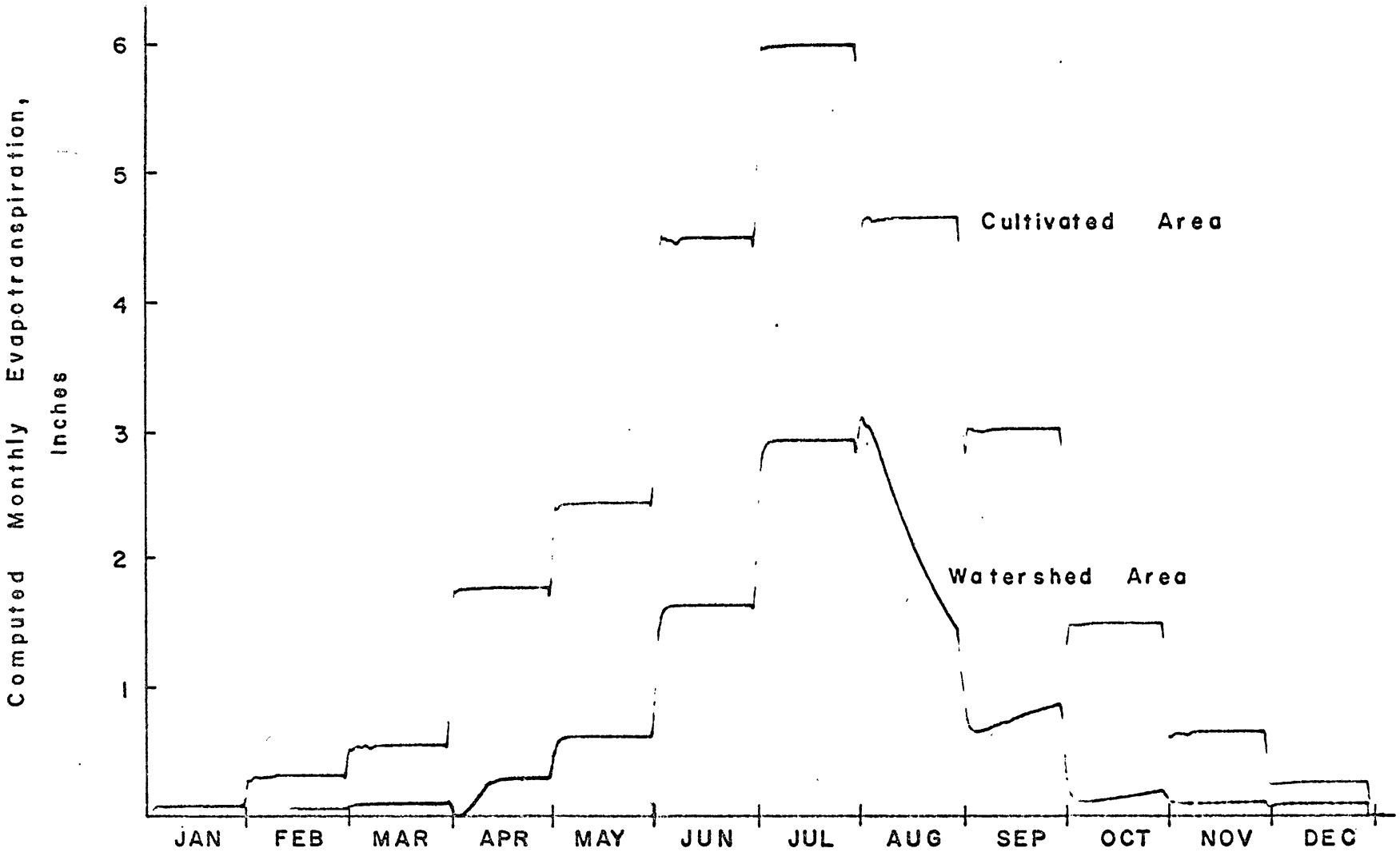

Figure B6. Computed mean monthly evapotranspiration rates, Circle Valley, 1962.

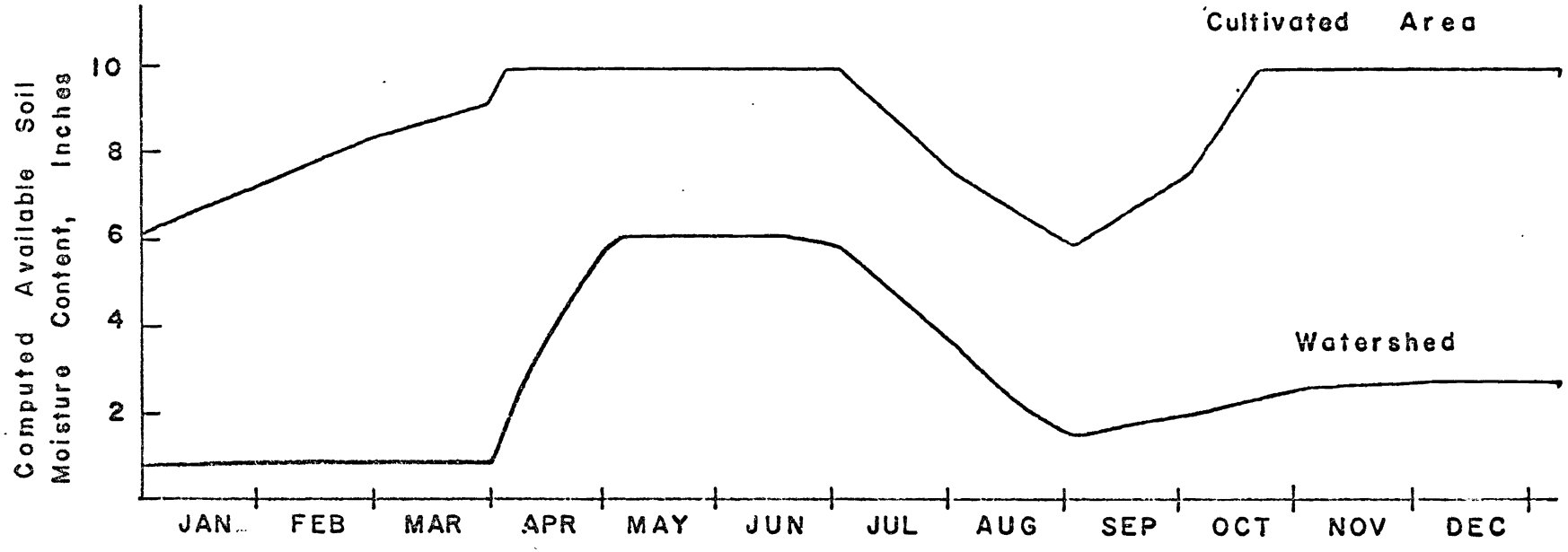

Figure B7. Computed average available soil moisture values within the cultivated and watershed areas of Circle Valley during 1962.

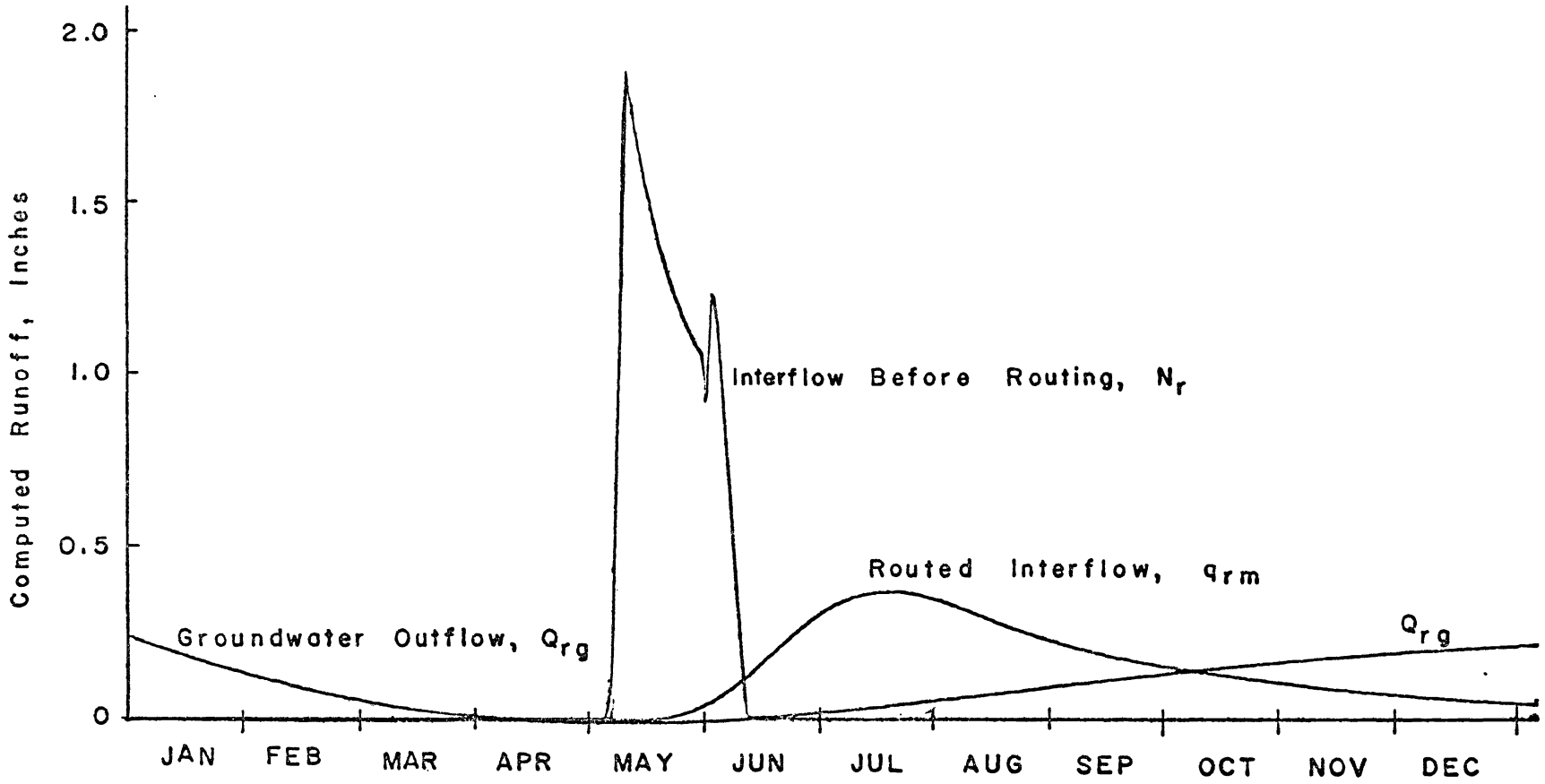

Figure B8. Components of runoff from the watershed area, Circle Valley, 1962.

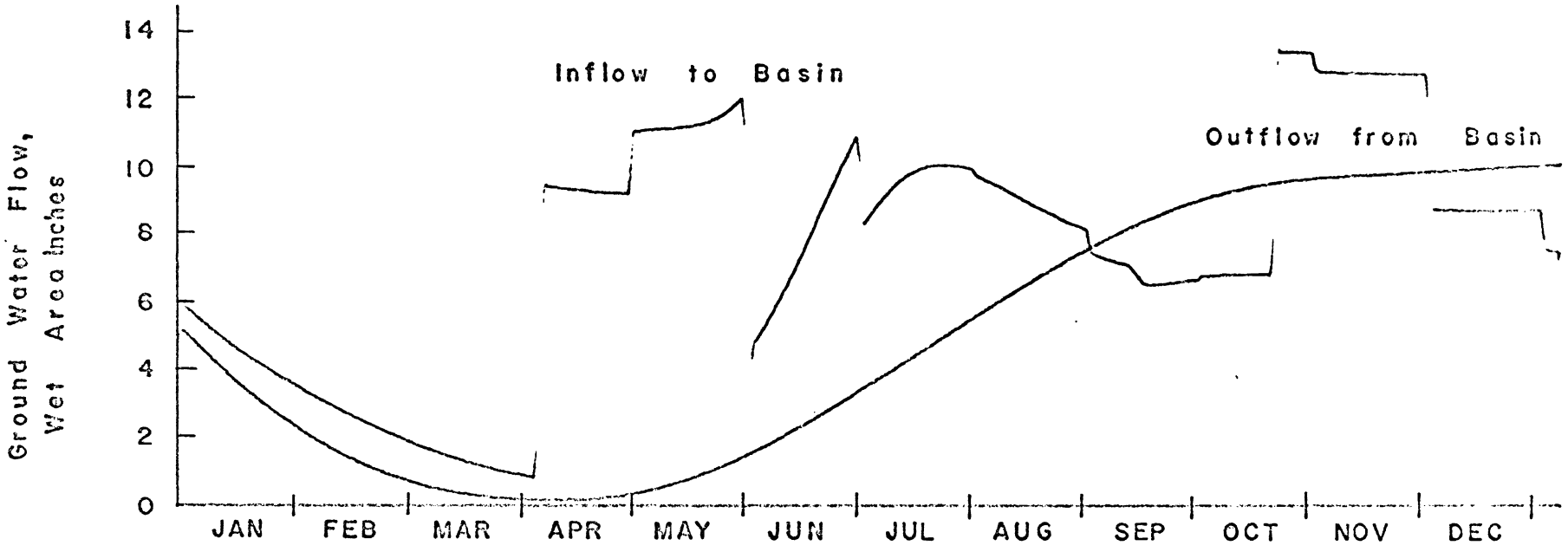

Figure B9. Computed values of inflow and outflow rates for the groundwater basin beneath the cultivated area of Circle Valley during 1962.

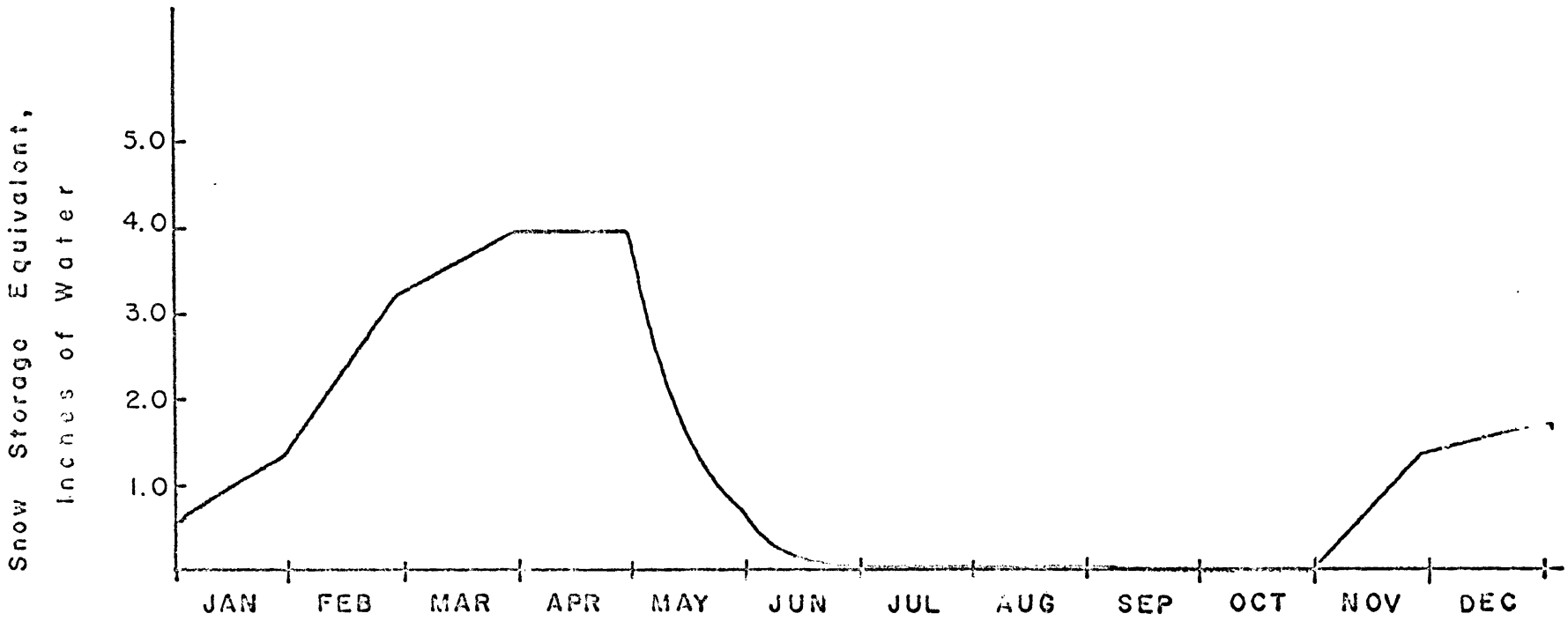

Figure B10. Computed accumulated snow storage equivalent in the watershed area of Circle Valley during 1963.

Appendix C

Hydrologic Data for Walnut Gulch Model

Table C1. Precipitation data for event of July 20, 1966, on subwatershed 11, Walnut Gulch, Arizona.

Gage No.	Theissen Area (acres)	Time from 1600 hours (minutes)[1]											
		5	10	15	20	25	30	35	40	45	50	55	60
44	27.1	0.03	0.08	0.10	0.22	0.20	0.21	0.15	0.04	0.04	0.02	0.01	0.00
51	197.2	0.01	0.04	0.08	0.16	0.21	0.18	0.10	0.06	0.04	0.02	0.02	0.00
52	239.4	0.00	0.05	0.09	0.14	0.25	0.15	0.08	0.06	0.05	0.04	0.01	0.01
54	258.8	0.00	0.00	0.06	0.20	0.24	0.30	0.20	0.10	0.04	0.04	0.01	0.00
55	157.4	0.00	0.02	0.14	0.27	0.35	0.20	0.22	0.09	0.03	0.01	0.01	0.00
56	197.5	0.00	0.00	0.06	0.09	0.19	0.20	0.16	0.15	0.04	0.03	0.02	0.02
88	355.4	0.00	0.02	0.06	0.24	0.14	0.20	0.15	0.12	0.06	0.03	0.01	0.01
89	142.9	0.00	0.00	0.03	0.09	0.19	0.22	0.15	0.08	0.05	0.02	0.01	0.01
90	247.6	0.00	0.00	0.04	0.12	0.17	0.21	0.13	0.09	0.04	0.02	0.01	0.01
91	211.7	0.00	0.03	0.13	0.37	0.35	0.29	0.19	0.09	0.03	0.01	0.00	0.00

[1] The tabulated values in the main body of the table are the precipitation caught in inches during each five minute time interval.

Table C2. Constant input values for subwatershed 11, Walnut Gulch, Arizona.

Symbol	Description	Value
Δt	time increment or scale factor adopted for the model	5 minutes
b	average base width of the surface channels within a watershed zone	20 feet
l	total length of the surface channels within a watershed zone	52,800 feet
m	average side slope (horizontal to vertical) of the surface channels within a watershed zone	0.6
F_c	constant infiltration capacity rate under conditions of a saturated soil profile	0.15 in./Δt
F_o	soil infiltration capacity rate at the beginning of a storm	0.3 in./Δt
k	a constant in the Horton infiltration equation	0.40
k_g	a constant applied in the computation of channel seepage loss	0.20
k_r	a constant applied in the computation of capacity surface retention rate	1.0
k_s	a constant applied in the computation of outflow rate from surface detention storage	0.3
R_{cs}	retention storage capacity of the vegetation and land surfaces within a particular area (interception plus depression)	0.15 in.

DIGITAL COMPUTER PROGRAM FOR COMPUTING INCREMENTAL PRECIPITATION

```
    DIMENSION TP(50),T(50),P(50),DELT(10)
  1 READ 99,DT1,DT2,NTO,L,ND,(DELT(I),I=1,ND)
 99 FORMAT(2A3,I9,2I5,5F9.0)
    READ 100
    PUNCH 100
100 FORMAT(80H
   1                              )
    PUNCH 101,DT1,DT2,NTO
101 FORMAT(15X,5HDATE 2A3,8X,9HTIME ZERO16)
    PUNCH 110
110 FORMAT(7HGAGE NO3X,13HACC TIME(MIN)4X,19HINTERVAL PRECIP(IN)3X,20H
   1ACC STORM PRECIP(IN))
  2 READ102,K,NGA
102 FORMAT(2I5)
    READ 104,(TP(J),J=1,K)
104 FORMAT (20X,10F6.2)
    DO324 J=1,K
    I=TP(J)*0.1
    T(J)=I
    B=I*10
324 P(J)=TP(J)-B
323 DO 15KK=1,ND
    PUNCH 360,DELT(KK)
360 FORMAT(20HTIME INCREMENT(MIN)=F4.0)
    CR=1.0
    AP=P(1)
    AT=DELT(KK)
    J=1
    ASP=0
  3 IF(AT-T(J+1))5,7,8
  5 DT=DELT(KK)
    API=AP
    GO TO 10
  8 J=J+1
    IF((J+1)-K)6,6,14
  6 IF(AT-T(J+1))9,7,8
  7 TAP=P(J+1)
    GO TO 11
  9 DT=AT-T(J)
    API=P(J)
    GO TO 10
 14 TAP=P(K)
    GO TO 11
 10 TAP=DT*(P(J+1)-P(J))/(T(J+1)-T(J))+API
```

```
   11 PI=TAP-AP
      PIR=PI+0.005
      ASP=ASP+PI
      ASPR=ASP+0.005
      NAT=AT
      PUNCH 106,NGA,NAT,PIR,ASPR
  106 FORMAT(I5,I12,2F22.2)
      IF(AT-T(K))12,15,15
   12 CR=CR+1.0
      AT=CR*DELT(KK)
      AP=TAP
      GO TO 3
   15 CONTINUE
      L=L-1
      IF(L)20,20,2
   20 PAUSE
      GO TO 1
      END
```

Sample Output

```
PRECIPITATION DATA FOR WALNUT GULCH    SUB WATERSHED 11    PROJECT WG'
                DATE 072066         TIME ZERO  1600
GAGE NO   ACC TIME(MIN)    INTERVAL PRECIP(IN)   ACC STORM PRECIP(IN)
TIME INCREMENT(MIN)=  5.
   32            5                .02                  .02
   32           10                .06                  .08
   32           15                .06                  .14
   32           20                .07                  .21
   32           25                .13                  .34
   32           30                .15                  .49
   32           35                .11                  .60
   32           40                .07                  .67
   32           45                .03                  .70
   32           50                .01                  .71
   32           55                .01                  .71
   32           60                .01                  .72
   32           65               0.00                  .72
TIME INCREMENT(MIN)= 10.
   32           10                .08                  .08
   32           20                .13                  .21
   32           30                .28                  .49
   32           40                .18                  .67
   32           50                .03                  .71
   32           60                .01                  .72
   32           70               0.00                  .72
```

TIME INCREMENT(MIN)= 15.			
32	15	.14	.14
32	30	.35	.49
32	45	.21	.70
32	60	.02	.72
32	75	0.00	.72
TIME INCREMENT(MIN)= 5.			
33	5	.03	.03
33	10	.04	.07
33	15	.06	.13
33	20	.05	.17
33	25	.09	.26
33	30	.12	.38
33	35	.15	.53
33	40	.10	.63
33	45	.04	.67
33	50	.02	.68
33	55	.01	.69
33	60	.01	.70
33	65	.01	.71
TIME INCREMENT(MIN)= 10.			
33	10	.07	.07
33	20	.10	.17
33	30	.21	.38
33	40	.25	.63
33	50	.06	.68
33	60	.02	.70
33	70	.01	.71
TIME INCREMENT(MIN)= 15.			
33	15	.13	.13
33	30	.26	.38
33	45	.29	.67
33	60	.04	.70
33	75	.01	.71
TIME INCREMENT(MIN)= 5.			
38	5	0.00	0.00
38	10	.05	.05
38	15	.11	.16
38	20	.11	.27
38	25	.16	.43
38	30	.21	.64
38	35	.14	.78
38	40	.05	.83
38	45	.04	.87
38	50	.03	.90
38	55	.03	.92
TIME INCREMENT(MIN)= 10.			
38	10	.05	.05
38	20	.22	.27
38	30	.37	.64
38	40	.19	.83
38	50	.07	.90
38	60	.03	.92

TIME INCREMENT(MIN)= 15.			
38	15	.16	.16
38	30	.48	.64
38	45	.23	.87
38	60	.05	.92
TIME INCREMENT(MIN)= 5.			
39	5	0.00	0.00
39	10	.03	.03
39	15	.09	.12
39	20	.14	.26
39	25	.13	.39
39	30	.08	.48
39	35	.13	.60
39	40	.10	.70
39	45	.06	.76
39	50	.02	.78
39	55	.01	.79
39	60	.01	.80
39	65	0.00	.80
TIME INCREMENT(MIN)= 10.			
39	10	.03	.03
39	20	.23	.26
39	30	.22	.48
39	40	.23	.70
39	50	.08	.78
39	60	.01	.80
39	70	0.00	.80
TIME INCREMENT(MIN)= 15.			
39	15	.12	.12
39	30	.36	.48
39	45	.29	.76
39	60	.04	.80
39	75	0.00	.80
TIME INCREMENT(MIN)= 5.			
44	5	.03	.03
44	10	.08	.11
44	15	.10	.21
44	20	.22	.43
44	25	.20	.63
44	30	.21	.84
44	35	.15	.99
44	40	.04	1.03
44	45	.04	1.07
44	50	.02	1.09
44	55	.01	1.10
44	60	0.00	1.10
TIME INCREMENT(MIN)= 10.			
44	10	.11	.11
44	20	.32	.43
44	30	.41	.84
44	40	.19	1.03
44	50	.07	1.09
44	60	.01	1.10